

REPORT NO.
UCB/EERC-83/04
FEBRUARY 1983

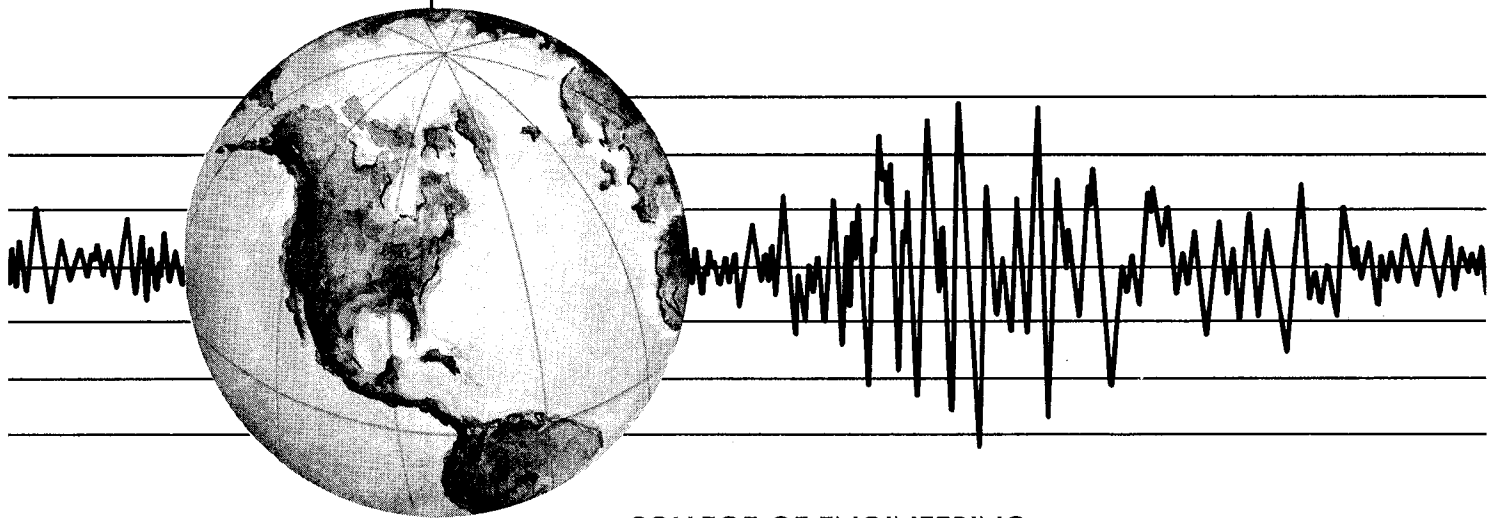
EARTHQUAKE ENGINEERING RESEARCH CENTER

NUMERICAL TECHNIQUES FOR THE EVALUATION OF SOIL-STRUCTURE INTERACTION EFFECTS IN THE TIME DOMAIN

by

EDUARDO BAYO
EDWARD L. WILSON

Report to the National Science Foundation



COLLEGE OF ENGINEERING
UNIVERSITY OF CALIFORNIA · Berkeley, California

For sale by the National Technical Information Service, U.S. Department of Commerce, Springfield, Virginia 22161.

See back of report for up to date listing of EERC reports.

DISCLAIMER

Any opinions, findings, and conclusions or recommendations expressed in this publication are those of the authors and do not necessarily reflect the views of the National Science Foundation or the Earthquake Engineering Research Center, University of California, Berkeley

EARTHQUAKE ENGINEERING RESEARCH CENTER

NUMERICAL TECHNIQUES FOR THE
EVALUATION OF SOIL-STRUCTURE INTERACTION
EFFECTS IN THE TIME DOMAIN

by

Eduardo Bayo

and

Edward L. Wilson

A Report to the
National Science Foundation

Report No. UCB/EERC-83/04
College of Engineering
Department of Civil Engineering
University of California
Berkeley, California

February 1983

j.a



ABSTRACT

A time domain finite element method that efficiently solves the three dimensional soil-structure interaction problem is presented. In addition to all the factors currently considered by frequency domain approaches the new method allows the consideration of the nonlinear effects in the structure and foundation (separation of base mat from soil or nonlinear material).

The general equations of motion for the linear cases are expressed in terms of the relative displacements of the soil-structure system with respect to those of the nodes at the foundation level. This formulation allows the load vector to be an exclusive function of the free field accelerations at the soil-structure interface. In order to avoid the scattering problem the dynamic displacements can be defined with respect to those of the buried part of the structure. The nonlinear case requires that the equations of motion be established in terms of the total interaction displacements.

The energy radiation through the boundaries of the finite element model is accounted for by using frequency independent radiation boundaries obtained from a frequency dependent boundary defined at the fundamental frequency of the soil-structure system. The effects of this approximation are shown to be minimal for typical structures.

The soil-structure system is divided into substructures, namely the structure (one or more) and the soil. The latter is modelled with three dimensional solid elements in the near field and axisymmetric elements in the far field. The coupling between them is enforced by expanding the displacements of the solid elements in terms of the axisymmetric ones. A new method for the reduction in the number of degrees of freedom is presented that is based on component mode synthesis techniques and on the use of orthogonal sets of Ritz functions. These functions are obtained in a simpler and computationally faster way than the eigenvectors, while yielding improved accuracy.

In the linear case, the resulting reduced set of equations of motion is integrated by uncoupling the system using the complex mode shapes. The latter procedure becomes exact for piece-wise linear type of excitation and is computationally as efficient as the step-by-step methods for reduced systems.

For linear problems the present method becomes numerically far more efficient than the existing frequency domain approaches. This difference leads to substantial savings in computer time and storage.

ACKNOWLEDGEMENTS

The research described in this report constitutes the first author's dissertation, submitted in partial satisfaction of the requirements for the degree of Doctor of Philosophy in Engineering at the University of California, Berkeley. The study was carried out under the supervision of Professor Edward L. Wilson. His guidance and constructive ideas have been of fundamental importance in completing this work.

Financial support, provided by the National Science Foundation under the grant no. CEE-8105790 titled "Seismic Behavior of Structural Systems", is gratefully acknowledged. Gratitude is also due to the "Fundacion del Instituto Nacional de Industria", Madrid, Spain, who sponsored the first two years of the senior author's studies at Berkeley.

The authors wish to thank Professors B. Bolt and R. W. Clough for their valuable suggestions and for reviewing the manuscript. A word of thanks is also extended to T. J. Tzong for his help and enjoyable discussions, and to Erico Crespo for handwriting the equations.

The first author wishes to express his gratitude to his family for all their support and encouragement, and especially to his wife Elizabeth Anne for her love and emotional support during his graduate studies at Berkeley.



TABLE OF CONTENTS

1.- INTRODUCTION.....	1
2.- ANALYTICAL METHODS IN THE FREQUENCY DOMAIN.....	4
2.1.- Intoduction.....	4
2.2.- Simplified model.....	5
2.3.- Complete methods.....	7
2.4.- Substructure methods.....	9
2.4.1.- Boundary methods.....	9
2.4.2.- Volume methods.....	15
2.4.3.- Impedance problem.....	19
2.5.- Hybrid methods.....	21
2.6.- Summary of frequency domain methods.....	23
3.- ANALYTICAL METHODS IN THE TIME DOMAIN.....	26
3.1.- Introduction.....	26
3.2.- Complete methods.....	27
3.3.- Boundary methods.....	28
3.4.- Volume methods.....	33
3.5.- Summary of time domain methods.....	35
4.- RADIATION BOUNDARIES.....	37
4.1.- Introduction.....	37
4.2.- Nature of radiation boundaries.....	39
4.2.1.- One dimensional case.....	39
4.2.2.- Two and three dimensional cases.....	40

4.3.- Frequency independent radiation boundaries.	41
4.3.1.- One dimensional case.	41
4.3.2.- Two dimensional cases.	49
4.3.3.- Three dimensional cases.	56
4.3.4.- Conclusions.	59
5.- REDUCTION IN THE SIZE OF THE PROBLEM.	60
5.1.- Ritz-functions techniques.	60
5.1.1.- Introduction.	60
5.1.2.- One dimension.	61
5.1.3.- Two dimensions.	61
5.1.4.- Three dimensions.	70
5.2.- Substructures.	72
5.2.1.- Review of existing methods of substructuring.	72
5.2.2.- Reduction of equations and dynamic substructuring.	74
5.2.3.- Numerical example.	80
6.- SOLUTION TO THE SCATTERING AND NONLINEAR PROBLEMS.	84
6.1.- Scattering problem.	84
6.2.- Nonlinear analysis.	87
7.- MODELING AND SOLUTION OF SOIL-STRUCTURE INTERACTION PROBLEMS IN THE TIME DOMAIN.	90
7.1.- Modeling the soil-structure system.	90
7.2.- Damping.	92
7.3.- Numerical integration.	100

8.-NUMERICAL EXAMPLE,	102
9.-CONCLUSIONS,	117
REFERENCES,	121
APPENDIX A: FINITE ELEMENT FORMULATION FOR AXISYMMETRIC SOLIDS WITH NON-AXISYMMETRIC LOADS.....	129
Displacement expansion,	129
Stiffness matrix	133
Body forces,	135
Temperature loads,	136
Surface loads,	137
APPENDIX B: 8 TO 27 SOLID FINITE ELEMENT,	138
Formulation,	138
Numerical integration,	144
Coupling between solids and axisymmetric meshes,	150
APPENDIX C: SOLUTION TO THE EQUATIONS OF MOTIONS WITH THE COMPLEX MODE SHAPES,	154

CHAPTER 1

INTRODUCTION

Soil-structure interaction problems have been studied for the last three decades. The need for analyzing a given structure not as if it were isolated, but rather as a part of a seismic environment and as a part of an ensemble of soil and other structures interacting between each other, is making soil-structure analysis imperative for an increasing range of structures. Many aspects need be studied in order to completely analyze a soil-structure interaction problem. Some of these aspects are: the seismic environment, the dynamic properties of soils, the site response, impedance problems and structural analysis. The solutions to all these problems have required the attention of many researchers in the three different areas of seismology, geotechnical engineering and structural engineering.

Much has been written about soil-structure interaction problems. In recent years several authors, Lysmer(1978), Idriss and Kennedy(1977), Rosenblueth (1980), have summarized the dispersed literature by writing different reports that tend to classify the analytical methods, analyze their differences, study the nature of input motions, and discuss the future possibilities for solving the different types of problems. This literature is concerned principally with frequency domain methods. There are two main reasons:

- 1) This domain permits, through the use of frequency dependent impedance coefficients, the splitting of the problem into separate studies of soil and structure.
- 2) The radiation boundaries that count for the transmission of energy through the edges of the finite element model, and that have been obtained from wave propagation theory, are frequency dependent.

So far these two reasons have been powerful enough to inhibit the time domain as the effective environment for the solution of the soil-structure problem. However this trend has to have an end, because of certain limitations of the method. Frequency domain techniques can not solve true nonlinear soil and structural problems, and they become numerically inefficient for three dimensional problems. The purpose of this dissertation is to present efficient numerical techniques in the time domain that can solve the soil structure interaction problem in 3 dimensions, and at the same time to leave the door open for the solution of true nonlinear problems, feasible only in the time domain.

The presentation of this research is organized as follows:

An extensive review of the analytical methods in the frequency domain are discussed in Chapter 2. The complete, substructure, and hybrid methods are formulated and compared to each other. Special attention is given to the substructure methods, and more concretely to the recently introduced volume methods that eliminate the need for solving the scattering problem.

Chapter 3 deals with the analytical solutions to the soil-structure interaction problem in the time domain. The complete, boundary, and volume methods are formulated. The last one constitutes an innovation within the time domain framework. The substructuring approach, as done in the frequency domain, cannot be adopted in the time domain due to the practical impossibility of splitting the system and solving independently the equations of the soil and structure. Substructuring concepts in the time domain are used in the sense of reducing the number of equations in each of the substructures that subsequently are assembled and solved simultaneously.

Chapter 4 deals with the research towards the finding of a frequency independent radiation boundary to be used in the time domain computations. Results are given which demonstrate that the use of frequency independent boundaries defined at the fundamental frequency of the system leads to very good approximations in two and three dimensional problems.

The reduction in the number of degrees of freedom by the use of Ritz functions is described in Chapter 5. One, two, and three dimensional examples are given which demonstrate their accuracy in solving not only structural problems but wave propagation problems as well. General techniques for the reduction of the system of equations and dynamic substructuring are also explored. A new method of substructuring is presented that is not only suitable for soil-structure interaction problems, but for general dynamic substructuring as well. The results of a numerical example show the efficiency of this new technique.

The analytical methods formulated in Chapter 3 are extended in Chapter 6 for the solution of the scattering and nonlinear problem. The formulation of the nonlinear problem is mostly suited for the case of the existence of local nonlinearities at the foundation level, like uplifting of the structure or plastic behaviour of the soil close to the foundation. The proposed modeling of the near and far fields of the ensemble soil-structure system is presented in Chapter 7. The near field part of the soil is modeled with solid finite elements and the far field with axisymmetric elements that are coupled at the boundary interface with the solid ones. Some considerations are made regarding the material damping in the soil and the structure, and the numerical integration of the reduced set of equations. Results of a three dimensional problem are shown in Chapter 8. Conclusions of this research are summarized in Chapter 9.

CHAPTER 2

ANALYTICAL METHODS IN THE FREQUENCY DOMAIN

2.1- INTRODUCTION:

The following discussion summarizes all the current analytical methods with their complete formulations, for the solution of soil-structure interaction problems in the frequency domain. All the analysis is made under the assumption that the finite element method is the analytical tool used for the discretization of the problem.

The methods in the frequency domain are divided into three categories:

- a) Complete methods
- b) Substructure methods $\left\{ \begin{array}{l} \text{Continuum} \\ \text{Boundary} \\ \text{Volume} \end{array} \right.$
- c) Hybrid methods

The complete methods, Lysmer (1974) and (1975), solve the ensemble soil-structure system simultaneously in terms of the total displacements. The motion is specified at the bottom of the model, which is supposed to be rigid, and is obtained from the control motion at the surface by the deconvolution process.

The substructure methods, Chopra (1973), Gutierrez (1976), Kausel and Roesset (1975) and Kausel (1978), make use of the principles of compatibility of forces and displacements at the foundation level to split the complete model into two parts: soil and structure. The frequency dependent impedance coefficients, obtained in closed form solutions for a few cases (generally surface structures) and by finite elements for the rest, are attached to the foundation. By introducing the free field motion at the foundation level the dynamic response of the structure can be obtained independently.

It is possible to distinguish between surface and embedded structures, and in the latter between boundary and volume methods, depending upon at which points the motion is specified. For the boundary methods the motion is specified at the interface between soil and structure. For the volume methods the motion is specified at all the nodes of the structure that are buried.

The hybrid methods eliminate the impedance problem at the boundary between the soil and the structure, and create a far field impedance problem that is solved by system identification techniques. A detailed formulation of all these methods will be given below.

2.2.- SIMPLIFIED MODEL.

In order to better illustrate the concepts upon which the general formulations in both time and frequency domains, are based, a simple 2 degree of freedom problem will be analyzed first. The formulation for more complicated soil-structure systems with thousands of degrees of freedom is only an extension of this small case, the concepts do not vary.

Let m_1 and m_2 be a system of two masses connected by a beam of stiffness k , as shown in Figure (2.1). The system is vibrating due to a specified ground motion v_g applied at m_2 . No external forces are acting in the system. The equations of motions in total coordinates are:

$$\begin{bmatrix} m_1 & 0 \\ 0 & m_2 \end{bmatrix} \begin{Bmatrix} \ddot{v}_1^t \\ \ddot{v}_2^t \end{Bmatrix} + \begin{bmatrix} k_{11} & k_{12} \\ k_{21} & k_{22} \end{bmatrix} \begin{Bmatrix} v_1^t \\ v_g \end{Bmatrix} = \begin{Bmatrix} 0 \\ 0 \end{Bmatrix} \quad (2.1)$$

Since the system has no support the matrix k is singular. The first equation of the system (2.1) is:

$$m_1 \ddot{v}_1^t + k_{11} v_1^t + k_{12} v_g = 0$$

or

$$m_1 \ddot{v}_1^t + k_{11} v_1^t = -k_{12} v_g \quad (2.2)$$

In (2.2), the input vector is defined in the R.H.S. of the equation. A step further can be taken if we write the total displacements as the sum of the dynamic and pseudostatic components. The dynamic displacements represent the relative

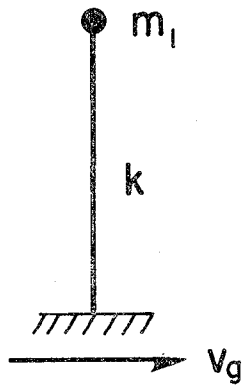
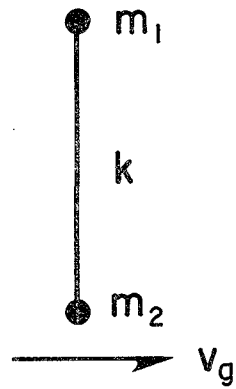


Fig 2.1.- Simplified 2 degree of freedom model.

displacements of degree of freedom 1 with respect to degree of freedom 2. The pseudostatic ones result from a static support displacement. (In this particular case it is a rigid body motion.)

$$v_1^t = v_1 + v^g = v_1 + v_g \quad (2.3)$$

The substitution of (2.3) in (2.2) yields:

$$m_1 \ddot{v}_1 + k_{11} v_1 = k_{12} v_g - m_1 \ddot{v}_g - k_{11} v_g \quad (2.4)$$

however

$$k_{11} v_g + k_{12} v_g = 0 \quad (2.5)$$

because a rigid body motion imposed in an unsupported structure (k is singular) does not create any internal forces. It may be seen also, that (2.5) comes from (2.4) by eliminating all the dynamic terms in it. Therefore (2.4) becomes:

$$m_1 \ddot{v}_1 + k_{11} v_1 = -m_1 \ddot{v}_g$$

which is the well known equation of motion of a single degree of freedom system under ground excitation (see Figure 2.1). The concepts outlined in this simple problem will be used throughout the time and frequency domain formulations. The next step will be to extend them to the general case of a large continuum or discrete model of a soil-structure system.

2.3.- COMPLETE METHODS, Lysmer (1974) and (1975)

Complete methods are defined as methods in which the motions of the soil and the structure are determined simultaneously. The equations of motion are derived with reference to Figure (2.2) which illustrates a complete, discretized soil-structure system. The soil degrees of freedom are designated by r_a , those of the structure by r_s , and the ones at the basement-rock by r_b . The concepts seen above for the 2 degree of freedom system apply similarly in this case. The equations of motion of the complete system in total coordinates are:

$$\begin{bmatrix} m_{ss} & m_{sa} & 0 \\ m_{as} & m_{aa} & m_{ab} \\ 0 & m_{ba} & m_{bb} \end{bmatrix} \begin{Bmatrix} \ddot{r}_s^t \\ \ddot{r}_a^t \\ \ddot{r}_b^t \end{Bmatrix} + \begin{bmatrix} c_{ss} & c_{sa} & 0 \\ c_{as} & c_{aa} & c_{ab} \\ 0 & c_{ba} & c_{bb} \end{bmatrix} \begin{Bmatrix} \dot{r}_s^t \\ \dot{r}_a^t \\ \dot{r}_b^t \end{Bmatrix} + \begin{bmatrix} k_{ss} & k_{sa} & 0 \\ k_{as} & k_{aa} & k_{ab} \\ 0 & k_{ba} & k_{bb} \end{bmatrix} \begin{Bmatrix} r_s^t \\ r_a^t \\ r_b^t \end{Bmatrix} = \begin{Bmatrix} 0 \\ 0 \\ 0 \end{Bmatrix}$$

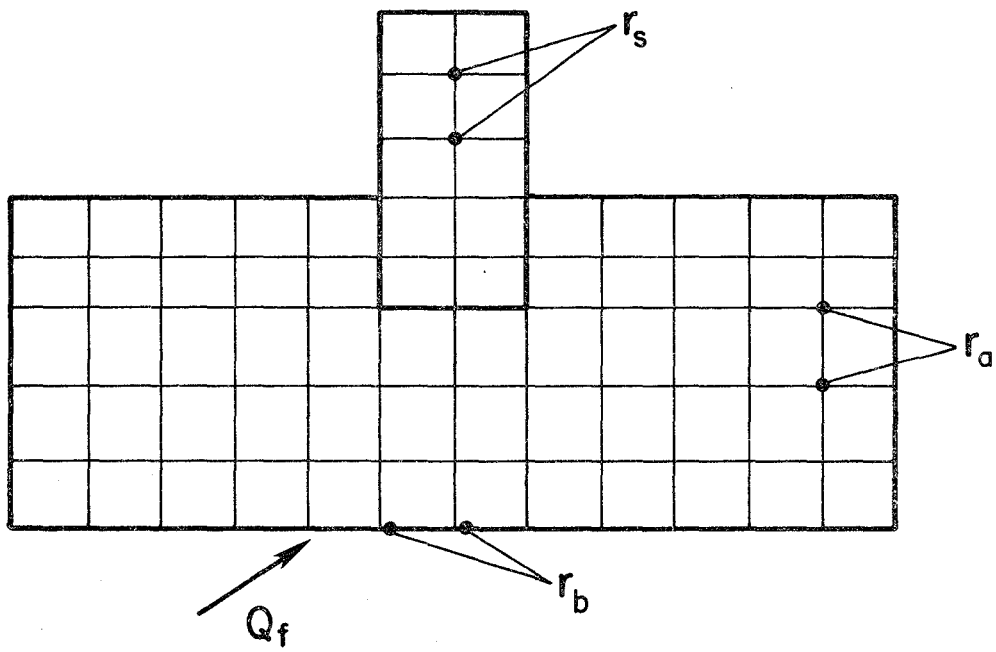


Fig 2.2.- Finite element mesh for the complete methods.

The input motion is specified at the basement-rock, and therefore no external forces are applied on the R.H.S. of the equation. The coupling terms expressing forces at the base level that correspond to the prescribed motion at the base of the model, can be transferred to the R.H.S. as done in the simple model (Equation 2.2, and 2.6) becomes:

$$\begin{bmatrix} m_{ss} & m_{sa} \\ m_{as} & m_{aa} \end{bmatrix} \begin{Bmatrix} \ddot{r}_s^t \\ \ddot{r}_a^t \end{Bmatrix} + \begin{bmatrix} c_{ss} & c_{sa} \\ c_{as} & c_{aa} \end{bmatrix} \begin{Bmatrix} \dot{r}_s^t \\ \dot{r}_a^t \end{Bmatrix} + \begin{bmatrix} k_{ss} & k_{sa} \\ k_{as} & k_{aa} \end{bmatrix} \begin{Bmatrix} r_s^t \\ r_a^t \end{Bmatrix} = \begin{Bmatrix} 0 \\ -m_{ab}\ddot{r}_b^t - c_{ab}\dot{r}_b^t - k_{ab}r_b^t \end{Bmatrix}$$

(2.7)

or in a simplified notation

$$M\ddot{r}^t + C\dot{r}^t + K r^t = Q_f \quad (2.8)$$

where Q_f is the input force vector with only nonzero elements at the base of the model. (See Figure 2.1)

This method does not use any superposition of displacements, therefore it has the advantage over the substructure methods of the possibility of including nonlinear effects by making use of the equivalent linear method, Lysmer (1975). However, it requires a much larger computational effort and overall it is numerically inefficient. The extension to three dimensional analysis is currently prohibitive. Another problem arises from the fact that the motion is specified at the boundary of the mesh, which leads to conflict with the radiation elements situated on it. The solution adopted in FLUSH is to assume that the lower boundary is rigid and specify the input motion at this location.

2.4.- SUBSTRUCTURE METHODS.

2.4.1.- BOUNDARY METHODS: Chopra(1973), Gutierrez (1976), Roesset(1975), Kausel(1978)

Formulation in total displacements:

The ensemble soil-structure may be divided as shown in Figure 2.2. r_s represents the motions at the structure, r_b and R_b the motions and the contact forces at the boundary with the soil respectively. The displacements at the soil are designated as r_a and those at the boundary as r_f .

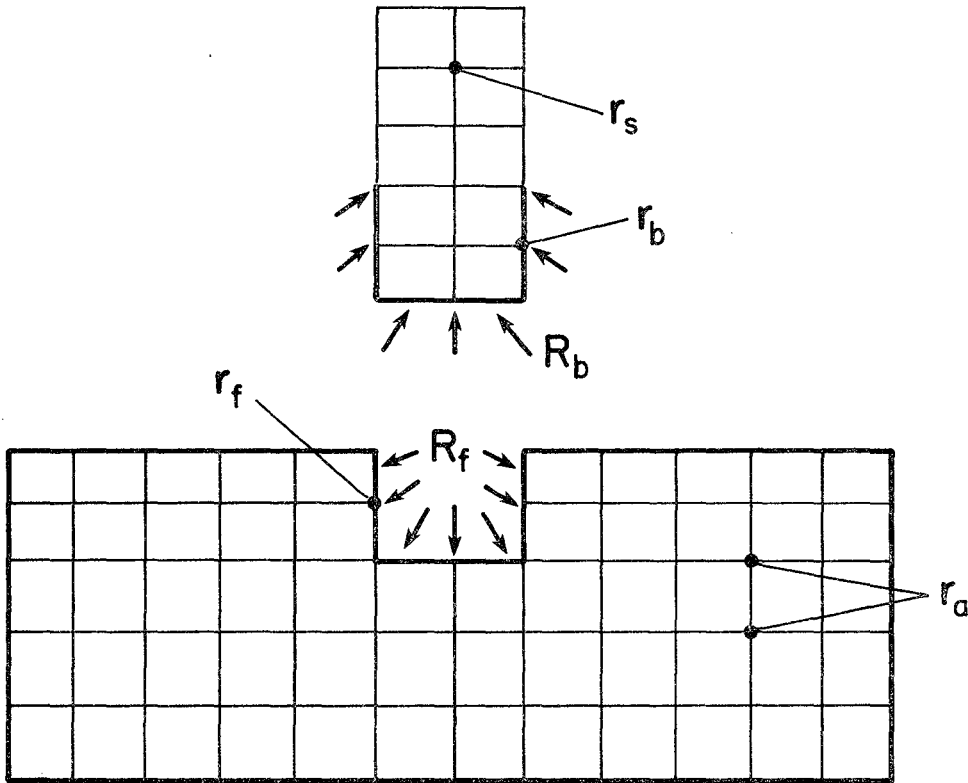


Fig 2.3.- Finite element mesh partition for the boundary methods.

The equations of motion for each of the substructures are:

For the structure:

$$\begin{bmatrix} m_s & 0 \\ 0 & m_b \end{bmatrix} \begin{Bmatrix} \ddot{r}_s^t \\ \ddot{r}_b^t \end{Bmatrix} + \begin{bmatrix} c_{ss} & c_{sb} \\ c_{bs} & c_{bb} \end{bmatrix} \begin{Bmatrix} \dot{r}_s^t \\ \dot{r}_b^t \end{Bmatrix} + \begin{bmatrix} k_{ss} & k_{sb} \\ k_{bs} & k_{bb} \end{bmatrix} \begin{Bmatrix} r_s^t \\ r_b^t \end{Bmatrix} = \begin{Bmatrix} 0 \\ R_b \end{Bmatrix} \quad (2.9)$$

where R_b is the interaction forces between the soil and the structure that would not exist if the influence of the structure upon the soil were negligible. Note that the stiffness matrix is singular, that is the structure is vibrating as the 2 degree of freedom model studied above with the addition of the interaction forces, as shown in Figure 2.2.

For the soil:

$$\begin{bmatrix} m_f & 0 \\ 0 & m_a \end{bmatrix} \begin{Bmatrix} \ddot{r}_f^t \\ \ddot{r}_a^t \end{Bmatrix} + \begin{bmatrix} c_{ff} & c_{fa} \\ c_{af} & c_{aa} \end{bmatrix} \begin{Bmatrix} \dot{r}_f^t \\ \dot{r}_a^t \end{Bmatrix} + \begin{bmatrix} k_{ff} & k_{fa} \\ k_{af} & k_{aa} \end{bmatrix} \begin{Bmatrix} r_f^t \\ r_a^t \end{Bmatrix} = \begin{Bmatrix} -R_b \\ 0 \end{Bmatrix} \quad (2.10)$$

The free field equations for the soil part are (scattering problem):

$$\begin{bmatrix} m_f & 0 \\ 0 & m_a \end{bmatrix} \begin{Bmatrix} \ddot{r}_f^o \\ \ddot{r}_a^o \end{Bmatrix} + \begin{bmatrix} c_{ff} & c_{fa} \\ c_{af} & c_{aa} \end{bmatrix} \begin{Bmatrix} \dot{r}_f^o \\ \dot{r}_a^o \end{Bmatrix} + \begin{bmatrix} k_{ff} & k_{fa} \\ k_{af} & k_{aa} \end{bmatrix} \begin{Bmatrix} r_f^o \\ r_a^o \end{Bmatrix} = \begin{Bmatrix} 0 \\ 0 \end{Bmatrix} \quad (2.11)$$

if we define the interaction displacements as:

$$\begin{aligned} r_f &= r_f^t - r_f^o \\ r_a &= r_a^t - r_a^o \end{aligned}$$

and subtract (2.11) from (2.10) we obtain:

$$\begin{bmatrix} m_f & 0 \\ 0 & m_a \end{bmatrix} \begin{Bmatrix} \ddot{r}_f \\ \ddot{r}_a \end{Bmatrix} + \begin{bmatrix} c_{ff} & c_{fa} \\ c_{af} & c_{aa} \end{bmatrix} \begin{Bmatrix} \dot{r}_f \\ \dot{r}_a \end{Bmatrix} + \begin{bmatrix} k_{ff} & k_{fa} \\ k_{af} & k_{aa} \end{bmatrix} \begin{Bmatrix} r_f \\ r_a \end{Bmatrix} = \begin{Bmatrix} -R_b \\ 0 \end{Bmatrix} \quad (2.12)$$

It should be noted that up to this point everything has been done in the time domain. The continuation of the substructure method in the time domain is possible by using influence coefficients that lead to a system of Volterra integro differential equations, but this poses a complicated and certainly inefficient technique of analysis. The frequency domain offers a much easier solution, as it will be seen in what follows.

Equation (2.12) may be written in the frequency domain as :

$$\left[-\bar{\omega}^2 \begin{bmatrix} m_f & 0 \\ 0 & m_a \end{bmatrix} + i\bar{\omega} \begin{bmatrix} c_{ff} & c_{fa} \\ c_{af} & c_{aa} \end{bmatrix} + \begin{bmatrix} k_{ff} & k_{fa} \\ k_{af} & k_{aa} \end{bmatrix} \right] \begin{Bmatrix} \hat{r}_f \\ \hat{r}_a \end{Bmatrix} = \begin{Bmatrix} -\hat{R}_b \\ 0 \end{Bmatrix} \quad (2.13)$$

where the symbol $\hat{}$ stands for the Fourier transform. The vibration of the soil due to forces $-\hat{R}_b(\omega)e^{i\omega t}$ applied at the soil-structure interface and without the excitation at the lower boundary is also governed by Equation (2.13). This constitutes the impedance problem. Equation (2.13) may be condensed for each frequency ω to the F degrees of freedom to obtain:

$$S_f(\omega) \hat{r}_f(\omega) = \hat{R}_f(\omega) \quad (2.14)$$

Compatibility between soil and structure leads for each frequency to:

$$\hat{r}_f^t = \hat{r}_b^t \quad (2.15)$$

The substitution of (2.15) and (2.14) in (2.9) yields:

$$\left[-\bar{\omega}^2 \begin{bmatrix} m_s & 0 \\ 0 & m_b \end{bmatrix} + i\bar{\omega} \begin{bmatrix} c_{ss} & c_{sb} \\ c_{bs} & c_{bb} \end{bmatrix} + \begin{bmatrix} k_{ss} & k_{sb} \\ k_{bs} & k_{bb} \end{bmatrix} \right] \begin{Bmatrix} \hat{r}_s^t \\ \hat{r}_b^t \end{Bmatrix} = \begin{Bmatrix} 0 \\ -S_f(\bar{\omega}) \hat{r}_b \end{Bmatrix} \quad (2.16)$$

now

$$\hat{r}_b = \hat{r}_b^t - \hat{r}_b^o = \hat{r}_b^t - \hat{r}_f^o$$

and (2.16) becomes:

$$\left[-\bar{\omega}^2 \begin{bmatrix} m_s & 0 \\ 0 & m_b \end{bmatrix} + i\bar{\omega} \begin{bmatrix} c_{ss} & c_{sb} \\ c_{bs} & c_{bb} \end{bmatrix} + \begin{bmatrix} k_{ss} & k_{sb} \\ k_{bs} & k_{bb} + S_f \end{bmatrix} \right] \begin{Bmatrix} \hat{r}_s^t \\ \hat{r}_b^t \end{Bmatrix} = \begin{Bmatrix} 0 \\ S_f(\bar{\omega}) \hat{r}_f^o \end{Bmatrix} \quad (2.17)$$

Equation (2.17) governs the motion of the structure in total coordinates with interaction effects due to any prescribed free field motions at the soil-structure interface. At this stage it is worth pausing to make some observations:

1) For surface structures and certain soil conditions (half space or single layer) analytical solutions for $S_f(\omega)$ are available, thus saving the effort of the impedance problem. The frequency dependency of $S_f(\omega)$ can be eliminated approximately by introducing the static values of S_f plus a virtual mass of the soil associated with the structure.

Several authors, Tsai, Niehof, Swatta, and Hadjian (1974) have demonstrated that the use of frequency independent impedance coefficients S_f , defined at $\omega=0$, leads to excellent results. The use of coefficients defined at the fundamental frequency of the system will lead to more accurate solutions than those obtained with the static values.

2) If the structure is embedded the free field motions r_f at the interface do not coincide with those at the surface, even in the case when the boundary is rigid. Since r_f are unknown, a scattering problem must be solved first. This consists of solving the free field problem with the shape of the embedded structure in it, as shown in the Figure (2.2), but without the interactions forces, so as to obtain the free field motions at the interface. Due to the lack of closed form solutions, this problem can only be solved at the present moment by finite element techniques.

Formulation in relative displacements.

First Case: Free field motions are identical at all nodal points.

In this case the structure behaves as if it were subjected to a single support excitation $r_b^0 = v_g$, where v_g is the ground motion at the interface level, and r_b^0 is defined in (2.17). The total displacements may be divided into the dynamic plus the pseudostatic components, as done with the 2 degree of freedom system in the previous section.

$$\begin{Bmatrix} r_s^t \\ r_b^t \end{Bmatrix} = \begin{Bmatrix} r_s \\ r_b \end{Bmatrix} + \begin{Bmatrix} r_s^q \\ r_b^0 \end{Bmatrix} \quad (2.18)$$

where r_s and r_b are the dynamic components, and r_s^q and r_b^0 are the free field and the quasi-static components respectively. Substituting (2.18) in (2.17):

$$[-\bar{\omega}^2 \underline{M} + i\bar{\omega} \underline{C} + \underline{K}] \begin{Bmatrix} \hat{r}_s \\ \hat{r}_b \end{Bmatrix} = \begin{Bmatrix} 0 \\ S_f \hat{r}_b^0 \end{Bmatrix} - [-\bar{\omega}^2 \underline{M} + i\bar{\omega} \underline{C} + \underline{K}] \begin{Bmatrix} \hat{r}_s^q \\ \hat{r}_b^0 \end{Bmatrix} \quad (2.19)$$

\underline{M} , \underline{C} and \underline{K} are defined in (2.17). The S_f terms vanish in the R.H.S, yielding:

$$\begin{bmatrix} -\bar{\omega}^2 \begin{bmatrix} m_s & 0 \\ 0 & m_b \end{bmatrix} + i\bar{\omega} \begin{bmatrix} c_{ss} & c_{sb} \\ c_{bs} & c_{bb} \end{bmatrix} + \begin{bmatrix} k_{ss} & k_{sb} \\ k_{bs} & k_{bb} \end{bmatrix} \end{bmatrix} \begin{Bmatrix} \hat{r}_s^q \\ \hat{r}_b^0 \end{Bmatrix}$$

The quasi-static displacements can be defined in terms of the free field ones

$$\begin{Bmatrix} \hat{r}_s^q \\ \hat{r}_b^o \end{Bmatrix} = \underline{r} \hat{v}_g$$

\underline{r} is a matrix containing zeros and ones, because the quasi-static displacements are rigid body motions. Since \underline{K} is singular $\underline{K}\underline{r} = \underline{0}$, thus if the damping terms are neglected (2.19) becomes:

$$\left[-\bar{\omega}^2 \underline{M} + i\bar{\omega} \underline{C} + \underline{K} \right] \begin{Bmatrix} \hat{r}_s \\ \hat{r}_b \end{Bmatrix} = -\bar{\omega}^2 \underline{M} \underline{r} \hat{v}_g(\bar{\omega})$$

or

$$\left[-\bar{\omega}^2 \begin{bmatrix} m_s & 0 \\ 0 & m_b \end{bmatrix} + i\bar{\omega} \begin{bmatrix} c_{ss} & c_{sb} \\ c_{bs} & c_{bb} \end{bmatrix} + \begin{bmatrix} k_{ss} & k_{sb} \\ k_{bs} & k_{bb} \end{bmatrix} \right] \begin{Bmatrix} \hat{r}_s \\ \hat{r}_b \end{Bmatrix} = - \begin{bmatrix} m_s & 0 \\ 0 & m_b \end{bmatrix} \underline{r} \hat{v}_g(\bar{\omega}) \quad (2.20)$$

Equation (2.20) expresses the dynamic equilibrium of the structure as a function of the ground accelerations, considering that these are all the same at the soil structure interface, and in terms of the relative displacements.

Second case: The free-field motion is different at each point of contact between soil and structure.

The structure is subjected now to a multiple support excitation. Again the total displacements can be decomposed into the dynamic and pseudostatic components:

$$\begin{Bmatrix} \hat{r}_s^t \\ \hat{r}_b^t \end{Bmatrix} = \begin{Bmatrix} \hat{r}_s \\ \hat{r}_b \end{Bmatrix} + \begin{Bmatrix} \hat{r}_s^q \\ \hat{r}_b^o \end{Bmatrix}$$

where the first term in the R.H.S. represents the dynamic components and the second the free-field and quasi-static components. The latter ones are the displacements produced in the structure due to unit displacements at the base.

$$\begin{bmatrix} k_{ss} & k_{sb} \\ k_{bs} & k_{bb} \end{bmatrix} \begin{Bmatrix} \hat{r}_s^q \\ \hat{r}_b^o \end{Bmatrix} = \begin{Bmatrix} 0 \\ \hat{R}_b \end{Bmatrix}$$

Thus,

$$k_{ss} \hat{r}_s^q + k_{sb} \hat{r}_b^o = 0$$

or

$$\hat{r}_s^q = -k_{ss}^{-1} k_{sb} \hat{r}_b^o = L \hat{r}_b^o$$

where

$$L = -k_{ss}^{-1} k_{sb}$$

therefore

$$\begin{Bmatrix} r_s^t \\ r_b^t \end{Bmatrix} = \begin{Bmatrix} \hat{r}_s \\ \hat{r}_b \end{Bmatrix} + \begin{Bmatrix} L \hat{r}_b^o \\ \hat{r}_b^o \end{Bmatrix} \quad (2.21)$$

Now substituting (2.21) in (2.17) yields :

$$\left[-\bar{\omega}^2 \underline{M} + i\bar{\omega} \underline{C} + \underline{K} \right] \begin{Bmatrix} \hat{r}_s \\ \hat{r}_b \end{Bmatrix} = \begin{Bmatrix} 0 \\ S_f \hat{r}_b^o \end{Bmatrix} - \left[-\bar{\omega}^2 \underline{M} + i\bar{\omega} \underline{C} + \underline{K} \right] \begin{Bmatrix} L \hat{r}_b^o \\ \hat{r}_b^o \end{Bmatrix}$$

The S_f term vanishes in the R.H.S., and after some manipulation it becomes:

$$\begin{aligned} \left[-\bar{\omega}^2 \begin{bmatrix} m_s & 0 \\ 0 & m_b \end{bmatrix} + i\bar{\omega} \begin{bmatrix} c_{ss} & c_{sb} \\ c_{bs} & c_{bb} \end{bmatrix} + \begin{bmatrix} k_{ss} & k_{sb} \\ k_{bs} & k_{bb} \end{bmatrix} \right] \begin{Bmatrix} \hat{r}_s \\ \hat{r}_b \end{Bmatrix} = \\ - \begin{Bmatrix} m_s & L \hat{V}_g \\ m_b & \hat{V}_g \end{Bmatrix} + \frac{i}{\bar{\omega}} \underline{C} \begin{Bmatrix} L \hat{V}_g \\ \hat{V}_g \end{Bmatrix} + \frac{1}{\bar{\omega}^2} \begin{Bmatrix} 0 \\ k^* \hat{V}_g \end{Bmatrix} \quad (2.22) \end{aligned}$$

Where

$$k^* = k_{bb} - k_{bs} k_{ss}^{-1} k_{sb}$$

This is the most general Equation of the boundary methods. Note that if there is no soil-structure interaction the term r_b vanishes and Equation (2.22) represents a standard multiple support excitation problem.

2.4.2.- VOLUME METHODS. (Lysmer 1981)

The volume methods avoid the scattering problem present in the boundary methods. They basically consider the interaction effects between soil and structure not only at the interface nodes but in all the buried degrees of freedom (see Figure (2.4)). The trick necessary to accomplish this is to reduce the mass, stiffness, and damping of the embedded structure by the corresponding properties of the excavated soil.

Formulation in total displacements:

As in the boundary methods, the structure and the soil are considered separately. The same notation is used in this case.

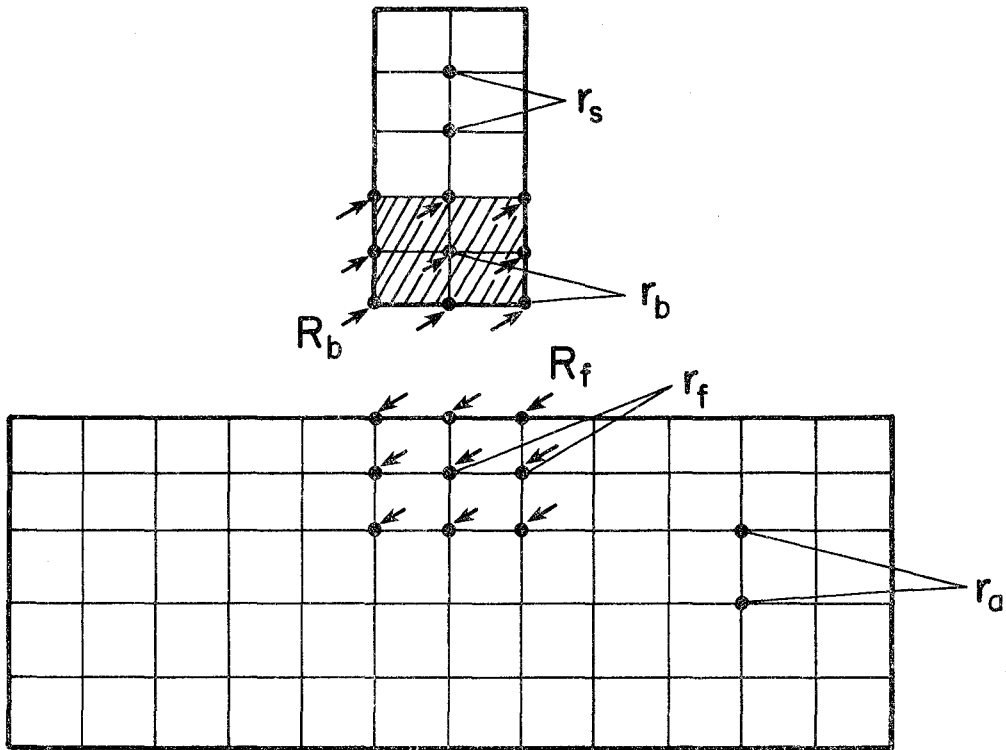


Fig 2.4.- Finite element mesh partition for the volume methods.

Structure:

$$\begin{bmatrix} m_s & 0 \\ 0 & m_b + m_f \end{bmatrix} \begin{Bmatrix} \ddot{r}_s^t \\ \ddot{r}_b^t \end{Bmatrix} + \begin{bmatrix} c_{ss} & c_{sb} \\ c_{bs} & c_{bb} \end{bmatrix} \begin{Bmatrix} \dot{r}_s^t \\ \dot{r}_b^t \end{Bmatrix} + \begin{bmatrix} k_{ss} & k_{sb} \\ k_{bs} & k_{bb} \end{bmatrix} \begin{Bmatrix} r_s^t \\ r_b^t \end{Bmatrix} = \begin{Bmatrix} 0 \\ R_b \end{Bmatrix} \quad (2.23)$$

The interaction forces are now acting in all the buried degrees of freedom.

Soil:

$$\begin{bmatrix} m_f & 0 \\ 0 & m_a \end{bmatrix} \begin{Bmatrix} \ddot{r}_f^t \\ \ddot{r}_a^t \end{Bmatrix} + \begin{bmatrix} c_{ff} & c_{fa} \\ c_{af} & c_{aa} \end{bmatrix} \begin{Bmatrix} \dot{r}_f^t \\ \dot{r}_a^t \end{Bmatrix} + \begin{bmatrix} k_{ff} & k_{fa} \\ k_{af} & k_{aa} \end{bmatrix} \begin{Bmatrix} r_f^t \\ r_a^t \end{Bmatrix} = \begin{Bmatrix} R_b^f \\ 0 \end{Bmatrix} \quad (2.24)$$

It is clear that if we sum up (2.23) and (2.24) we will obtain the Equations of the assembly as in the case of the boundary methods. The free field Equations now refer to the whole soil system without the excavated part; thus a scattering problem need not be solved.

$$\begin{bmatrix} m_f & 0 \\ 0 & m_a \end{bmatrix} \begin{Bmatrix} \ddot{r}_f^o \\ \ddot{r}_a^o \end{Bmatrix} + \begin{bmatrix} c_{ff} & c_{fa} \\ c_{af} & c_{aa} \end{bmatrix} \begin{Bmatrix} \dot{r}_f^o \\ \dot{r}_a^o \end{Bmatrix} + \begin{bmatrix} k_{ff} & k_{fa} \\ k_{af} & k_{aa} \end{bmatrix} \begin{Bmatrix} r_f^o \\ r_a^o \end{Bmatrix} = \begin{Bmatrix} 0 \\ 0 \end{Bmatrix} \quad (2.25)$$

Subtracting (2.25) from (2.24) yields

$$\begin{bmatrix} m_f & 0 \\ 0 & m_a \end{bmatrix} \begin{Bmatrix} \ddot{r}_f^t \\ \ddot{r}_a^t \end{Bmatrix} + \begin{bmatrix} c_{ff} & c_{fa} \\ c_{af} & c_{aa} \end{bmatrix} \begin{Bmatrix} \dot{r}_f^t \\ \dot{r}_a^t \end{Bmatrix} + \begin{bmatrix} k_{ff} & k_{fa} \\ k_{af} & k_{aa} \end{bmatrix} \begin{Bmatrix} r_f^t \\ r_a^t \end{Bmatrix} = \begin{Bmatrix} -R_b \\ 0 \end{Bmatrix} \quad (2.26)$$

where $r_f^t = r_f^t - r_f^o$ and $r_a^t = r_a^t - r_a^o$;

Equation (2.26) defines the impedance problem, which will have more unknowns than the corresponding impedance problem in the boundary method. Thus at the cost of having to solve an impedance problem with more unknowns, the volume methods eliminate the need to solve the scattering problem. Transferring to the frequency domain, defining the impedance relation as $S_f(\omega)r_b(\omega) = R_f(\omega)$, and following the same procedure as in the boundary methods, Equation (2.23) becomes:

$$\begin{bmatrix} -\bar{\omega}^2 \begin{bmatrix} m_s & 0 \\ 0 & m_b + m_f \end{bmatrix} + i\bar{\omega} \begin{bmatrix} c_{ss} & c_{sb} \\ c_{bs} & c_{bb} \end{bmatrix} + \begin{bmatrix} k_{ss} & k_{sb} \\ k_{bs} & k_{bb} + S_f - k_{ff} \end{bmatrix} \end{bmatrix} \begin{Bmatrix} \hat{r}_s^t \\ \hat{r}_b^t \end{Bmatrix} = \begin{Bmatrix} 0 \\ S_f(\bar{\omega}) \hat{r}_f^o \end{Bmatrix} \quad (2.27)$$

Equation (2.27) defines the motion of the structure in terms of the total displacements and as a function of the free-field ground motion at the buried degrees of freedom. The free field motion may be obtained from a site response analysis. Assuming one dimensional vertical propagation of P and S waves, Schnabel

(1972), the problem becomes very simple. More complicated wave patterns, like inclined P and S waves and surface waves, can be considered also, Gomez-Masso (1979), Chen (1981), and Wolf (1982).

Formulation in Relative Displacements:

Since the free-field motion is different at each point of the buried degrees of freedom, a multiple support analysis is needed. The formulation is identical to that described for the boundary methods and there is no need to proceed in much detail.

Again

$$\begin{Bmatrix} \hat{r}_s^t \\ \hat{r}_b^t \end{Bmatrix} = \begin{Bmatrix} \hat{r}_s \\ \hat{r}_b \end{Bmatrix} + \begin{Bmatrix} \hat{r}_s^g \\ \hat{r}_b^g \end{Bmatrix}$$

are obtained from static condensation as:

$$\hat{r}_s^g = L \hat{r}_b^g$$

where

$$L = -k_{ss}^{-1} k_{sb}$$

Substituting in (2.27):

$$[-\bar{\omega}^2 M + i\bar{\omega} C + K] \begin{Bmatrix} \hat{r}_s \\ \hat{r}_b \end{Bmatrix} = \begin{Bmatrix} 0 \\ S_f \hat{r}_b^g \end{Bmatrix} - [-\bar{\omega}^2 \bar{M} + i\bar{\omega} \bar{C} + \bar{K}] \begin{Bmatrix} L \hat{r}_b^g \\ \hat{r}_b^g \end{Bmatrix}$$

Since

$$\bar{K} = \begin{bmatrix} k_{ss} & k_{sb} \\ k_{bs} & k_{bb} + S_f - k_{ff} \end{bmatrix}$$

the S_f term vanishes on the R.H.S. Thus:

$$\begin{aligned} & [-\bar{\omega}^2 \begin{bmatrix} m_s & 0 \\ 0 & m_b - m_f \end{bmatrix} + i\bar{\omega} \begin{bmatrix} c_{ss} & c_{sb} \\ c_{bs} & c_{bb} - c_f \end{bmatrix} + \begin{bmatrix} k_{ss} & k_{sb} \\ k_{bs} & k_{bb} + S_f - k_{ff} \end{bmatrix}] \begin{Bmatrix} \hat{r}_s \\ \hat{r}_b \end{Bmatrix} = \\ & = - \begin{Bmatrix} m_s L \hat{v}_g \\ m_b \hat{v}_g \end{Bmatrix} + \frac{i}{\bar{\omega}} \bar{C} \begin{Bmatrix} L \hat{v}_g \\ \hat{v}_g \end{Bmatrix} + \frac{1}{\bar{\omega}^2} \begin{Bmatrix} 0 \\ k^* \hat{v}_g \end{Bmatrix} \end{aligned} \quad (2.28)$$

where

$$k^* = k_{bb} - k_{bs} k_{ss}^{-1} k_{sb} - k_{ff}$$

Equation (2.28) constitutes the most general Equation for the structural displacements in terms of the free-field motions at the buried structural degrees of freedom.

2.4.3.- IMPEDANCE PROBLEM:

In order to obtain the frequency dependent impedance matrix S_f , Equation (2.13) has to be solved as many times as the number of frequencies in the frequency range of interest. Equation (2.13) can be written as:

$$\begin{bmatrix} G_{ff} & G_{fa} \\ G_{of} & G_{aa} \end{bmatrix} \begin{Bmatrix} \hat{r}_f(\omega) \\ \hat{r}_a \end{Bmatrix} = \begin{Bmatrix} \hat{R}_f \\ 0 \end{Bmatrix} \quad (2.29)$$

where

$$G_{ff} = -\bar{\omega}^2 m_{ff} + i\bar{\omega} c_{ff} + k_{ff}$$

$$G_{fa} = i\bar{\omega} c_{fa} + k_{fa}$$

$$G_{aa} = -\bar{\omega}^2 m_{aa} + i\bar{\omega} c_{aa} + k_{aa}$$

Two methods are commonly used to determine the impedance matrix S_f :

a) Static condensation may be applied to the r_f degrees of freedom:

$$(G_{ff} - G_{fa}^T G_{aa}^{-1} G_{of}) \hat{r}_f = \hat{R}_f$$

and

$$S_f(\bar{\omega}) = G_{ff} - G_{fa}^T G_{aa}^{-1} G_{of} \quad (2.30)$$

Because G_{aa} and G_{ff} are usually very large matrices, this method requires excessive computational effort.

b) An alternative procedure is to first calculate the dynamic flexibility matrix for the foundation. This involves the direct solution of Equation (2.13) for unit harmonic loads applied at the boundary interface to obtain the displacements at the correspondent degrees of freedom. The impedance matrix is the inverse of the dynamic flexibility matrix:

$$S_f(\bar{\omega}) = F^{-1}(\bar{\omega})$$

It is worth noticing that all the operations have to be repeated for each frequency. However since the impedance matrix S_f typically varies slowly with frequency, a common simplification is to analyze the soil region at a relatively coarse frequency interval and then calculate S_f at intermediate frequencies by interpolation. Another important point to consider is the fact that frequency dependent radiation boundaries may be used at this stage to reduce the size of the finite element mesh.

No attempt has yet been made to reduce the size of the system of Equations (2.13) by the use of Ritz functions. As shown in more detail later in this thesis, the use of a total number of Ritz functions equal to 10% of the total number of degrees of freedom of the impedance problem leads to results within 96% accuracy. The main consequence of this is that typical wave propagation problems can be analyzed very accurately using Ritz functions.

Another important aspect to take into consideration is that the impedance problem has been solved analytically for cases of surface structures under certain conditions regarding the number of soil layers and the rigidity of the foundation. This eliminates the need to solve Equation (2.13) with finite elements, and the impedance coefficients can be directly assembled in the stiffness matrix of the structural system. This type of solution constitutes the basis of the so-called "continuum methods", that may be considered as a particular case of the substructure methods.

Analytical solutions to the impedance problem are provided in the literature. Lysmer and Richart (1966), Luco and Westman (1971), Veletsos and Wei (1971) obtained the impedance functions for the case of rigid massless circular plates resting on homogeneous isotropic elastic half-space. Arnold (1955), Bycroft (1956), Warbuton (1957), Kashio (1970), Wei (1971) and Luco (1974) have provided solutions for a layered elastic half-space. Solutions for a viscoelastic half-space are given by Veletsos, Verbic and Nair (1973) and (1974) and Chopra (1975), and for viscoelastic layered systems by Luco (1976). Impedance functions for rigid strip footings have been obtained by Oien (1971) and Luco (1972). Luco (1977) and Savidis (1977) have obtained the response of rectangular footings to horizontally propagating waves in a half-space. Flexible rectangular footings on a half-space have been studied by Iguchi (1981), and rigid foundations of arbitrary shapes in a half-space by Rucker (1982) and Wang (1976)

In all the cases the solutions are obtained for surface structures, or at the most for one layer. Studies of the effect of foundation embedment on the response have been rather limited and only a very small number of continuum solutions, all for very special cases, are now available.

In summary then, for the impedance problem of surface structures a limited number of closed form solutions are available, for embedded structures however, the only general approach to the impedance problem, now available is to solve Equation (2.13) by the finite element method as explained at the beginning of this section.

2.5.- HYBRID METHODS: (Gupta, Lin, Penzien and Chen (1980))

Except for the cases for which a continuum solution is available, the solution for the impedance functions poses the major computational problem in the substructure approach. Since continuum solutions are only available for surface structures, whenever any structural embedment is present a three dimensional finite element model will have to be analyzed (Equation 2.13) for a wide range of frequencies of excitation. Since a three dimensional analysis is still very impractical, due to the tremendous amount of degrees of freedom involved, two dimensional approximations are made under the assumption of plane strain conditions, which are not always satisfactory, Lysmer and Seed (1977) and Idriss and Kennedy (1979).

In order to avoid the impedance problem for the case of buried structures, Gupta, Lin, Penzien and Yen (1980) developed a hybrid method which basically consists of partitioning the soil into a near field and a far field. The far field is modeled in the form of an impedance matrix. In other words, the substructure concepts are extended in such a way that the superstructure contains not only the building but the near field part of the soil as well. (See Figure (2.5)) Equation (2.17) holds in this case:

$$\begin{bmatrix} -\bar{\omega}^2 \begin{bmatrix} m_s & 0 \\ 0 & m_b \end{bmatrix} + i\bar{\omega} \begin{bmatrix} c_{ss} & c_{sb} \\ c_{bs} & c_{bb} \end{bmatrix} + \begin{bmatrix} k_{ss} & k_{sb} \\ k_{bs} & k_{bb} \end{bmatrix} \end{bmatrix} \begin{Bmatrix} \hat{r}_s^t \\ \hat{r}_b^t \end{Bmatrix} = \begin{Bmatrix} 0 \\ S_f(\bar{\omega}) \hat{r}_b^o \end{Bmatrix}$$

r_s^t represents the total displacements of the structure in the near field, and r_b^o represents those at the boundary of the model, which include the far field coefficients.

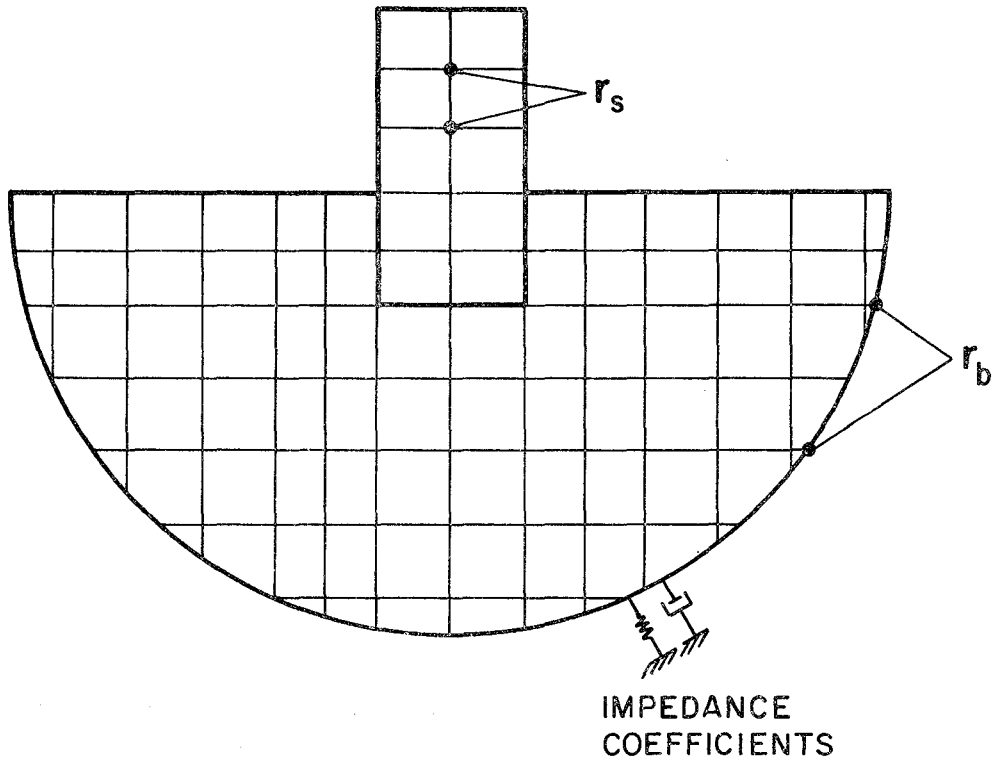


Fig 2.5.- Finite element layout for the hybrid methods.

The only problem remaining is to define the far field coefficients. Analytical solutions are only available for torsional excitation with a spherical boundary (Luco 1976). Gupta and Penzien solve the problem by system identification techniques, by insuring that the resulting hybrid model reproduces the known compliances of a rigid circular plate on an elastic half-space. Once the impedance coefficients are obtained they are assembled to the stiffness matrix and the Equations of motion can be solved in terms of the total displacements (Equation 2.17), or the relative ones (Equation 2.20).

A limitation of this method is that a scattering problem, involving the half-space in the absence of the near field, needs to be solved to define the input motions at the interface. Gupta and Penzien neglect this effect and assume that the input motion is uniform along the boundary and equal to the free-field motion. This assumption is generally not appropriate since large variations in the free-field motions are expected to occur along the boundary.

Tsong (1981) extended this method to the case of two dimensional problems. Again a method of system identification is used to determine the two dimensional far field frequency dependent impedance functions.

2.6.- SUMMARY OF FREQUENCY DOMAIN METHODS:

As has been shown above, the frequency domain methods can be classified into three major groups: complete, substructure, and hybrid methods. The substructure methods may be subdivided into continuum, boundary and volume methods. Figure (2.6) summarizes the steps involved in each one of them. The complete methods only require a site response analysis (deconvolution) to define the motions at the bedrock. These are introduced as input in the complete structure and soil analysis. The continuum approach avoids the site response and scattering problems. The impedance functions are obtained analytically and the input motion for the last stage is directly the surface ground motion. The boundary and volume methods are similar. The main advantage of the flexible volume methods is to eliminate the scattering problem, which requires a complete finite element solution, by paying a higher price in the impedance problem. A dramatic reduction in the size of the model can be obtained with frequency dependent radiation boundaries. In the hybrid methods the

finite element solution of the impedance problem is avoided by using system identification techniques.

The free field solution (site response problem) is usually obtained assuming one dimensional vertical propagation of elastic waves. Chen (1981) and Lysmer (1980) have studied the free field problem including inclined body waves and horizontal (Rayleigh, Love) waves. They have demonstrated that, for both soil sites and rock sites, the major part of the response is due to vertically propagated P and S waves. An exception is the case of buried structures, such as pipelines and tunnels, for which an analysis assuming horizontally propagating waves is needed.

In the case of axisymmetry of material properties and geometry, the number of degrees of freedom of the three dimensional problem may be reduced by using axisymmetric elements, and by expanding the load and displacements in terms of Fourier Series.

METHOD	COMPLETE	CONTINUUM	BOUNDARY	VOLUME	HYBRID
SITE RESPONSE PROBLEM ↑ EARTHQUAKE		NONE			
SCATTERING PROBLEM	NONE	NONE		NONE	
IMPEDANCE PROBLEM • LOADED NODE	NONE				SYSTEM IDENTIFICATION
SCATTERING ANALYSIS • INPUT MOTION					

Fig 2.6.- Summary of the frequency domain methods.

CHAPTER 3

ANALYTICAL METHODS IN THE TIME DOMAIN

3.1.- INTRODUCTION.

Chapter 2 has outlined the formulation of the common methods in the frequency domain. As pointed out at the beginning, the reasons for the popularity of the frequency domain approach are, firstly, the possibility of dividing the problem into substructures that can be analyzed independently, and secondly, the frequency radiation boundaries that help to reduce considerably the size of the finite element models. As a consequence very little attention has been given to the time domain approach. In fact there is only one formal method, the one presented in Dynamic of Structures, Clough and Penzien (1975), for the solution of the problem in this domain.

The following discussion will describe the current analytical methods and their complete formulations for the soil-structure interaction problem in the time domain, and then will extend them to eliminate the scattering problem (volume methods). These approaches constitute the basis for the formulation of the scattering and nonlinear problems that will be discussed in Chapter 6. The methods in the time domain can be divided into three main groups:

- 1) Complete methods.
- 2) Boundary methods.
- 3) Volume methods.

The complete methods are formulated as was done for the frequency domain. By virtue of the principle of superposition the total displacements may be divided, as explained below, into the free field displacements and the interaction displacements. By doing so the input motion may now be established, not at the bottom boundary, but at either the interface between soil and structure (boundary methods), or at the

buried part of the structure (volume methods). These formulations simplify the problem and make the use of frequency independent boundaries more feasible, since the source of excitation is not close to the boundary as in the complete method but far away from it. The volume methods have never been proposed before in the time domain, and have, as shown later, a major advantage over the boundary methods by eliminating the scattering problem.

A drastic reduction of the size of the problem can be achieved by using Ritz functions, and by dynamic substructuring. These methods will be discussed later in this work.

It should be noted that the substructure concept used in the frequency domain is not similar to that of the time domain. The splitting of the model, as done in the frequency domain, is very cumbersome in the time domain due to the need of using Volterra integro-differential equations. In order to avoid this problem the equations of motion of the soil-structure ensemble have to be solved simultaneously. Therefore when we refer to substructuring concepts in the time domain we refer to the reduction in the number of degrees of freedom in certain parts of the system, structure and soil, that subsequently, are assembled and solved simultaneously.

3.2.- COMPLETE METHODS.

There is no difference in formulation of the complete methods between the time and frequency domains. The only difference is in the numerical technique used for the solution of the set of equations. In one case transformation to the frequency domain is done by means of the Fast Fourier Transform, and in the other case a direct implicit or explicit integration is done with a time step scheme.

Because of obvious limitations, the use of frequency dependent transmitting boundaries is not possible in this case, and in general large models will have to be used to avoid spurious results coming from the reflections and refractions of elastic waves in the boundary of the finite element model. Currently a three dimensional analysis of a soil-structure interaction problem by a complete method is prohibitive due to the large amount of computer time and storage that is needed.

3.3.- BOUNDARY METHODS.

The complete problem may be divided, as shown in Figure (3.1), into a free field problem without the excavated part of the soil (scattering problem), and a source problem in which the input is defined only at the interface boundary between the soil and the structure.

The notation corresponding to each part of the problem is as follows: \mathbf{v} represents the motions at the structure, \mathbf{v}_g represent those at the soil-structure interface and \mathbf{v}_a the soil displacements. Furthermore

$\tilde{\mathbf{m}}_c, \tilde{\mathbf{c}}_c, \tilde{\mathbf{k}}_c$ are the properties of the system in free field motion, meaning without the structure,

$\tilde{\mathbf{v}}_c, \tilde{\mathbf{v}}_g, \tilde{\mathbf{v}}_a$ are the free field motions,

$\mathbf{m}_c, \mathbf{c}_c, \mathbf{k}_c$ are the properties of the added system (building) and

$\mathbf{v}_c^t, \mathbf{v}_g^t, \mathbf{v}_a^t$ are the added or interaction motions resulting from locating the building in the site.

The partitions of the displacements are:

$$\mathbf{v}_c^t = \begin{Bmatrix} \mathbf{v}^t \\ \mathbf{v}_g^t \\ \mathbf{v}_a^t \end{Bmatrix} \quad \text{and} \quad \tilde{\mathbf{v}}_c = \begin{Bmatrix} \mathbf{0} \\ \tilde{\mathbf{v}}_g \\ \tilde{\mathbf{v}}_a \end{Bmatrix} \quad (3.1)$$

and the property matrices:

$$\mathbf{m}_c = \begin{bmatrix} m & m_g & 0 \\ m_g^T & m_{gg} & 0 \\ 0 & 0 & 0 \end{bmatrix} \quad \tilde{\mathbf{m}}_c = \begin{bmatrix} 0 & 0 & 0 \\ 0 & \tilde{m}_{gg} & \tilde{m}_{ga} \\ 0 & \tilde{m}_{ag} & \tilde{m}_{aa} \end{bmatrix} \quad (3.2)$$

and in the same manner for the stiffness and damping matrices.

The free field equations are:

$$\begin{bmatrix} \tilde{\mathbf{m}}_c & \tilde{\mathbf{m}}_b \\ \tilde{\mathbf{m}}_b^T & \tilde{\mathbf{m}}_{bb} \end{bmatrix} \begin{Bmatrix} \tilde{\mathbf{v}}_c \\ \tilde{\mathbf{v}}_b \end{Bmatrix} + \begin{bmatrix} \tilde{\mathbf{c}}_c & \tilde{\mathbf{c}}_b \\ \tilde{\mathbf{c}}_b^T & \tilde{\mathbf{c}}_{bb} \end{bmatrix} \begin{Bmatrix} \tilde{\mathbf{v}}_c \\ \tilde{\mathbf{v}}_b \end{Bmatrix} + \begin{bmatrix} \tilde{\mathbf{k}}_c & \tilde{\mathbf{k}}_b \\ \tilde{\mathbf{k}}_b^T & \tilde{\mathbf{k}}_{bb} \end{bmatrix} \begin{Bmatrix} \tilde{\mathbf{v}}_c \\ \tilde{\mathbf{v}}_b \end{Bmatrix} = \begin{Bmatrix} \mathbf{0} \\ \mathbf{0} \end{Bmatrix} \quad (3.3)$$

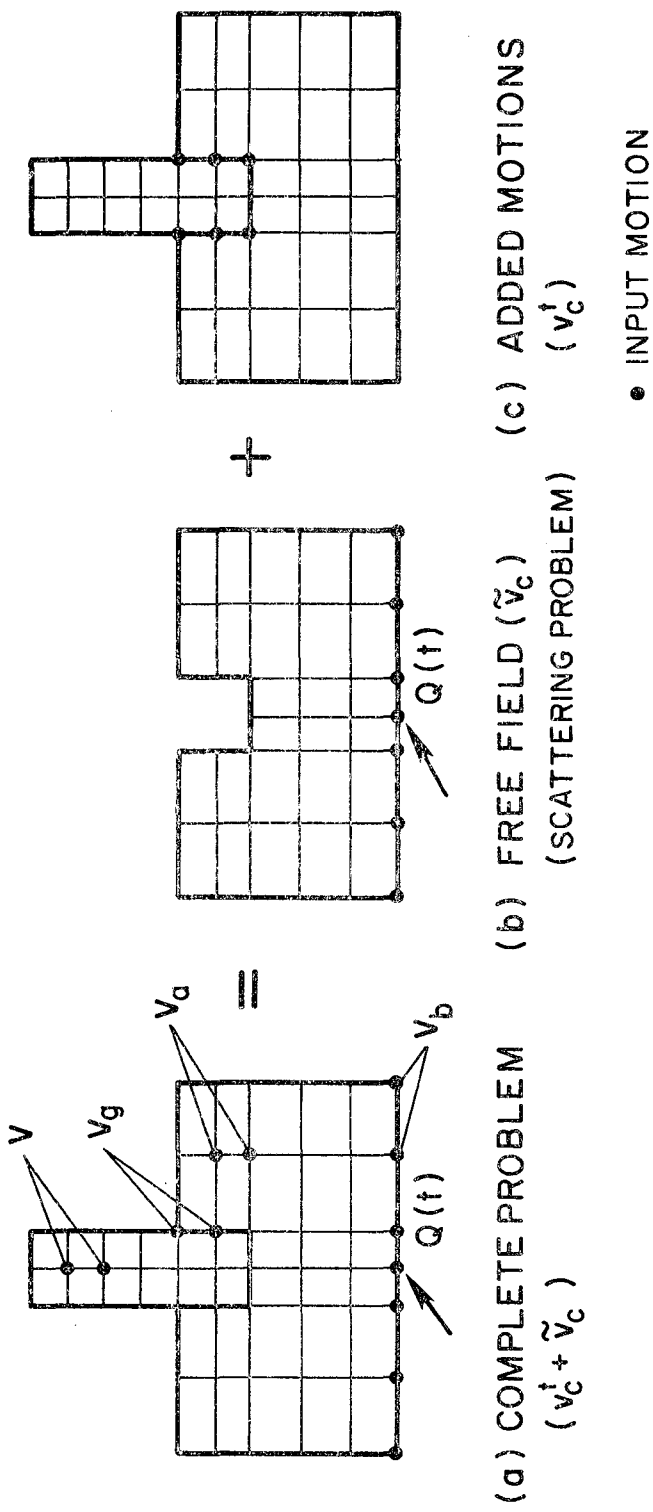


Fig 3.1.- Division of the complete problem into a scattering and an interaction problem.

The first matrix equation leads to:

$$\tilde{m}_c \ddot{\tilde{v}}_c + \tilde{c}_c \dot{\tilde{v}}_c + \tilde{k}_c \tilde{v}_c = -\tilde{m}_b \ddot{\tilde{v}}_b - \tilde{c}_b \dot{\tilde{v}}_b + \tilde{k}_b \tilde{v}_b \quad (3.4)$$

where the R.H.S. represents the input motion at the base of the model. When the building is superimposed on the foundation, the properties and motions on the L.H.S. of Equation (3.4) are modified by the added building and displacements. However, the input motion remains the same. This is due to the fact that far from the structure the input is not considered to be modified by the presence of the structure, even when the basement is not rigid, as in the case of a half-space. The Equation that controls the motion of the whole system in total coordinates is:

$$\begin{aligned} [\tilde{m}_c + m_c] \{ \ddot{\tilde{v}}_c + \ddot{v}_c^t \} + [\tilde{c}_c + c_c^t] \{ \dot{\tilde{v}}_c + \dot{v}_c^t \} + [\tilde{k}_c + k_c] \{ \tilde{v}_c + v_c^t \} = \\ = -\tilde{m}_b \ddot{\tilde{v}}_b - \tilde{c}_b \dot{\tilde{v}}_b - \tilde{k}_b \tilde{v}_b \end{aligned} \quad (3.5)$$

By substituting (3.4) in (3.5) and reducing terms (3.5) becomes:

$$[\tilde{m}_c + m_c] \ddot{v}_c^t + [\tilde{c}_c + c_c] \dot{v}_c^t + [\tilde{k}_c + k] v_c^t = -m_c \ddot{\tilde{v}}_c - c_c \dot{\tilde{v}}_c - k_c \tilde{v}_c \quad (3.6)$$

This is the Equation for the added motions which corresponds to Figure 3.1.c By substituting (3.1) and (3.2) in (3.6), (3.6) becomes:

$$[\tilde{m}_c + m_c] \{ \ddot{v}_c^t \} + [\tilde{c}_c + c] \{ \dot{v}_c^t \} + [\tilde{k}_c + k] \{ v_c^t \} = - \begin{Bmatrix} m_g \\ m_{gg} \\ 0 \end{Bmatrix} \ddot{\tilde{v}}_g - \begin{Bmatrix} c_g \\ c_{gg} \\ 0 \end{Bmatrix} \dot{\tilde{v}}_g - \begin{Bmatrix} k_g \\ k_{gg} \\ 0 \end{Bmatrix} \tilde{v}_g \quad (3.7)$$

It is important to note, firstly, that the input motion is defined only at the interface between the soil and the structure, as shown in Figure 3.1.c, and secondly, that the added motions in the structure are total displacements, and consequently Equation (3.7) is suitable for nonlinear analysis in the structure. For a surface structure, the input motion \tilde{v}_g coincides with the free field at the surface. For embedded structures, \tilde{v}_g contains the different free field motions at the interface nodes. In this case, unless direct data are available or an assumption is made regarding these motions, a scattering problem must be solved in order to obtain \tilde{v}_g .

In the case of a rigid foundation, the same input motion may be specified at all the contact nodes, and equal to the surface motion. In general, however, a scattering problem will be needed, which is an inconvenience that may be avoided by using the volume methods described below.

Equation (3.7) may be further simplified by dividing the added displacements in two parts: a dynamic component, v_c , plus a pseudostatic component, v_c^s . The pseudostatic displacements may be derived from (2.37) by eliminating the dynamic terms. Hence:

$$[\bar{k}_c + k] v_c^s = - \begin{Bmatrix} k_g \\ k_{gg} \\ 0 \end{Bmatrix} \tilde{v}_g \quad (3.8)$$

or

$$v_c^s = r_c \tilde{v}_g$$

where

$$r_c = - [\bar{k}_c + k_c]^{-1} \begin{Bmatrix} k_g \\ k_{gg} \\ 0 \end{Bmatrix} \quad (3.9)$$

Thus

$$v_c^t = v_c + r_c \tilde{v}_g \quad (3.10)$$

Substituting (3.10) in (3.7) we get:

$$[\bar{m}_c + m_c] \ddot{v}_c + [\bar{c}_c + c] \dot{v}_c + [\bar{k}_c + k] v_c = - \left\{ [\bar{m}_c + m_c] r_c + \begin{Bmatrix} m_g \\ m_{gg} \\ 0 \end{Bmatrix} \right\} \ddot{\tilde{v}}_g \quad (3.11)$$

The main advantage of Equation (3.11) is that the R.H.S. is in terms of the free field accelerations only. This is so because the displacements have dropped out, and the velocity effects are usually neglected. Once the dynamic displacements v_c are obtained from (3.11) the total forces f may be obtained as follows:

$$f = [k_c + k] \begin{Bmatrix} v \\ v_g \\ v_a \end{Bmatrix} + r_c v_g + \begin{Bmatrix} 0 \\ \tilde{v}_g \\ \tilde{v}_a \end{Bmatrix} = [k_c + k] \begin{Bmatrix} v \\ v_g \\ v_a \end{Bmatrix} + \begin{Bmatrix} 0 \\ \tilde{v}_g \\ \tilde{v}_a \end{Bmatrix} - \begin{Bmatrix} k_g \\ k_{gg} \\ 0 \end{Bmatrix} \tilde{v}_g$$

The forces in the superstructure are:

$$f_s = kv + k_g v_g \quad (3.12)$$

Note that these forces depend only on the dynamic displacements v and v_g , and therefore no superposition with the free field motion is needed.

Up to this point there are two major disadvantages:

1) No energy radiation mechanism at the boundary has been considered. To avoid reflections very large models will be necessary.

2) The final Equation (3.11) is expressed in terms of all the geometric degrees of freedom of the system. For most cases their number will be very large (several hundred to several thousands). The reduction of this system to normal coordinates requires obtaining the eigenvectors which can be very costly. Also since the damping is nonproportional the system will be coupled. Therefore mode superposition will not be applicable and a step-by-step integration or the uncoupling the system with complex mode shapes will have to be carried out for the numerical integration.

These disadvantages and the scattering problem may be avoided in the following manner:

1) The scattering problem may be eliminated by using the volume methods described below.

2) Energy radiation may be accounted for by using frequency independent radiation boundaries which, as will be seen later in this work, prove to be very efficient. The resulting boundary will add new terms in the damping, stiffness, and mass matrices.

3) The final Equation of motion (3.11) may be reduced by Wilson-Yuan Ritz vectors, Wilson, Yuan and Dickens (1982), which can be obtained more easily than the undamped eigenvectors, while yielding a better accuracy.

4) The resulting set of coupled equations can be uncoupled by the damped mode shapes and integrated exactly for linear type of excitation, avoiding the inaccuracies inherent in the step-by-step procedures.

3.4.- VOLUME METHODS.

The complete problem may be divided now, as shown in the Figure (3.2), into a free field with the excavated soil included, plus the source problem for the added motions, in which the input is defined only at all the buried structural nodes, and in which the structure properties at its embedded level are reduced by those of the soil. The formulation of this method, though different, will follow the same line as that of the boundary methods. Up to Equation (3.4), the same formula apply, however the partitions are now as follows:

$$v_c^t = \begin{Bmatrix} v^t \\ v_f^t \\ v_g^t \\ v_a^t \end{Bmatrix} \quad \text{and} \quad \tilde{v}_c = \begin{Bmatrix} 0 \\ \tilde{v}_f \\ \tilde{v}_g \\ \tilde{v}_a \end{Bmatrix} \quad (3.13)$$

where v^t represent the total motions at the structure, v_f^t at the buried part, v_a^t at the soil and v_g^t at the boundary of the model. The partitions for the property matrices are:

$$m_c = \begin{bmatrix} m & m_f & 0 & 0 \\ m_f & m_{ff} - \tilde{m}_{ff} & m_{fg} - \tilde{m}_{gf} & 0 \\ 0 & m_{gf} - \tilde{m}_{gf} & m_{gg} & 0 \\ 0 & 0 & 0 & 0 \end{bmatrix} \quad \tilde{m}_c = \begin{bmatrix} 0 & 0 & 0 & 0 \\ 0 & \tilde{m}_{ff} & \tilde{m}_{fg} & 0 \\ 0 & \tilde{m}_{gf} & \tilde{m}_{gg} & \tilde{m}_{ga} \\ 0 & 0 & \tilde{m}_{ga}^T & \tilde{m}_{aa} \end{bmatrix} \quad (3.14)$$

and in the same manner for the stiffness and damping matrices. Substituting (3.13) and (3.14) in (3.4), (3.4) becomes:

$$\begin{aligned} & [\tilde{m}_c + m_c] \{\dot{v}_c^t\} + [\tilde{c}_c + c] \{\dot{v}_c^t\} + [\tilde{k}_c + k_c] \{v_c^t\} = \\ & = - \begin{bmatrix} m_f & 0 \\ m_{ff} - \tilde{m}_{ff} & m_{gf} - \tilde{m}_{fg} \\ m_{gf} - \tilde{m}_{gf} & m_{gg} \\ 0 & 0 \end{bmatrix} \begin{Bmatrix} \tilde{v}_f \\ \tilde{v}_g \end{Bmatrix} - \begin{bmatrix} c_f & 0 \\ c_{ff} - \tilde{c}_{ff} & c_{gf} - \tilde{c}_{fg} \\ c_{gf} - \tilde{c}_{gf} & c_{gg} \\ 0 & 0 \end{bmatrix} \begin{Bmatrix} \dot{\tilde{v}}_f \\ \dot{\tilde{v}}_g \end{Bmatrix} - \begin{bmatrix} k_f & 0 \\ k_{ff} - \tilde{k}_{ff} & k_{fg} - \tilde{k}_{fg} \\ k_{gf} - \tilde{k}_{gf} & k_{gg} \\ 0 & 0 \end{bmatrix} \begin{Bmatrix} \tilde{v}_f \\ \tilde{v}_g \end{Bmatrix} \quad (3.15) \end{aligned}$$

To simplify the notation let the matrices on the R.H.S. be called, X_m , X_c and X_k respectively. The L.H.S. of Equation (3.15) is identical to that of Equation (3.7). The R.H.S., although more involved, has the main advantage of being defined in terms of the free field motion without excavation, and therefore no scattering problem need be solved.

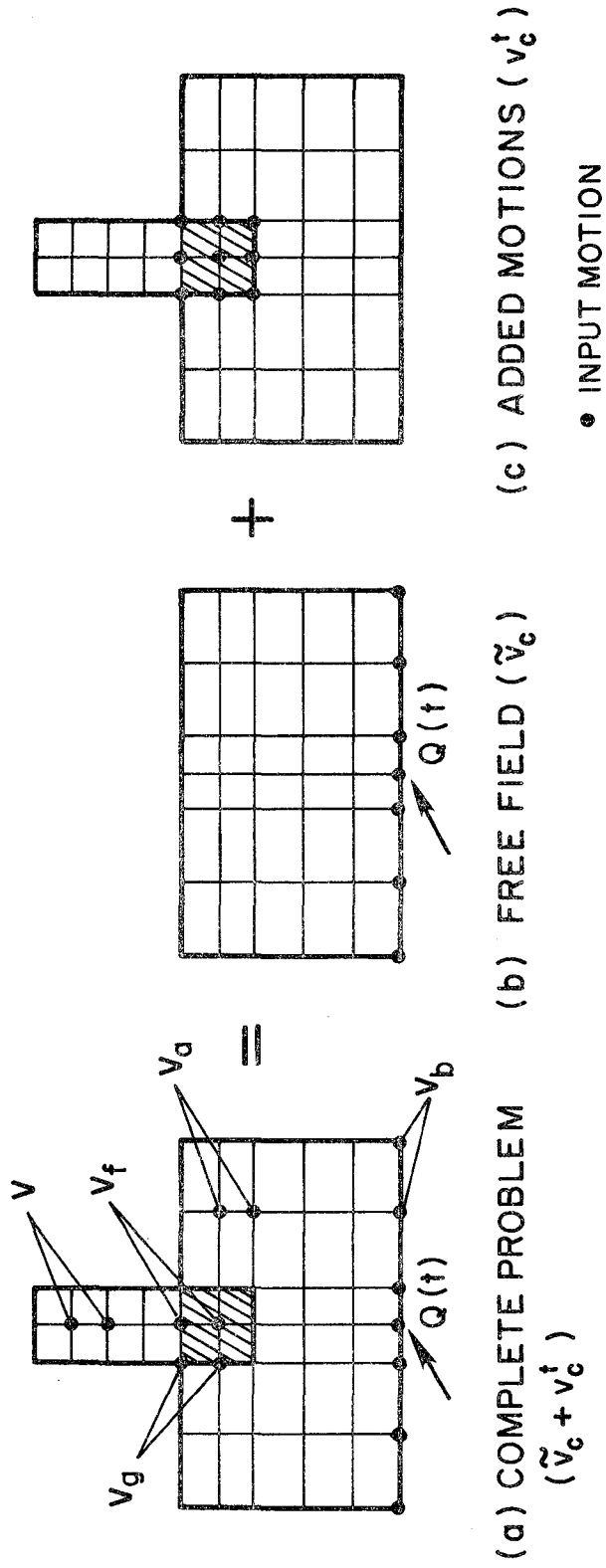


Fig 3.2.- Division of the complete problem into a free field and an interaction problem.

The free field motions at the embedded nodes may be obtained assuming a desired wave propagation pattern. The simplest one, as mentioned already, is to assume vertical propagation of P and S waves. The added displacements may be written, as done before, as the sum of the dynamic and pseudostatic components.

$$v_c^{\ddagger} = v_c + v_c^s = v_c + r_c \begin{Bmatrix} \tilde{v}_f \\ \tilde{v}_g \end{Bmatrix} \quad (3.16)$$

again:

$$r_c = - [\tilde{k}_c + k] \begin{bmatrix} k_f & 0 \\ k_{ff} - \tilde{k}_{ff} & k_{fg} - \tilde{k}_{fg} \\ k_{gf} - \tilde{k}_{gf} & k_{gg} \\ 0 & 0 \end{bmatrix} \quad (3.17)$$

substituting (3.17) into (3.15):

$$[\tilde{m}_c + m_c] \ddot{v}_c + [\tilde{c}_c + c_c] \dot{v}_c + [\tilde{k}_c + k] v_c = - \left\{ [\tilde{m}_c + m_c] r_c + X_M \right\} \begin{Bmatrix} \tilde{v}_f \\ \tilde{v}_g \end{Bmatrix} \quad (3.18)$$

It can easily be seen that the forces in the nonburied part of the structure will depend only on the dynamic displacements. However, the forces in the buried part will now depend on the dynamic as well as on the free field displacements. Their computation will be a little more involved than in the case of the boundary methods. With the inclusion of the radiation boundaries the only problem left is the reduction of the number of degrees of freedom.

3.5.- SUMMARY OF TIME DOMAIN METHODS.

A classification analogous to that done with the frequency domain methods is illustrated in Figure (3.3) for the time domain. The site response problem needs to be solved prior to any analysis, except for the case of surface structures for which the control motion is directly the ground motion at the surface. The scattering problem needs to be solved for the boundary methods only. The input motion is defined in different places as shown in the Figure (3.3), depending on the different methods. The main difference with the frequency domain methods is the need to solve the whole system of equations simultaneously. This is why the use of radiation boundaries and the reduction in the number of degrees of freedom is crucial.

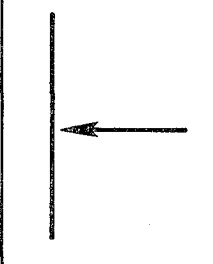
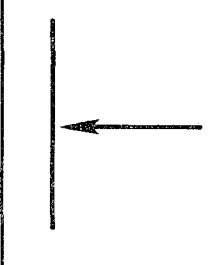
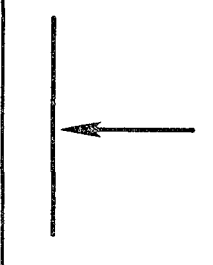
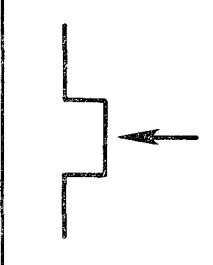
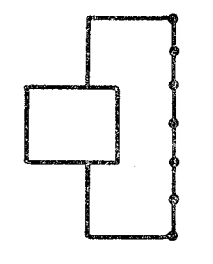
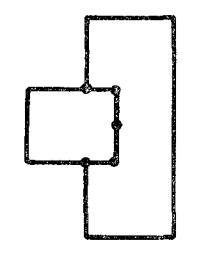
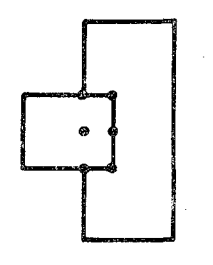
METHOD	COMPLETE	BOUNDARY	VOLUME
SITE RESPONSE PROBLEM			
SCATTERING PROBLEM	NONE		NONE
STRUCTURAL ANALYSIS • LOADED NODE			

Fig 3.3.- Summary of the time domain methods.

CHAPTER 4

RADIATION BOUNDARIES

4.1.-INTRODUCTION.

The finite element model of the soil-structure system has to account for the energy radiation at the boundaries. Boundary conditions that are not adequate will produce reflections of wave fronts that will impinge back in the structure producing spurious results. One way of solving the problem is by extending the finite element mesh as much as necessary in order to prevent the reflected waves from reaching the structure during the time of the analysis. This approach will certainly lead to very large models and the computational effort may be extraordinary.

Following this line of thought, Day (1977) proposed a method for attenuation of waves based on prolonging the finite element mesh with elements whose size gradually increase with increasing distances from the structure. The zone of growing grid is made dissipative with internal viscous damping, and terminates at a large distance from the structure. The method is successful depending on the rate of grid growth and viscous damping. Day proposes a constant viscous damping and a factor for element size increase equal to 1.1.

Another approach to the problem of mesh finiteness is due to Smith (1974). In his method first order reflections from plane boundaries are rigorously eliminated by averaging independently computed solutions for the Dirichlet and Newman boundary conditions. The method requires 2^n independent solutions, where n is the number of boundaries at which reflections are canceled, and it does not eliminate higher order reflections (the waves that impinge in the boundary more than once). Therefore even though the theory is exact, the efficiency of the technique is limited since at least 2^n solutions are necessary for a given problem.

Cundall et al (1978) devised an ingenious trick that is based on Smith's theory of superposition and is formulated in finite differences. The trick consists of superimposing the solutions not in all the domain but in two small meshes attached at the boundaries of the model, where the reflections are to take place. The superposition is carried out every few time steps and consequently the reflections do not propagate out of the small meshes. In order to avoid the numerical shock created by the sudden jumps in accelerations and velocities due to the Newman and Dirichlet conditions, they use constant force and constant velocity as boundary conditions. The method gives good results but so far it has only been implemented in two dimensions, Kunar and Ovejero (1980).

Boundary conditions obtained by the integration of wave equations at the boundary of a given model are only available in the frequency domain because of the frequency dependency of the problem. Lysmer and Kulhemeyer (1969) presented an approximate transmitting boundary based on the assumption of energy being transmitted in the form of P and S waves through the bottom of the model and the fundamental mode of Rayleigh waves through the sides of the model. The results were quite good for relatively small models. Waas (1972) perfected the method and solved the case of a steady state plane motion of a system of horizontal layers of infinite lateral extent, terminated below by a rigid boundary. The theory has been extended to include axysimmetric geometries, Waas (1972) and Kausel et al (1975), but it is still restricted to horizontal layers with rigid bottom boundaries, and to steady state problems. No theoretical solution for the boundary element is available in the time domain.

The following discussion gives some examples that demonstrate that the use of frequency independent radiation boundaries obtained in a very simple way from a frequency dependent one defined at the fundamental frequency of the soil-structure system, leads to very acceptable approximations. Prior to the examples, however, some observations will be made about the nature of a radiation boundary.

4.2.- NATURE OF THE RADIATION PROBLEM.

4.2.1- One dimensional case.

The perfect absorbing energy mechanism in the one dimensional case is a frequency independent viscous dashpot. In order to find its characteristics let's consider a semi-infinite bar. The expressions for the displacements and velocities at a point x due to an outgoing harmonic wave are:

$$u = A e^{i(\omega t - kx)}$$

$$\dot{u} = A \omega i e^{i(\omega t - kx)}$$

where ω is the frequency, k is the wave number and A is the amplitude of the wave. At a certain point x the horizontal stress will be:

$$\sigma_x = E \frac{\partial u}{\partial x} = -E A i k e^{i(\omega t - kx)}$$

Expressed in terms of the velocities, this yields

$$\sigma = -E \dot{u} \frac{k}{\omega}$$

now

$$k = \frac{\omega}{V_p}$$

thus:

$$\sigma = -V_p \rho \dot{u} \tag{4.1}$$

Relation (4.1) is satisfied at any point of the bar. The stress is identical to the one produced by a simple damped oscillator with a damping value equal to $-V_p \rho$. Therefore if we cut the bar at any location and colocate as boundary a dashpot equal to $V_p \rho$, tractions will be applied to the boundary which will be equal in magnitude and opposite in direction to the stresses caused by the incident wave, thus becoming the one dimensional perfect energy absorbing mechanism. Since its characteristics do not depend upon frequency, it can be used equivalently in the time or frequency domains.

4.2.2.- Two and three dimensional cases.

The general equation for the propagation of a plane wave in a general anisotropic medium is: (Synge (1956))

$$\{u\} = A \{n\} \exp [i\omega (\{k\}^T \{r\} - t)] \quad (4.2)$$

where $\{u\}$ is the vector of particle displacements, $\{n\}$ is the vector of direction cosines, $\{k\}$ is the horizontal wave number vector, $\{r\}$ is the vector of particle coordinates, ω is the frequency of the wave and, A is its amplitude. For simplicity, only the two dimensional case as done by White (1977), will be considered. The extrapolation to the three dimensional case is straightforward. Equation (4.2) has two independent solutions for the plane case.

$$u = \sum_{m=1}^2 A_m \{n_m\} \exp [i\omega \{k_m\}^T \{r\} - t]$$

The strains are:

$$\epsilon_x = u_{x,x} = i\omega \sum_{m=1}^2 A_m n_{mx} k_{mx} \exp [i\omega (\{k_m\}^T \{r\} - t)]$$

$$\epsilon_y = u_{y,y} = i\omega \sum_{m=1}^2 A_m n_{my} k_{my} \exp [i\omega (\{k_m\}^T \{r\} - t)]$$

$$\epsilon_{xy} = u_{x,y} + u_{y,x}$$

The velocities will be :

$$\dot{u}_x = -i\omega \sum_{m=1}^2 A_m n_{mx} \exp [i\omega (\{k_m\}^T \{r\} - t)]$$

$$\dot{u}_y = -i\omega \sum_{m=1}^2 A_m n_{my} \exp [i\omega (\{k_m\}^T \{r\} - t)]$$

The strains can be expressed (as done in the one dimensional case) in terms of the velocities as follows:

$$\underline{\epsilon} = \underline{B} \underline{\dot{u}}$$

where

$$\underline{B} = -\Delta^{-1} \begin{bmatrix} n_{1x} k_{1x} & n_{1y} k_{1y} & n_{1x} k_{1y} + n_{1y} k_{1x} \\ n_{2x} k_{2x} & n_{2y} k_{2y} & n_{2x} k_{2y} + n_{2y} k_{2x} \end{bmatrix}$$

in which

$$\Delta = \begin{bmatrix} n_{1x} & n_{1y} \\ n_{2x} & n_{2y} \end{bmatrix}$$

The normal and shear stresses at a given boundary can be expressed as:

$$\sigma = \underline{D} \underline{B} \dot{u} = \underline{B}^* \dot{u}$$

where \underline{D} is the matrix representing the constitutive characteristics of the material. It must be noticed that the matrix \underline{B}^* is independent of frequency and amplitude of the waves, and only depends on the physical characteristics of the material and the direction of the wave propagation. Therefore, if we knew the direction of propagation of a given wave we could get the perfect energy absorbing frequency independent mechanism by simply satisfying the boundary condition:

$$\sigma = -\underline{B}^* \dot{u}$$

This ideal solution is impossible to carry out due to the practical impossibility of finding in a given finite element mesh all the directions of all the wave trains impinging at the boundaries. This is why analytical solutions to the radiation boundary, based on wave propagation theory have not been obtained in the time domain. It is because of this that all the methods mentioned in the introduction have been developed.

4.3.- FREQUENCY INDEPENDENT RADIATION BOUNDARY.

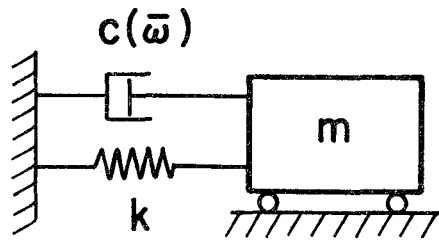
4.3.1.- One dimensional cases.

a) Single dof:

Consider a SDOF system with the characteristics shown in Figure (4.1). As can be seen the damping varies parabolically with respect to frequency from the value 0 at $\omega=0$ to 60 at $\omega=40$. At the fundamental frequency ω_1 the damping value is 20, which corresponds to a damping ratio of 10%. The expression for the dynamic amplification factor is:

$$DAF(\bar{\omega}) = [k(-m\bar{\omega}^2 + i\bar{\omega}c(\bar{\omega}))]^{-1}$$

Figure (4.2) shows the results obtained computing the DAF with the damping depending on frequency and with the frequency independent damping that has been matched at the fundamental frequency $\omega_1=10$. As we can see they are practically the same, and the maximum response is obviously perfectly matched.



$$\begin{aligned}
 k &= 1000 \\
 m &= 10 \\
 \omega_0 &= 10 \\
 C_c &= 200 \\
 \xi &= 10\%
 \end{aligned}$$

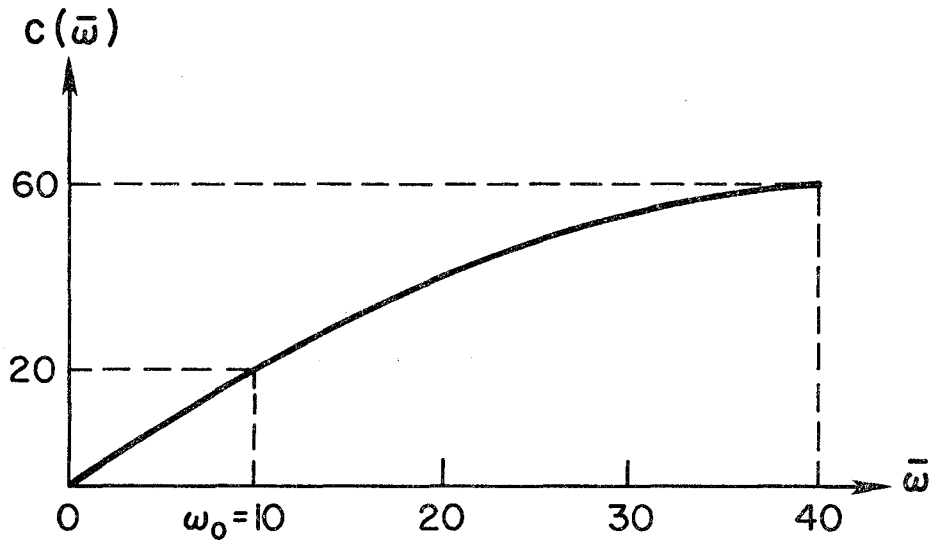


Fig 4.1.- Characteristics of a SDOF system and damping variation with frequency.

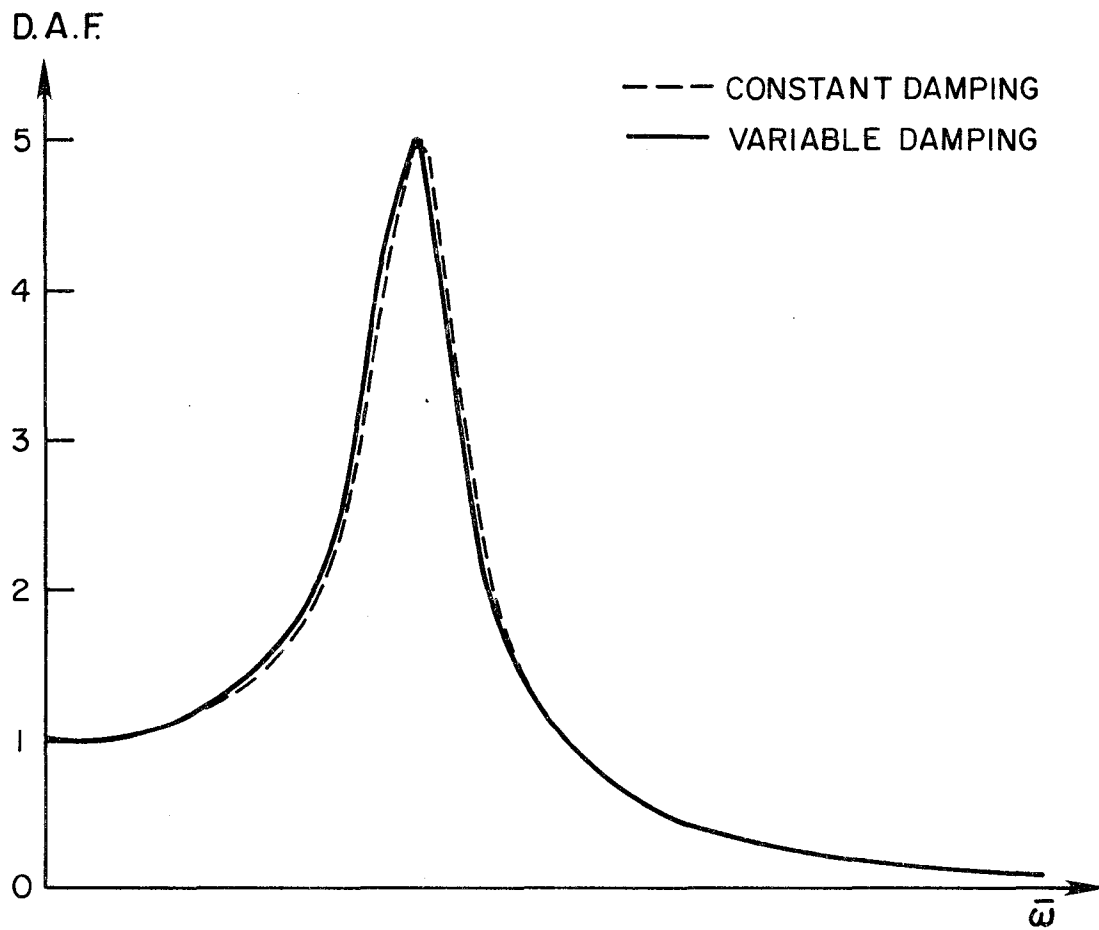


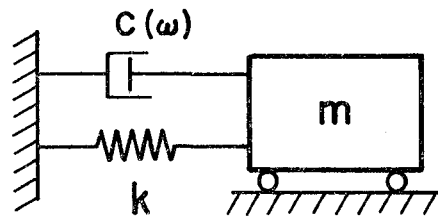
Fig 4.2.- Dynamic Amplification Factor versus frequency for constant and variable damping.

Figure (4.3) shows a second example in which the variation of damping with respect to frequency is increased. At the fundamental frequency the damping value is equal to 80, which corresponds to a damping ratio equal to 40%. In this case due to the high damping ratio the fundamental damped frequency differs from the undamped frequency and is equal to 9.27. The values of the DAF considering frequency dependent and independent damping are shown in Figure (4.4). This Figure also includes the results obtained by matching the damping at the undamped fundamental frequency.

b) Multidegree of freedom systems :

Consider now the case of a bar with the characteristics given in Figure (4.5), that is modeled with linear finite elements and subjected to harmonic loads at its tip, as shown. The damping constant attached at the end of it varies parabolically as illustrated in the same Figure. The value of $\zeta = 1$ corresponds to the case of perfect energy transmission. The variation of ζ with respect to frequency is considered sharp enough to give a good idea of how much effect the consideration of frequency dependent coefficients has on the system response. Impedance coefficients attached at the foundation of building models experience a proportionally smaller variation than those considered here. The amplitude of the complex response function at the degrees of freedom 1 and 2 are illustrated in Figures (4.6) and (4.7) respectively.

As we can see, the differences between both structures are very small for degree of freedom 1 and almost negligible for degree of freedom 2. It is worth noticing that the maximum response is always computed exactly at the fundamental frequency of the system and that both solutions practically coincide along the part of the frequency spectrum where the maximum responses are expected. These results are in agreement with those obtained by Tsai, Niehoff, Swatta and Hadjian (1974) with the difference that they took the static values of the frequency dependent impedances. Due to this fact they do not obtain total agreement in the peak response given by the two approaches at the fundamental frequency of the system.



$$\begin{aligned}
 k &= 1000 \\
 m &= 10 \\
 \omega_0 &= 10 \\
 C_c &= 200 \\
 \xi &= 10\%
 \end{aligned}$$

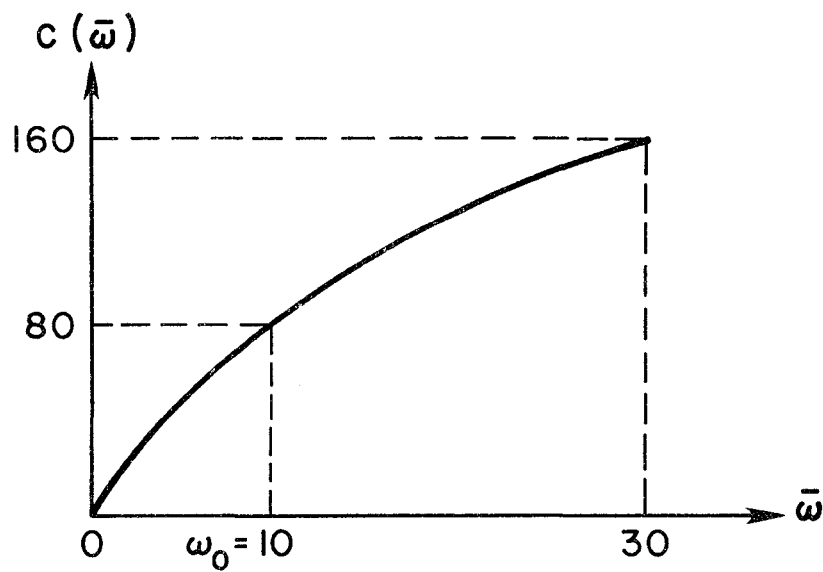


Fig 4.3.- Characteristics of a SDOF system and damping variation with respect to frequency.

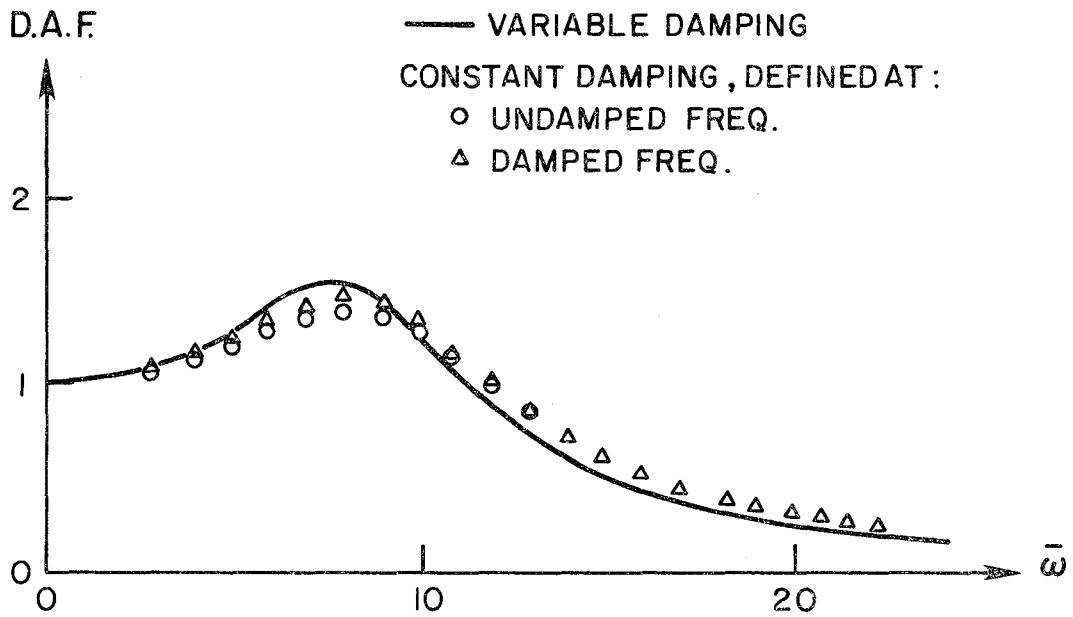


Fig 4.4.- Dynamic Amplification Factor versus frequency for variable and constant damping.

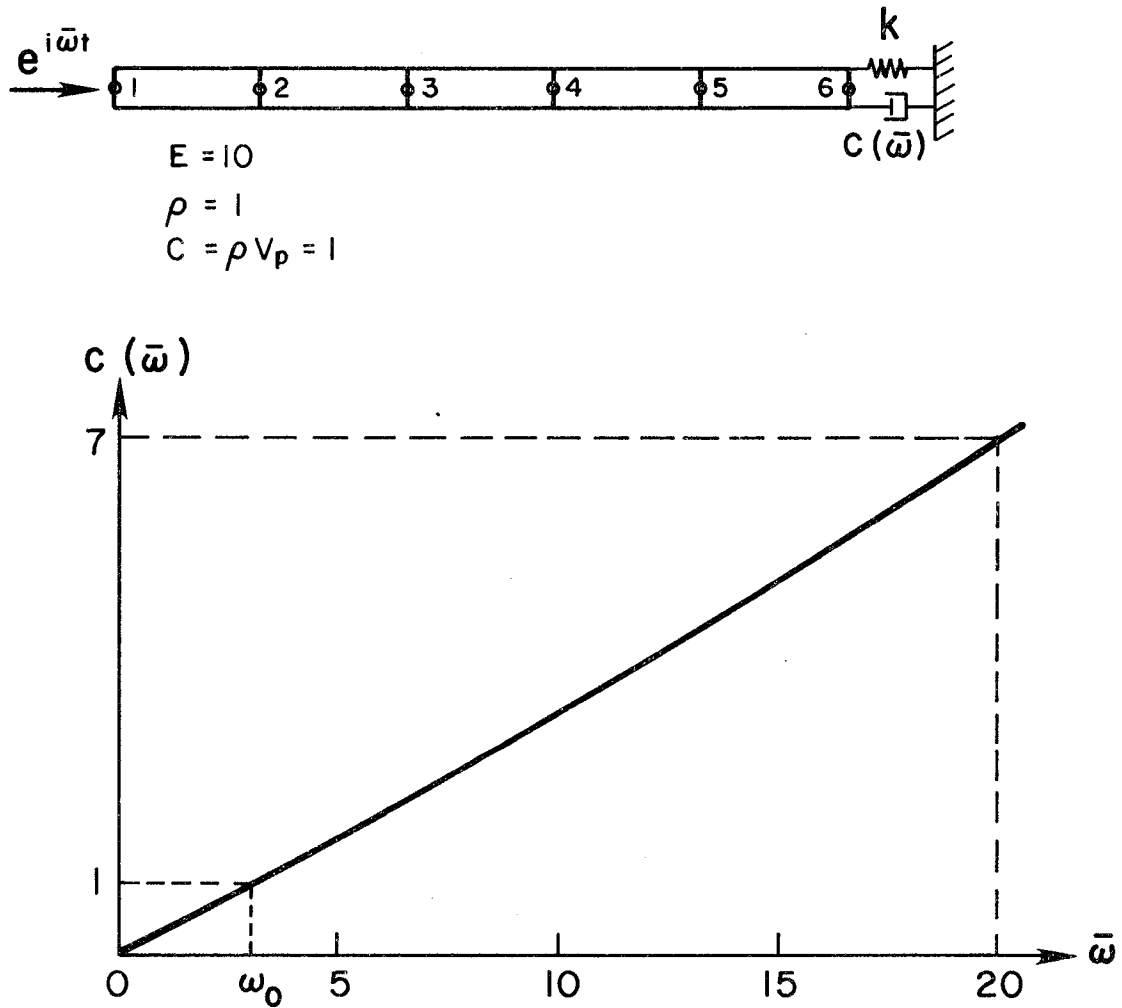


Fig 4.5.- Modelling of a discrete bar and variations of the dashpot characteristics with respect to frequency.

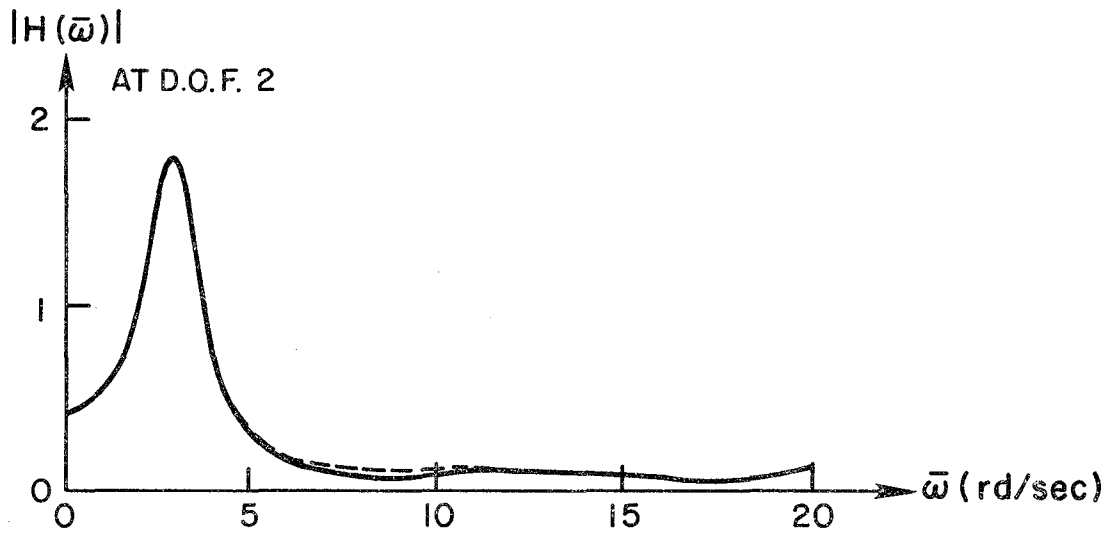
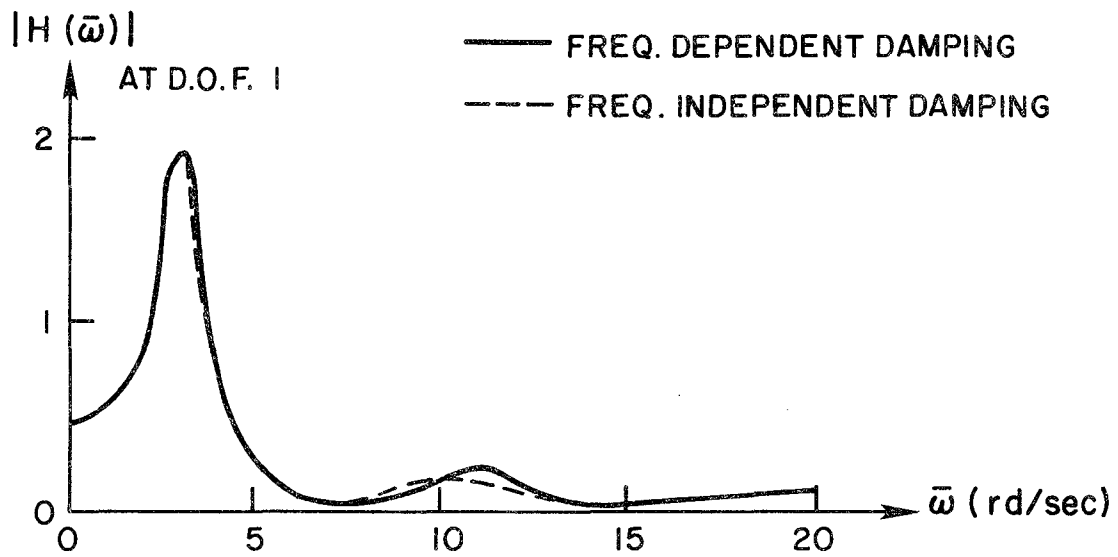


Fig 4.6 and Fig 4.7, - Amplitude of the complex response functions at degrees of freedom 1 and 2 of the discrete bar.

4.3.2.- TWO DIMENSIONAL CASES.

As mentioned before, Lysmer and Kulhemeyer (1969) developed a frequency dependent boundary under the assumption of energy being radiated in the form of body waves through the bottom of the model and in the form of Rayleigh waves through the lateral boundaries. They obtained rather good approximations with relatively small models for the case of a vertical vibration of a rigid footing in an elastic half-space. The improvement over a frequency independent solution capable of radiating only body waves through both the lateral and the bottom boundaries was significant.

The aim in this case (as in the one dimensional case) is to demonstrate that the assumption of a frequency independent boundary, matched at the fundamental frequency of the system leads to very good approximations in the frequency range of interest.

Three examples are considered in this case. The first two are the vertical and horizontal excitations of a rigid footing in an elastic half-space with characteristics shown in Figure (4.8). The third corresponds to the horizontal excitation of a single layer over a bedrock. For each case two different models of different dimensions are considered. The first one has a length equal to four times the radius and depth equal to three times the radius. For the second model, the depth does not change and the length is doubled to eight times the radius. To see the influence that the material damping in the soil has in the response, the same models are considered including viscous Rayleigh damping with a damping ratio equal to 20%.

For all cases the fundamental frequency of the system is computed at which the frequency independent boundary is defined. The responses in the form of compliance functions are obtained by subjecting the system to harmonic unit loads with varying frequencies. The compliance functions of the models that do not include viscous damping are checked against the exact solutions for the half-space that are given by Luco and Westman (1972) and Oien (1971). The compliances for the cases that consider viscous damping can not be checked against any exact solution, however their purpose is to show the influence that the viscosity has in the frequency independence of the boundary.

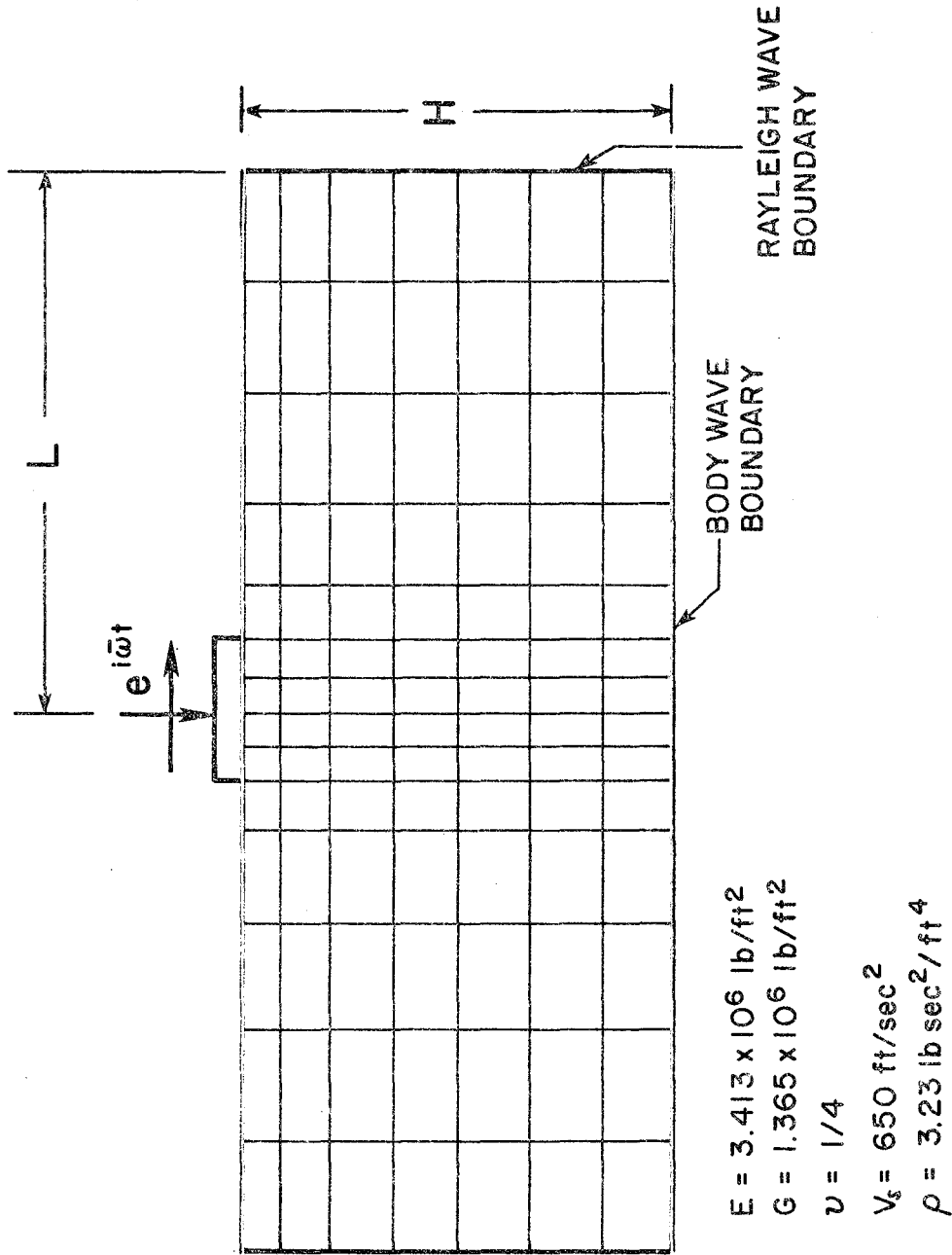


Fig 4.8.- Characteristics of a halfspace for a horizontal and vertical impedance problem.

Figures (4.9) and (4.10) illustrate the results in the half-space for the vertical cases without and with internal viscous damping respectively. Figures (4.11) and (4.12) illustrate those corresponding to the horizontal cases. In view of these results the following conclusions may be drawn:

Vertical excitation in the half-space:

a) The differences between the results obtained with frequency dependent and independent boundaries are small for the small model ($L=4R$), and almost negligible for the large model ($L=8R$). In both cases the approximations achieved for the frequency range of interest are very significant.

b) The errors that both solutions give with respect to the exact solution in the low frequency range is due to the limited size in the vertical direction of the finite element model, and the limitations of the Lysmer- Kuhemeyer boundary itself.

c) In the two dimensional vertical case most of the energy is dissipated in the form of P and S waves. The energy radiated through the lateral boundary in the form of Rayleigh waves is not significant. Therefore, the differences between a frequency dependent and independent Rayleigh boundary are not important.

d) Viscous damping in the soil tends to decrease the differences between the results obtained with both types of boundaries. In this particular case both sets of results completely coincide.

Horizontal excitation in the half-space:

a) Figures (4.9) and (4.10) show that the differences between the results obtained with both boundaries are small (within 10%). This differences are smaller for the large model than for the small one, which tends to indicate that the frequency dependency of the boundary decreases when the size of the model increases.

b) Enlarging the model has a definite effect on the importance in the results. Not only does the frequency dependency lose importance, but also the response gets much closer to the exact solution. This leads to the conclusion that the Lysmer-Kulhemeyer boundary should only be applied at a moderate distance from the structure (6-8 times the semi-width of the footing).

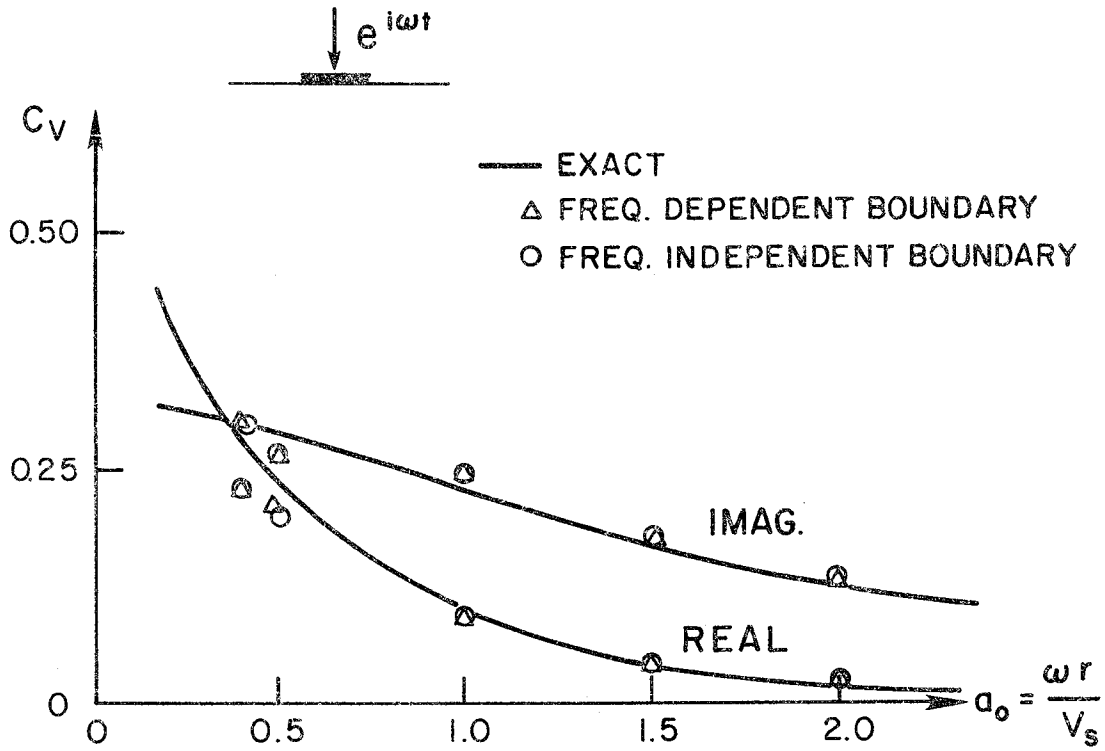
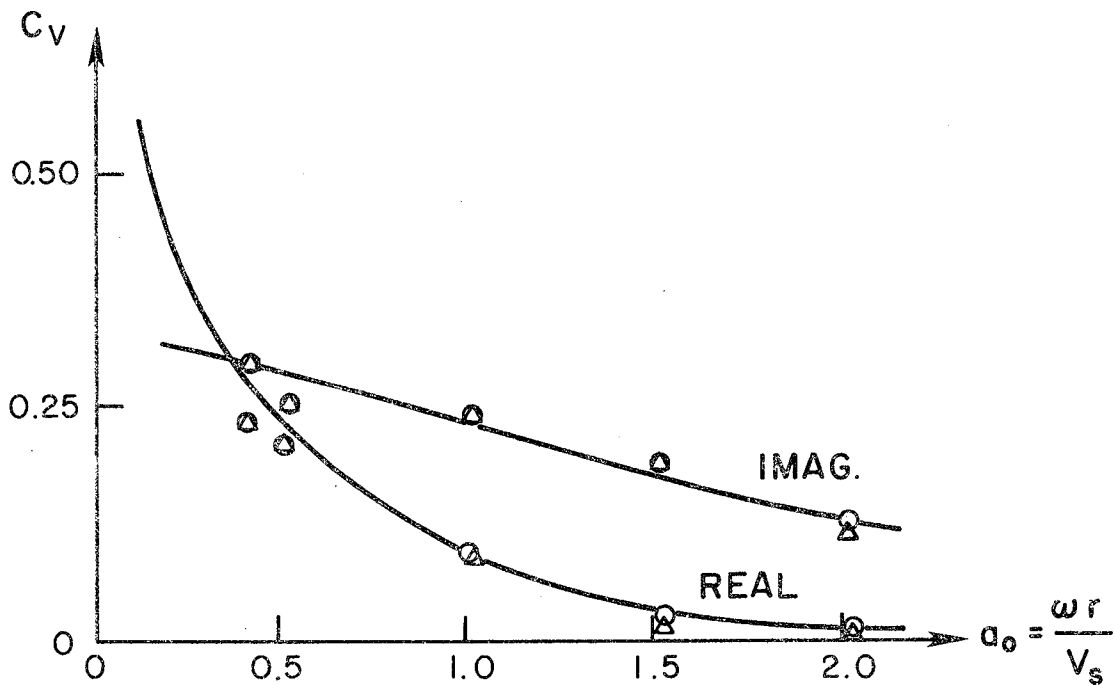
(a) DIMENSIONS $L=4R$ AND $H=3R$ (b) DIMENSIONS $L=8R$ AND $H=3R$

Fig 4.9.- Vertical compliances of a rigid strip footing on an elastic halfspace.

a) Dimensions $L=4R$, $H=3R$. b) Dimensions $L=8R$, $H=3R$.

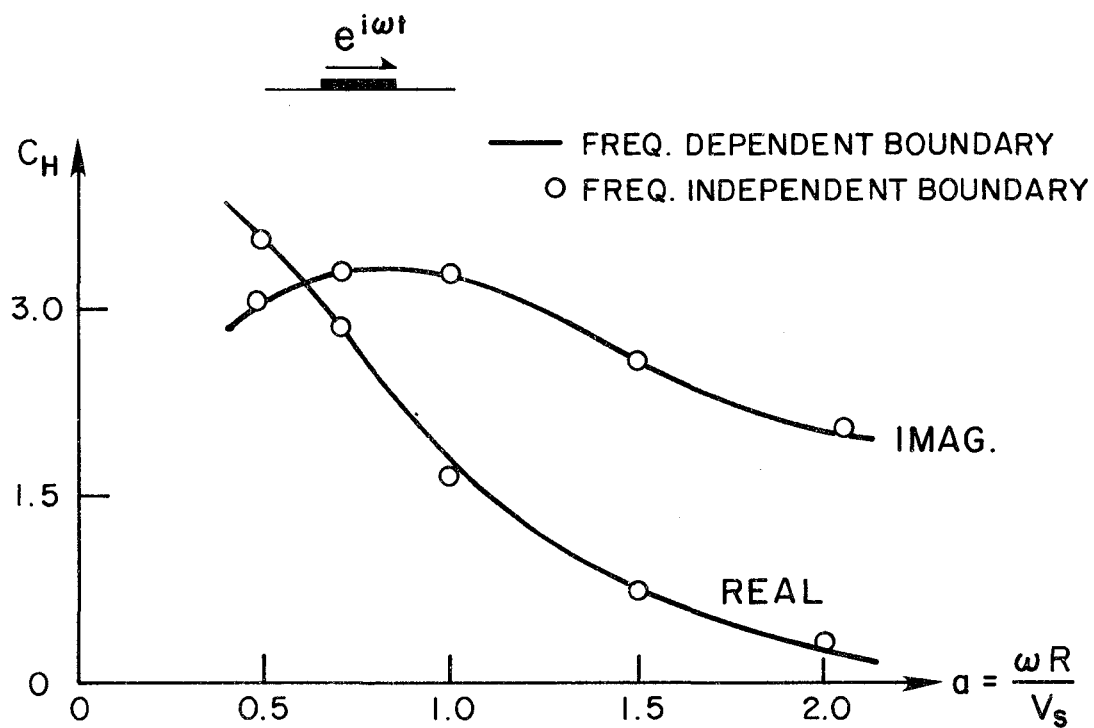
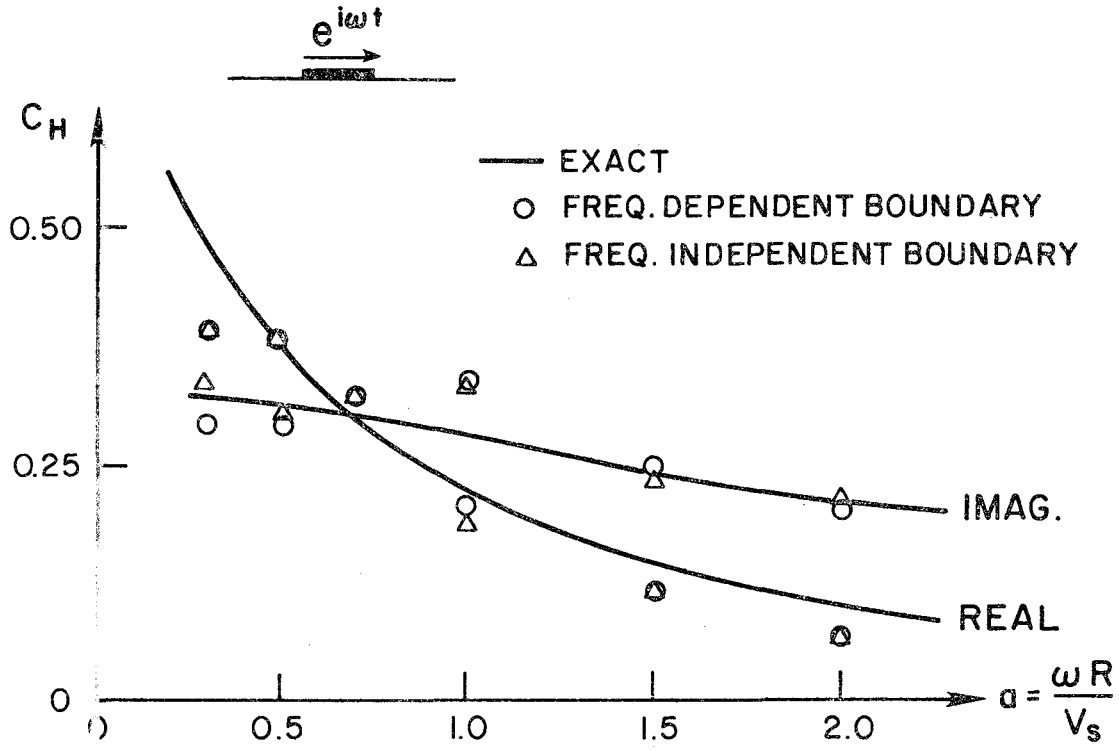
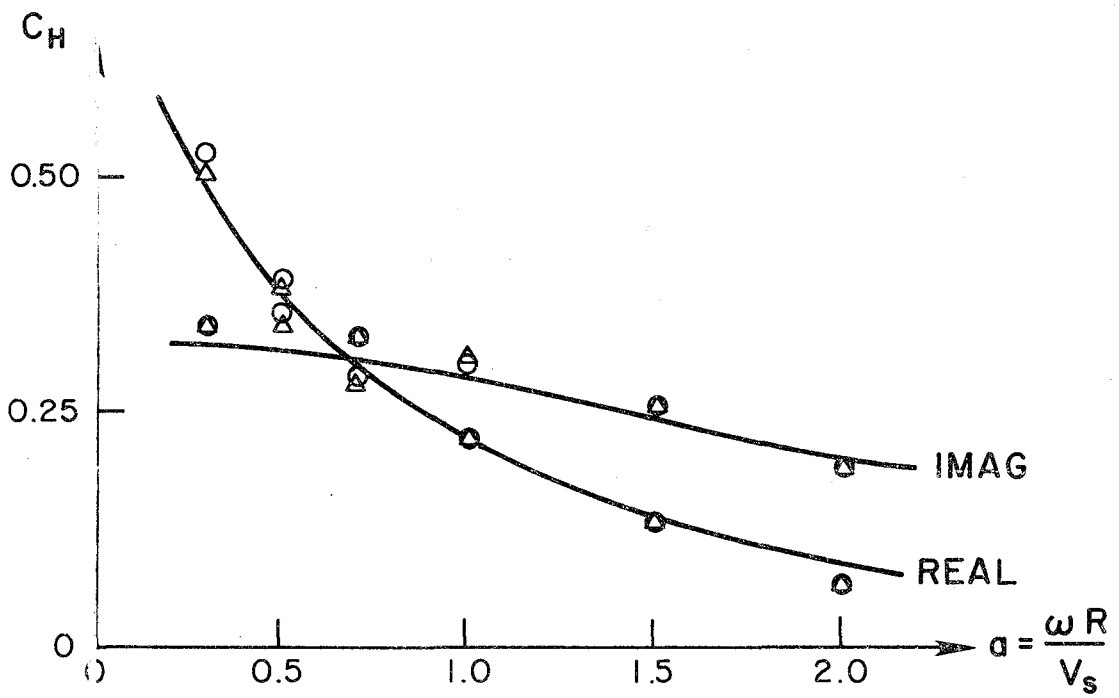


Fig 4.10.- Vertical Compliances of a rigid strip footing resting on a viscoelastic halfspace. Dimensions of the model $L=8R$ and $h=3R$.



(a) DIMENSIONS $L = 4R$ AND $H = 3R$



(b) DIMENSIONS $L = 8R$ AND $H = 3R$

Fig 1.11.- Horizontal compliances of a rigid footing resting on an elastic halfspace.
a) Dimensions $L=4R$ and $H=3R$. b) Dimensions $L=8R$ and $H=3R$.

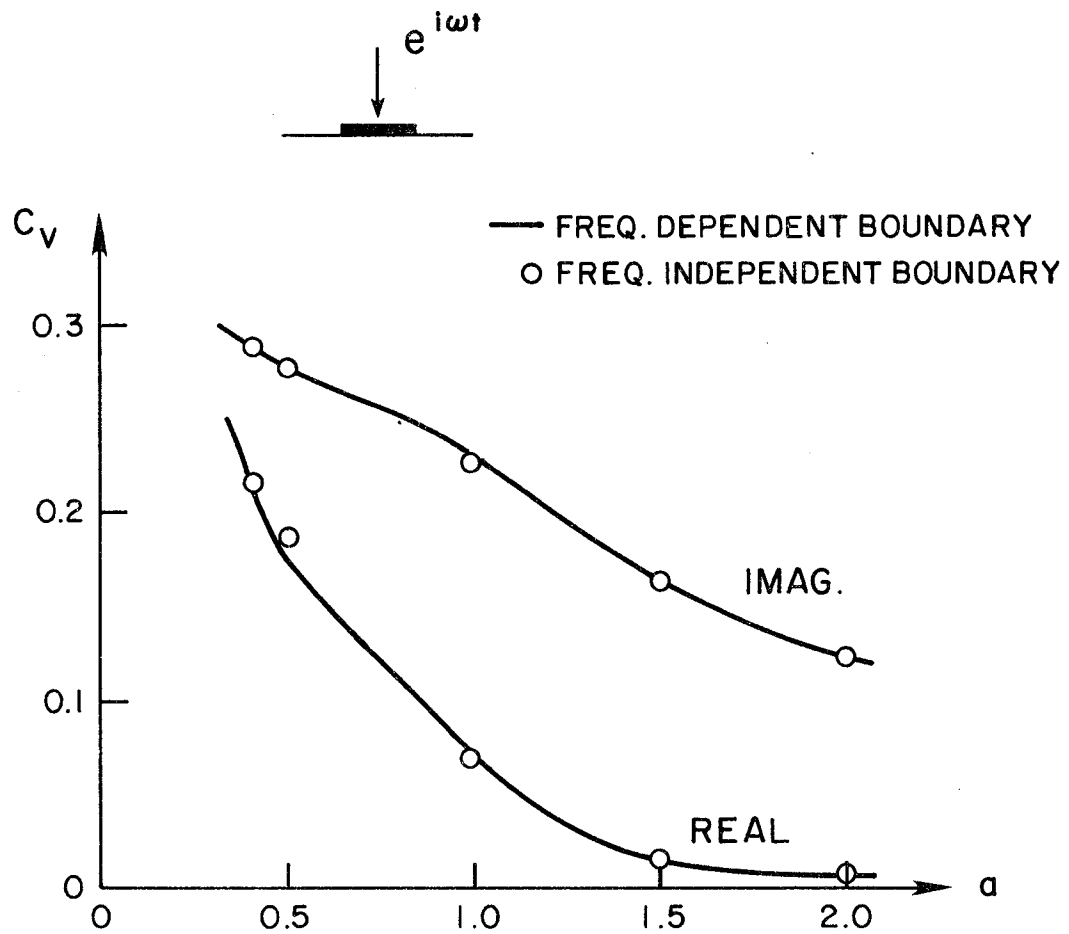


Fig 4.12.- Horizontal compliance of a rigid strip footing resting on a viscoelastic halfspace. Dimensions of the model $L=8R$ and $H=3R$.

c) Since the nature of the wave propagation in this case is such that most of the energy is dissipated through the lateral boundaries in the form of Rayleigh waves, the results obtained demonstrate the validity of the proposed approach.

d) Again the inclusion of viscous damping decreases the differences between both methods to such an extent that they become almost negligible.

Horizontal excitation in one layer over a rigid base.

Results in the large model for the frequency dependent and independent boundaries are so close in this case that their corresponding plots are superimposed on each other. Figure (4.13) shows the differences between the responses of the large model $L=8R$ and a model of length $L=14R$. It can be seen how close both solutions are. In both cases there is no difference between the frequency dependent and independent boundary.

4.3.3.- THREE DIMENSIONAL CASES.

The Lysmer-Kulhemeyer boundary is again used to obtain the vertical compliance of a rigid circular footing bonded to an elastic half-space. Since the results in the two dimensional cases gave a good idea of the dimensions of the model, only one finite element model will be used for the three dimensional problem. Its length and depth are $L=6R$ and $H=5R$. The material damping is not considered in this example. The results are illustrated in Figure (4.14), where they are compared to the exact solutions obtained by Lucio and Westman (1971).

The boundary is defined at a frequency equal to 6.5 rd/sec which corresponds to an adimensional frequency of $\omega=0.5$. The differences between the exact and the approximate solution at that particular frequency are due to the size of the finite element model and the limitations of the viscous Lysmer-Kulhemeyer boundary itself. Overall, the approximations obtained with the frequency independent boundary over the frequency range of interest are quite good, especially in this case where, according to Miller and Pursey (1955), 67% of the energy is transmitted in the form of Rayleigh waves that are supposed to be radiated with frequency dependent radiation boundaries only.

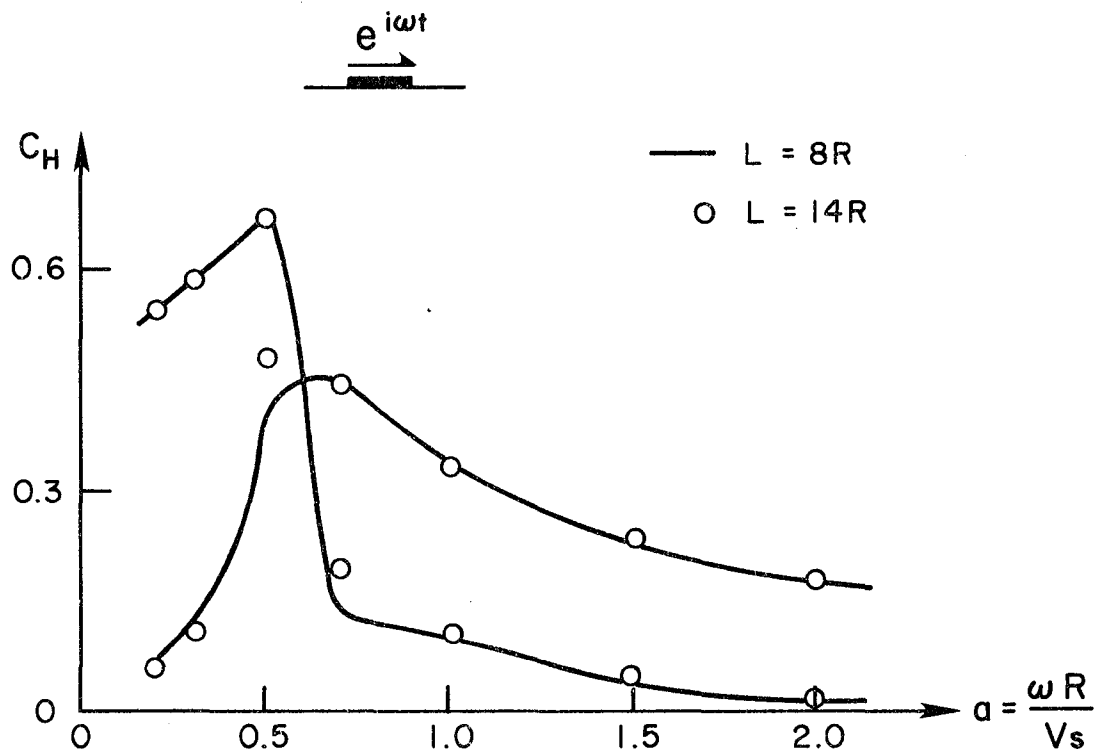


Fig 4.13.- Horizontal compliances of a rigid footing resting on a layer over a rigid base for different dimensions of the finite element model.

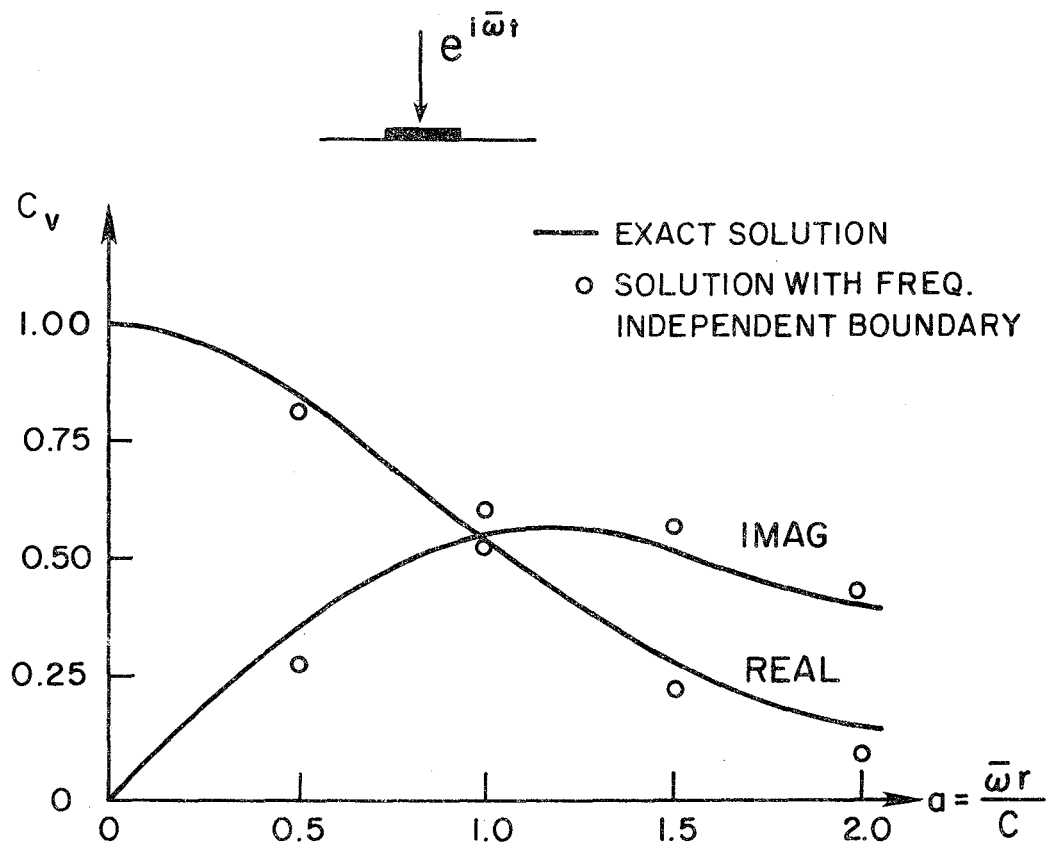


Fig 4.14,- Vertical compliance of a circular footing resting on an elastic halfspace.

4.3.4.- CONCLUSIONS.

Two important conclusions can be drawn from these results.

a) The frequency dependent viscous Lysmer-Kulhemeyer boundary provides quite good results for two and three dimensional models with moderate sizes (length equal to 6-10 times the semi-width of the footing). This consideration is in agreement with the results obtained by Roesset and Ertorrey (1977).

b) For those cases in which the frequency independent boundary is obtained from the frequency dependent one by defining it at the fundamental frequency of the system good approximations are obtained. Errors decrease when the size of the model is increased and when internal viscous damping is included.

CHAPTER 5

REDUCTION IN THE SIZE OF THE PROBLEM

The utilization of the frequency independent boundary allows us to limit the size of the finite element model, and consequently to reduce the computational effort involved in this ordinarily large problem. The use of sets of Ritz functions will further reduce the system of equations and render a solution of acceptable accuracy. We will see in this chapter that reduced systems of equations obtained with Wilson-Yuan Ritz functions yield very good results in solving not only structural problems but wave propagation problems as well. In this way the computational effort involved in solving the original set of equations is greatly reduced.

5.1.- RITZ FUNCTIONS TECHNIQUES.

5.1.1.- Introduction.

It is a well known fact that the use of only a few eigenvectors of a structural system renders a sufficiently accurate approximation to the total response of that system to an earthquake type of loading. Wilson, Yuan and Dickens (1982) have demonstrated that the use of subspaces expanded by a set of Ritz functions that are generated taking into account the spatial distribution of the load, yields more accurate results than the approximations obtained with the subspace expanded with the same number of eigenvectors.

Wilson and Yuan used typical building and cantilever cases to show their results. The following discussion will demonstrate by the use of several numerical examples how well these Ritz vectors approximate wave propagation and impedance type of problems in one, two and three dimensions. The Ritz vectors are automatically generated in a much faster and less costly way than the eigenvectors and therefore they become excellent candidates for the reduction of large systems of equations, i.e. the soil-structure systems.

5.1.2.- One dimension.

Figure (5.1) shows the the problem of the transmission of a wave generated in a semi-infinite bar by a rectangular pulse applied at its tip. According to wave theory the pulse will propagate to infinity leaving a constant deformation δ in the bar as shown in the lower half of figure (5.1). In order to check the efficiency of the Ritz vector approach in modeling the problem, the bar, whose characteristics are given in the same figure, is modeled with linear elements. The total number of degrees of freedom is 20. A dashpot is attached to the right end of the bar to simulate the infinite length of the bar.

Sets of 3,5, and 7 Ritz functions are used to reduce the systems of equations. The analysis is carried out by step-by-step integration using the Newmark method, Newmark (1959). Figures (5.2),(5.3),(5.4) and (5.5) show, firstly the approximation to the exact solution obtained by the finite element approach, and secondly the degree of accuracy with which the Ritz functions approximate the finite element solution. As can be seen, the wave pattern and final deformation in the bar are approximated very well by the sets of 5 and 7 Ritz functions. The solution given by the set of 3 Ritz vectors shows significant dispersions at several points. It may be concluded that only a few Ritz vectors provide an excellent approximation to wave propagation problems in one dimension.

5.1.3.- Two dimensions.

The impedance problem shown in Figure (4.8) is now solved again using different sets of Ritz functions. Two cases are considered: first, the horizontal excitation in the half-space, and second, the horizontal excitation of one layer over a rigid bedrock. In both cases the dimensions were $L=8R$. Internal viscous damping and a frequency independent boundary are included. The total number of degrees of freedom in the first and second cases was 428 and 400 respectively.

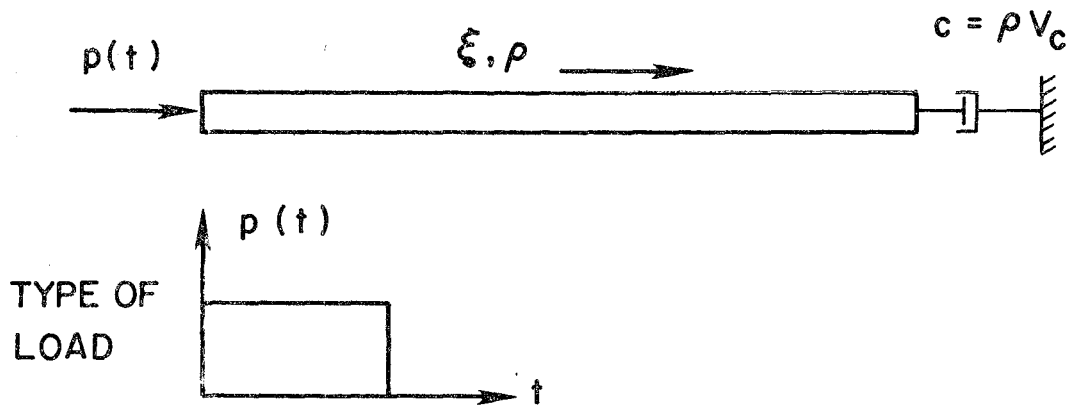
Tables (5.1) and (5.2) show how the results obtained with sets of 5,8,12,16,20,25,35, and 50 Ritz vectors compared with those obtained with the complete set of equations. Maximum errors over the frequency range of study are also shown. By increasing the number of Ritz vectors the approximation converges to the exact solution, and as seen in the tables, the results are outstanding.

W (rad/sec)	DIFFERENT SETS OF RITZ VECTORS								Compl. Set
	5	8	12	16	20	25	35	50	428
2.6	.591	.600	.604	.610	.614	.614	.618	.622	.645
3.9	.550	.556	.563	.571	.572	.572	.575	.577	.613
6.5	.468	.489	.498	.501	.498	.500	.500	.496	.492
9.16	.373	.408	.409	.405	.402	.402	.401	.400	.395
13.0	.320	.320	.315	.313	.314	.313	.312	.312	.310
19.5	.291	.223	.218	.217	.217	.217	.217	.217	.217
26.0	.238	.158	.159	.159	.159	.159	.159	.159	.159
Max Error%	33.0	5.36	4.73	3.79	3.15	3.10	2.5	1.89	

TABLE 5.1 - Amplitudes of the horizontal compliances of a rigid strip footing resting on a viscoelastic halfspace.

DIFFERENT SETS OF RITZ VECTORS									Comp. Set
W(rd/sec)	5	8	12	16	20	25	35	50	400
3.9	.583	.583	.584	.585	.585	.585	.585	.585	.587
6.5	.752	.757	.760	.763	.768	.768	.770	.770	.777
9.16	.541	.531	.520	.509	.504	.502	.496	.494	.482
13.0	.326	.334	.337	.344	.344	.346	.348	.349	.354
19.5	.264	.235	.235	.235	.235	.235	.235	.235	.235
Max Error%	10.91	9.22	7.30	5.30	4.35	3.98	2.82	2.23	

TABLE 5.2 - Amplitudes of the horizontal compliances of a rigid strip footing resting on a layer over a rigid base.



EXACT DISPLACEMENT AT THREE DIFFERENT TIMES :

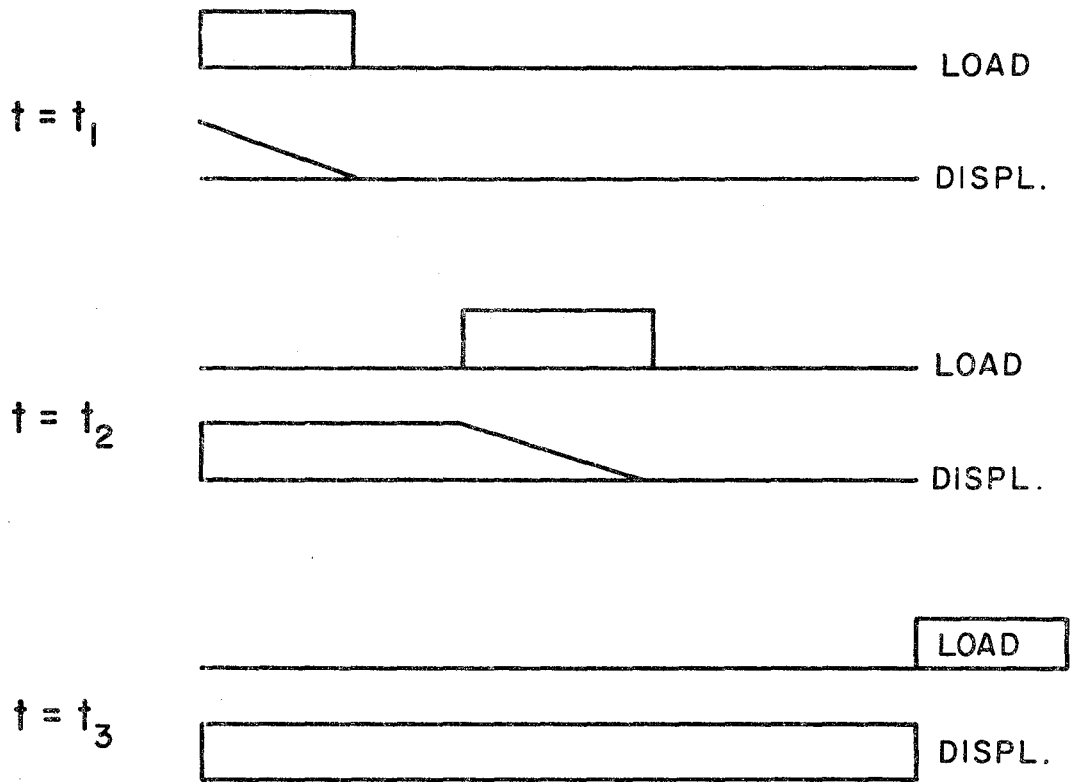


Fig 5.1.- One dimensional wave propagation example.

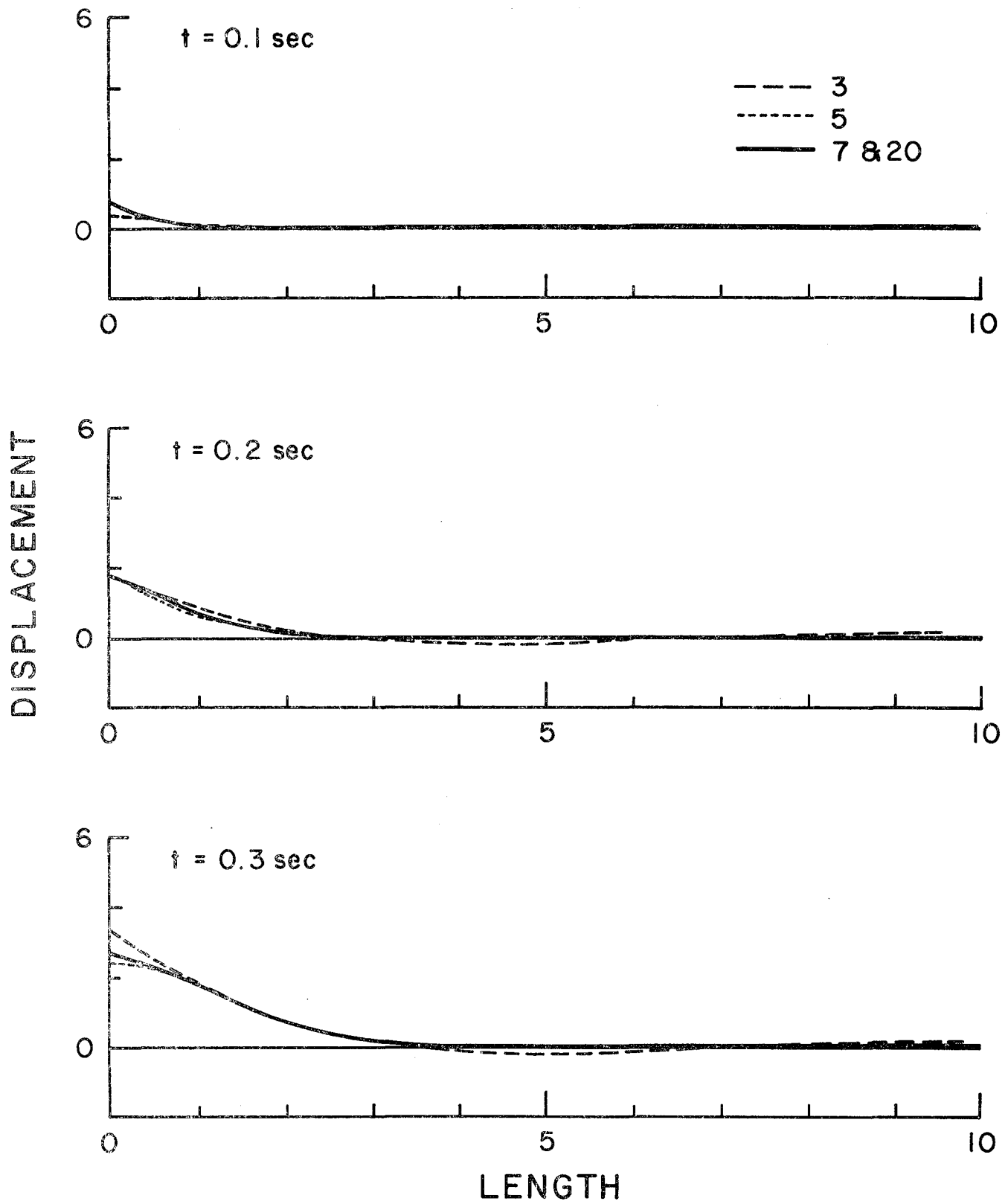


Fig 5.2,- Several instances of the wave front.

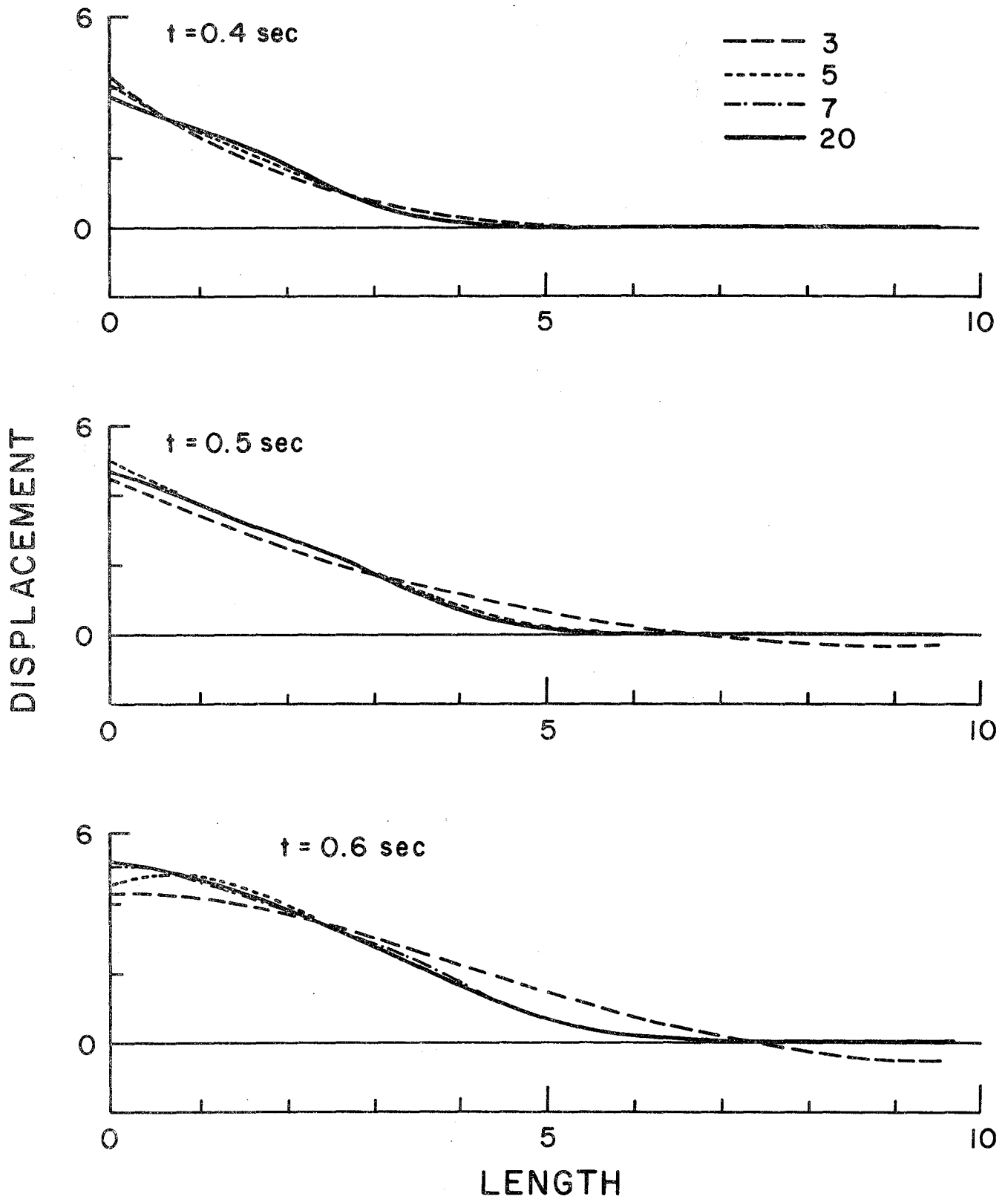


Fig 5.3.

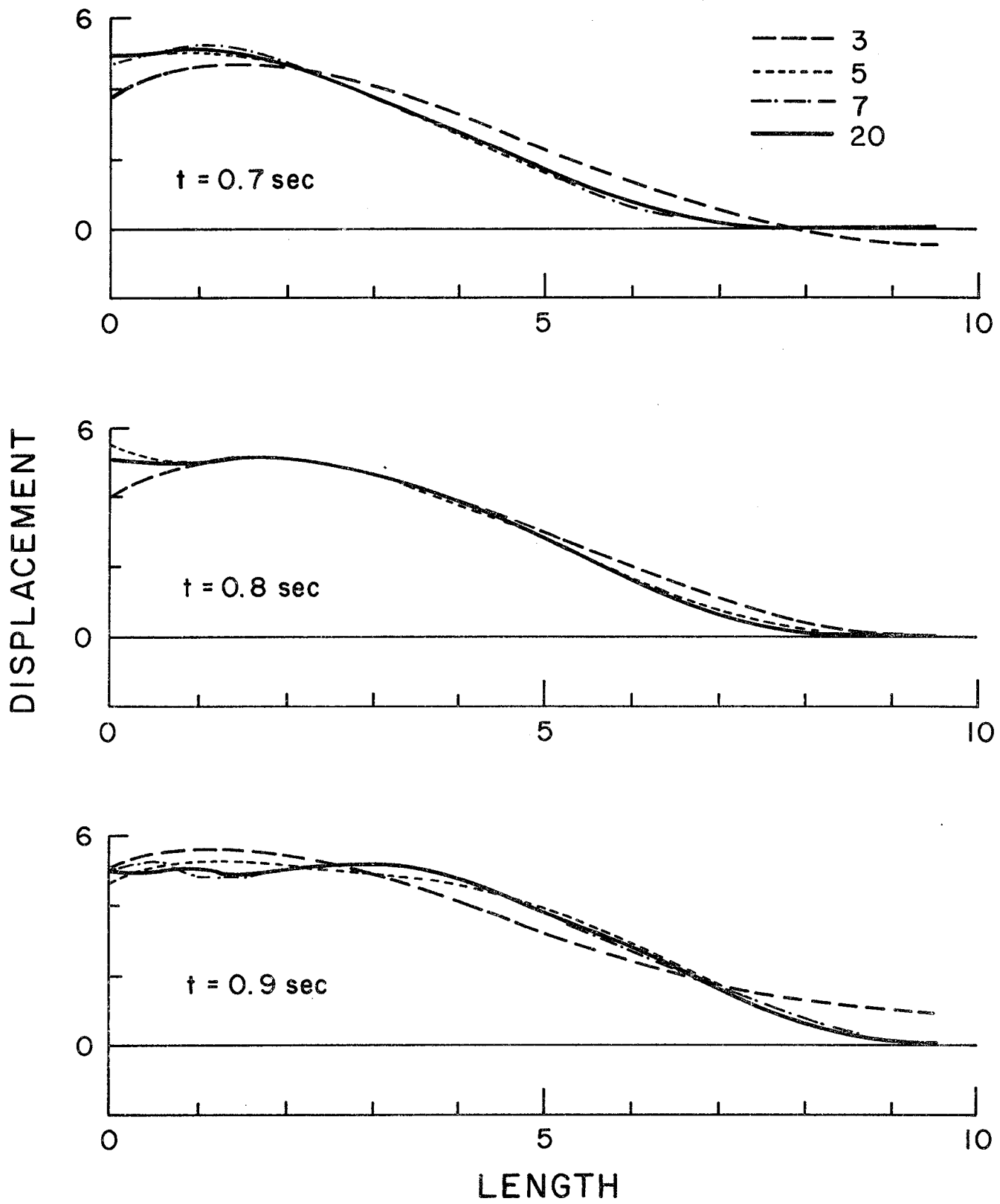


Fig 5.4.

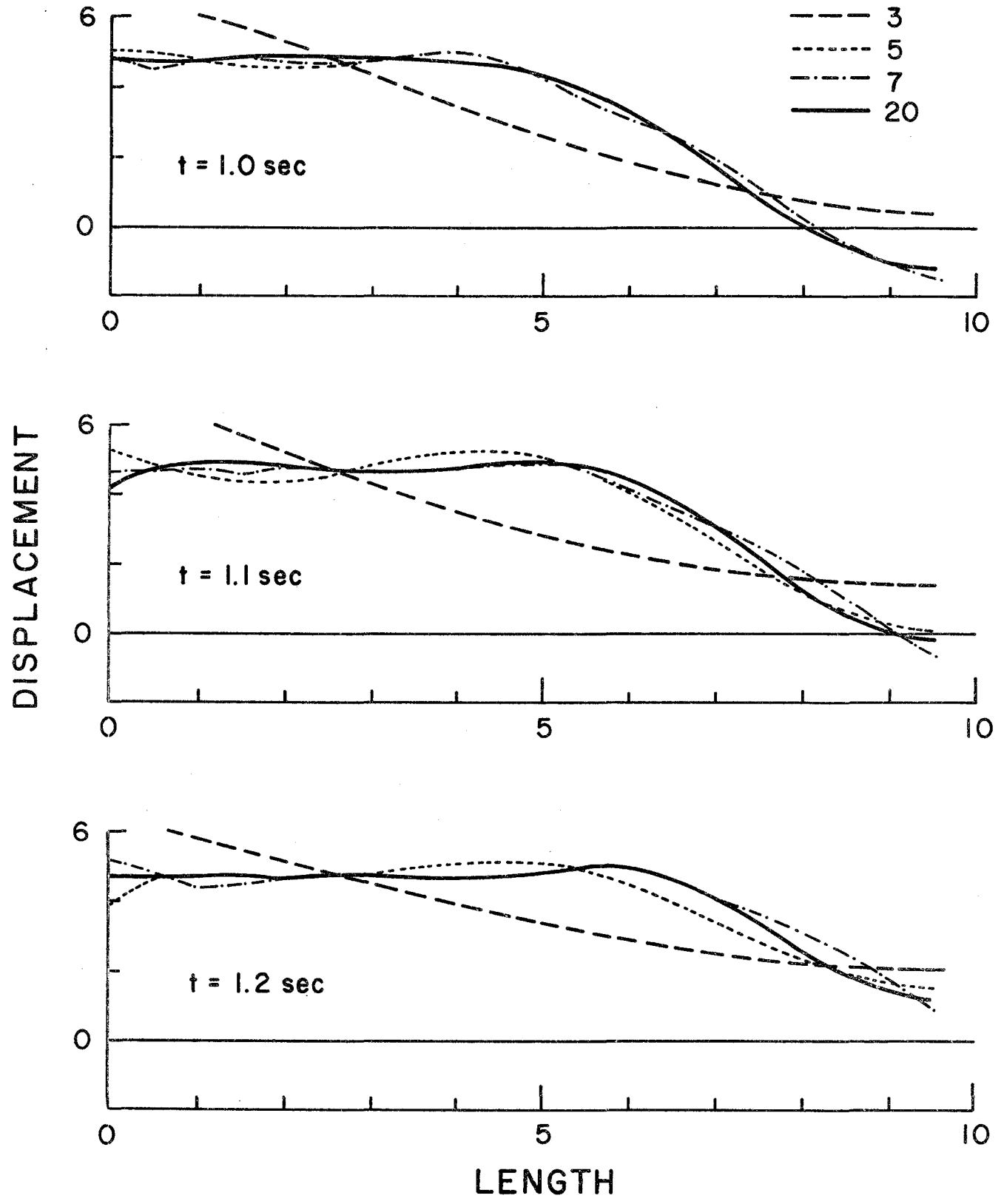


Fig 5.5.

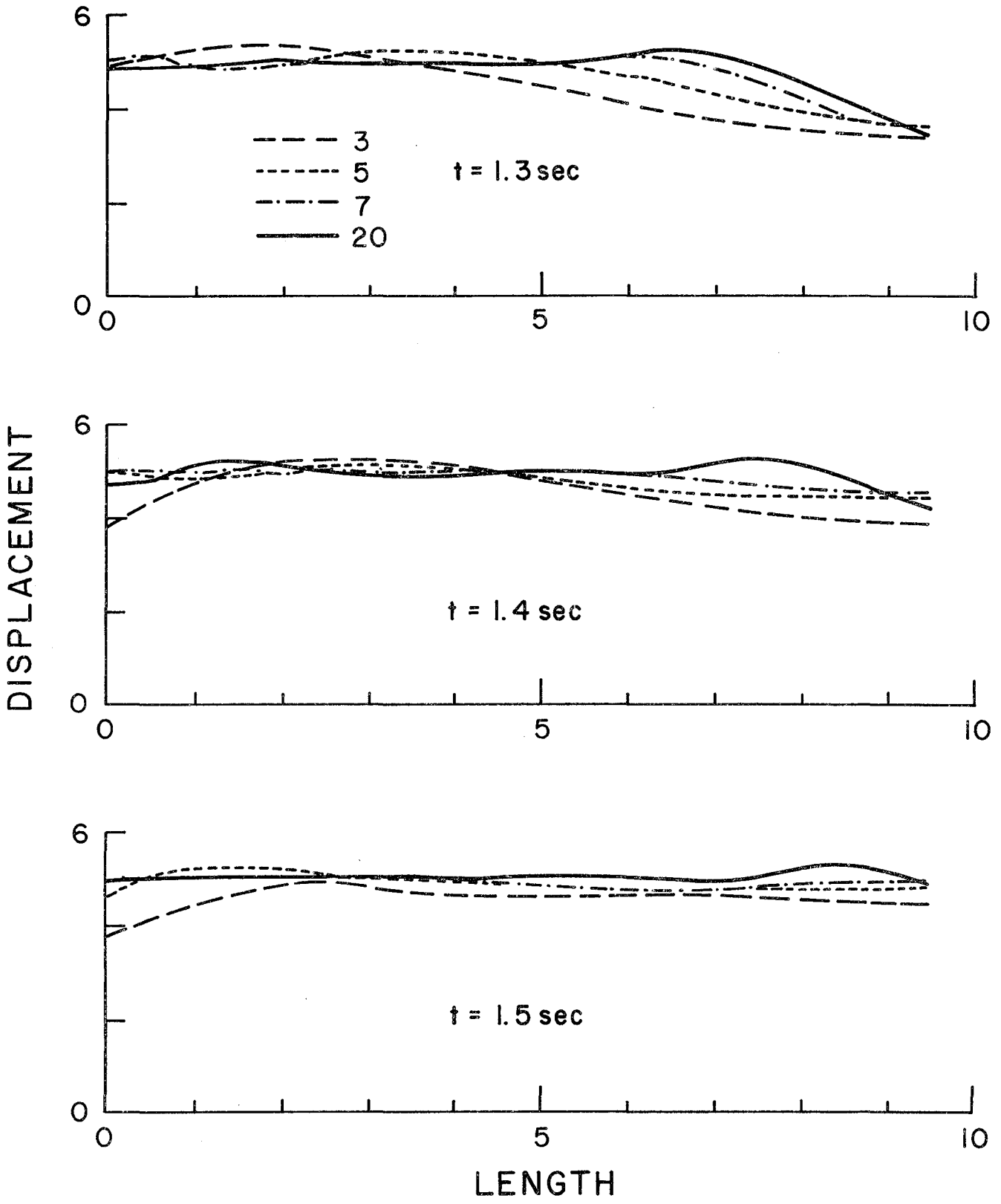


Fig 5.5 (cont.)

For a set of 35 Ritz vectors (less than 10% of the total number of degrees of freedom) the maximum error over the frequency range is 2.5%. The rapid convergence of the Ritz functions to the complete solution for high frequencies is due to the attenuation caused by the viscous damping.

5.1.4.- Three dimensions.

The impedance problem shown in Figure (4.14) is solved again using a set of 63 Ritz vectors which correspond to 10% of the total number of degrees of freedom. Table (5.3) shows the amplitude of the compliance functions obtained with the Ritz vectors and with the complete set of equations. This time no viscous damping is considered. The results show, as expected, more discrepancy in the high frequency range. This is contrary to the two dimensional case where the high frequency content was damped out by the material damping.

CONCLUSIONS.

It has been shown that a small number of Ritz functions suffice to give an excellent approximation not only to structural problems, but to wave propagation problems as well. The necessary number of functions will depend on the degree of accuracy desired for the high frequency content. Global functions fail to represent the propagation of high frequency waves. However, since in general material damping will be included in the soil, the high frequency content will be attenuated and a small set of Ritz functions will provide an excellent approximation throughout the frequency range.

Moreover, for most cases the major part of the structural response is contained in a few modes that are located in the low-medium frequency range. For this range the Ritz vectors provide an excellent approximation as seen above.

W(rd/sec)	Ritz Vect. 63.	Comp.Set 630	Error %
6.5	.873	.871	0.23
13.0	.862	.822	4.64
19.50	.617	.636	2.99
26.00	.400	.447	10.51

TABLE 5.3 - Amplitudes of the vertical compliances of a rigid circular footing resting on an elastic halfspace.

5.2.- SUBSTRUCTURES.

The dynamic substructuring concept is closely related to the idea of reducing the number of degrees of freedom of a certain structural system while retaining at the same time a high accuracy in its dynamic response. The reduction is not done globally as mentioned above, but at the substructure level, and compatibility of displacements and forces at the substructure interfaces generates the complete set of equations of the complete structure. Soil-structure interaction problems invite the idea of dynamic substructuring because of the size of the problem and because the structure (or structures) and the soil can be reduced separately to be coupled together for the global solution.

Many methods have been proposed for dynamic substructuring. The Guyan, Hurty, Hintz, and McNeal methods are several of the most used. Dickens (1980) analyzes them extensively and compares them with the subspace iteration algorithm. In what follows the concepts of each of the methods will be summarized, and a new method will be proposed that is more suitable for soil-structure interaction systems.

5.2.1.- Review of the existing methods of substructuring.

a) Guyan method:

Guyan (1965) proposed a method by which the degrees of freedom of each substructure are divided into master and slave. The slave degrees of freedom are defined in terms of the master ones by means of static condensation. The free vibration equations of a substructure are:

$$\begin{bmatrix} M_s & 0 \\ 0 & M_m \end{bmatrix} \begin{Bmatrix} \ddot{x}_s \\ \ddot{x}_m \end{Bmatrix} + \begin{bmatrix} K_{ss} & K_{sm} \\ K_{ms} & K_{mm} \end{bmatrix} \begin{Bmatrix} x_s \\ x_m \end{Bmatrix} = \begin{Bmatrix} 0 \\ 0 \end{Bmatrix} \quad (5.1)$$

From static condensation

$$x_s = -K_{ss}^{-1} K_{sm} x_m \quad (5.2)$$

thus

$$\begin{Bmatrix} x_s \\ x_m \end{Bmatrix} = \begin{bmatrix} -K_{ss}^{-1} K_{sm} \\ I \end{bmatrix} x_m \quad (5.3)$$

Note that (5.3) represents a set of Ritz vectors which are equal to the static displacements at the slave degrees of freedom obtained from unit displacements at the master degrees of freedom. Using (5.3) as a transformation of coordinates, Equation (5.1) can be reduced to

$$M_{mm} \ddot{x}_m + K_{mm} x_m = 0 \quad (5.4)$$

where

$$\begin{aligned} M_{mm} &= M_m + K_{ms} K_{ss}^{-1} M_s K_{ss}^{-1} K_{sm} \\ K_{mm} &= K_m - K_{ms} K_{ss}^{-1} K_{sm} \end{aligned} \quad (5.5)$$

The application of this technique to dynamic substructuring is very simple. The boundary and selected internal nodes are taken as the master nodes. The inclusion of the boundary nodes allows the direct assemblage of all the substructure Equations, as in the direct stiffness method.

b) Hurty method (Component mode synthesis).

Hurty (1971) used two types of vectors to reduce the substructure system of Equations. First, like in the Guyan's method, the slave degrees of freedom are statically condensed to the boundary ones. In order to represent the dynamic characteristics of the substructure a second set of Ritz functions is formed with the eigenvectors obtained by fixing the boundary. Only a few of these eigenvectors are usually needed. The governing Equations are:

$$\begin{bmatrix} x_s \\ x_m \end{bmatrix} = \begin{bmatrix} \phi_s & -K_{ss}^{-1} K_{sm} \\ 0 & I \end{bmatrix} \begin{bmatrix} y_s \\ y_m \end{bmatrix} \quad (5.6)$$

where the subindices "s" and "m" represent slave and master respectively. The reduction of (5.1) according to (5.6) yields the following transformed stiffness and mass matrices:

$$\begin{aligned} M_{mm} &= \begin{bmatrix} I & -\phi_s^T m_s K_{ss}^{-1} K_{sm} \\ \text{(symm)} & M_m + K_{ms} K_{ss}^{-1} M_s K_{ss}^{-1} K_{sm} \end{bmatrix} \\ K_{mm} &= \begin{bmatrix} [\omega]^2 & 0 \\ 0 & K_m - K_{ms} K_{ss}^{-1} K_{sm} \end{bmatrix} \end{aligned}$$

As in the Guyan method all the boundary degrees of freedom have been retained and therefore the assemblage of each of the substructures into the total system is direct.

c) Hintz and McNeal methods:

Hintz (1976) used the same concept as that the component mode synthesis and proposes as a set of Ritz vectors the eigenvectors of the unrestrained substructure plus a set of vectors obtained from the static solution of unit forces at the boundary degrees of freedom. The transformation is now

$$\begin{Bmatrix} x_s \\ x_b \end{Bmatrix} = \begin{bmatrix} \phi_s & -K_{ss}^{-1} K_{sb} K_{bb}^{-1} \\ \phi_b & K_{bb}^{-1} \end{bmatrix} \begin{Bmatrix} y_s \\ \bar{x}_b \end{Bmatrix}$$

The expressions for the reduced mass and stiffness become more involved for this case and will not be included here. However this is not the main inconvenience. In order to assemble the substructures in the total system, compatibility conditions have to be met. If x_{b1} and x_{b2} represent the boundary displacements between substructure 1 and 2 respectively, the condition to be met is $x_{b1} = x_{b2}$. This means that

$$[(\phi_b)^i (K_{bb}^{-1})^i] \begin{Bmatrix} y_s^i \\ \bar{x}_b^i \end{Bmatrix} = [(\phi_b)^j (K_{bb}^{-1})^j] \begin{Bmatrix} y_s^j \\ \bar{x}_b^j \end{Bmatrix} \quad (5.7)$$

Thus prior to the assemblage of each of the substructures into the total system the above compatibility conditions have to be imposed at each set of connecting substructures.

McNeal's method (1971) is basically the same as the Hintz method with the exception that the eigenvectors are now obtained with at least a statically determinate set of boundary degrees of freedom restrained. Again compatibility conditions have to be satisfied before the assemblage of substructures can be carried out.

5.2.2. Reduction of Equations and dynamic substructuring.

The problem is now to find a substructuring procedure that will most conveniently suit the characteristics of soil-structure interaction systems.

The starting point will be the general Equation of motion in terms of the relative displacements derived for the boundary methods in Section 3.3.2. (The procedure will apply identically the same for the volume methods.) Equation (3.11) is rewritten again here

$$[\tilde{m}_c + m_c] \ddot{v}_c + [\tilde{c}_c + c_c] \dot{v}_c + [\tilde{k}_c + k_c] v_c = - \left[[\tilde{m}_c + m] r_c + \begin{Bmatrix} 0 \\ m_{gg} \\ 0 \end{Bmatrix} \right] \ddot{v}_g \quad (5.8)$$

The subindex "g" may represent either the boundary degrees of freedom for the boundary method or all the buried structural degrees of freedom for the volume methods. In this manner all the subsequent formulation can be applied to both methods simultaneously.

As mentioned before, one way of reducing the total system is by using global Ritz functions. Even though this can not be considered a real substructuring technique it is mentioned here because it will be used later to compare its results with those of the proposed substructuring procedure. Several methods of reducing the Equations of motion of the soil-structure systems are described next.

a) Define the following displacement transformation:

$$\begin{Bmatrix} v_s \\ v_g \\ v_a \end{Bmatrix} = \phi Y$$

Where v_s , v_g and v_a are the displacements at the structure, boundary interface, and soil respectively, and ϕ is a set of global Ritz vectors. Substituting this transformation into Equation (5.8) and premultiplying by ϕ leads to:

$$M^* \ddot{Y} + C^* \dot{Y} + KY = -\phi_i^T [(\tilde{m}_c + m_c) r_c + \begin{Bmatrix} 0 \\ m_g \\ 0 \end{Bmatrix}] \ddot{v}_g \quad (5.9)$$

where

$$\begin{aligned} M^* &= \phi^T [m_c + \tilde{m}_c] \phi \\ K^* &= \phi^T [k_c + \tilde{k}_c] \phi \\ C^* &= \phi^T [c_c + \tilde{c}_c] \phi \end{aligned} \quad (5.10)$$

Call S1 the procedure defined by Equation (5.9).

b) The R.H.S. of Equation (5.9) may be obtained once the mass and the stiffness have already been reduced. This would yield the following Equations:

$$M^* \ddot{\gamma} + C^* \dot{\gamma} + K^* \gamma = - \left[M^* r_c + \phi^T \begin{Bmatrix} 0 \\ m_g \\ 0 \end{Bmatrix} \right] \ddot{v}_g \quad (5.11)$$

where M^* , C^* and K^* are defined in Equation (5.10), and

$$r_c = - (K^*)^{-1} \phi^T \begin{Bmatrix} k_g \\ k_{gg} \\ 0 \end{Bmatrix}$$

Equation (5.11) defines the procedure S2.

Equation (5.11) may be obtained formally from the Equations of motion (3.7) (Section (3.3.2)) that is expressed in terms of the total added displacements by defining the following transformation

$$v_c^t = \begin{Bmatrix} v^t \\ v_g^t \\ v_a^t \end{Bmatrix} = \phi \gamma^t \quad (5.12)$$

where ϕ is the same set of global Ritz functions as that defined in part a. Applying the transformation defined by (5.12), Equation (3.7) becomes:

$$M^* \ddot{\gamma}_c^t + C^* \dot{\gamma}_c^t + K^* \gamma_c^t = - \phi^T \begin{Bmatrix} 0 \\ m_{gg} \\ 0 \end{Bmatrix} \ddot{v}_g - \phi^T \begin{Bmatrix} 0 \\ c_{gg} \\ 0 \end{Bmatrix} \dot{v}_g - \phi^T \begin{Bmatrix} k_g \\ k_{gg} \\ 0 \end{Bmatrix} v_g \quad (5.13)$$

Now we can express γ_c^t as the summation of a dynamic component plus a pseudo-static one. Following the same procedure as that of Section (3.3.2), the generalized coordinates can be expressed as:

$$\gamma_c^t = \gamma_c^d + r_c v_g = \gamma_c^d - (K^*)^{-1} \phi^T \begin{Bmatrix} k_g \\ k_{gg} \\ 0 \end{Bmatrix} v_g$$

thus

$$M^* \ddot{\gamma}_d + C^* \dot{\gamma}_d + K^* \gamma_d = \left[-M^* r_c + \phi^T \begin{Bmatrix} 0 \\ m_{gg} \\ 0 \end{Bmatrix} \right] \ddot{v}_g \quad (5.14)$$

where K^* , C^* and M^* are defined in (5.10) and r_c is:

$$r_c = - (K^*)^{-1} \phi^T \begin{Bmatrix} k_g \\ k_{gg} \\ 0 \end{Bmatrix}$$

Note that the L.H.S. of Equations (5.14) and (5.11) are identical. The R.H.S. of (5.14) is the Ritz approximation to the R.H.S. of (5.11). Once Equation (5.14) is solved for the generalized displacements, the relative coordinates will be $v = \phi y$. The total forces in the structure can be obtained from v .

c) A substructuring procedure that may suit the characteristics of soil-structure interaction problems can be obtained by extending the concepts of the component mode synthesis techniques. Consider the structure-soil system shown in Figure 5.1. The structure and soil can be separated into two different substructures. The displacements of the first may be expressed (as in component mode synthesis) in terms of a set of Ritz vectors obtained considering the structure fixed (see Fig 5.1), plus a set of vectors that statically condensate the structural degrees of freedom to the foundation. The transformation is then:

Superstructure:

$$\begin{Bmatrix} v_s \\ v_g \end{Bmatrix} = \begin{bmatrix} \phi_s & -K_{ss}^{-1} K_{sg} \\ 0 & I \end{bmatrix} \begin{Bmatrix} y_s \\ v_g \end{Bmatrix} = \Phi_s^* y_s \quad (5.15)$$

where Φ_s is the set of Ritz vectors and y_s is the generated Ritz coordinates. Figure 5.1c shows the second substructure, which consists on the soil system plus the foundation. This system is reduced entirely by Ritz vectors according to the following expression:

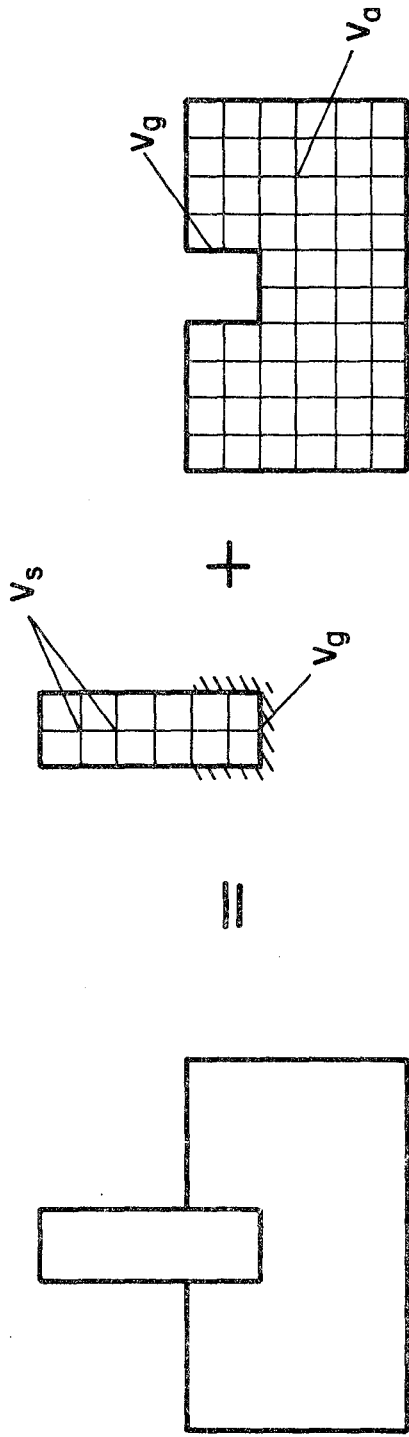
$$\begin{Bmatrix} v_g \\ v_a \end{Bmatrix} = \begin{bmatrix} \phi_g \\ \phi_a \end{bmatrix} y_a \quad (5.16)$$

The assemblage of both substructures can not be done directly, since the boundary displacements in the soil have been expressed in terms of the Ritz coordinates. As in the Hintz method compatibility conditions are necessary at the interface degrees of freedom. These constraints are defined by the first set of Equations of (5.16):

$$v_g = \phi_g y_a \quad (5.17)$$

The substitution of (5.17) into (5.15) yields:

$$\begin{Bmatrix} v_s \\ v_g \end{Bmatrix} = \begin{bmatrix} \phi_s & -K_{ss}^{-1} K_{sg} \\ 0 & I \end{bmatrix} \begin{Bmatrix} 0 \\ \phi_g \end{Bmatrix} \begin{Bmatrix} y_s \\ y_a \end{Bmatrix} = \begin{bmatrix} \phi_s & -K_{ss}^{-1} K_{sg} \phi_g \\ 0 & \phi_g \end{bmatrix} \begin{Bmatrix} y_s \\ y_a \end{Bmatrix} = \Phi_s^* \begin{Bmatrix} y_s \\ y_a \end{Bmatrix} \quad (5.18)$$



(a) SOIL-STRUCTURE SYSTEM (b) STRUCTURE ON FIXED BASE (c) SOIL & FOUNDATION

Fig 5/6.- Substructuring method for soil-structure interaction problems.

Equations (5.17) and (5.18) allow the direct assemblage of the substructure reduced matrices. The reason why a Hurty type of substructuring has not been used here is because the number of degrees of freedom at the foundation ψ will generally be large. They need be reduced as those in other parts of the total system. The compatibility condition imposed in Equation (5.17) is not difficult to implement numerically, since it merely consists of backsubstituting the vectors ϕ_g in the already triangularized superstructure stiffness matrix. Therefore, the vector $-\mathbf{K}_{ss}^{-1} \mathbf{K}_{sg}$ can be obtained directly, without the need to invert \mathbf{K}_{ss} . It is worth noting that the exposed substructure procedure is equivalent to a global transformation defined by the following expression:

$$\begin{Bmatrix} v_s \\ v_g \\ v_a \end{Bmatrix} = \begin{bmatrix} \phi_s & -\mathbf{K}_{ss}^{-1} \mathbf{K}_{sg} \phi_g \\ 0 & \phi_s \\ 0 & \phi_a \end{bmatrix} \begin{Bmatrix} Y_s \\ Y_a \end{Bmatrix}$$

Once the displacements transformation matrices have been defined, the reduction of the substructure mass, stiffness and damping matrices is straightforward:

Structure:

$$\mathbf{M}_s^* = \Phi_s^T \mathbf{M}_s \Phi_s$$

$$\mathbf{C}_s^* = \Phi_s^T \mathbf{C}_s \Phi_s$$

$$\mathbf{K}_s^* = \Phi_s^T \mathbf{K}_s \Phi_s$$

Soil:

$$\mathbf{M}_a^* = \Phi_a^T \mathbf{M}_a \Phi_a$$

$$\mathbf{C}_a^* = \Phi_a^T \mathbf{C}_a \Phi_a$$

$$\mathbf{K}_a^* = \Phi_a^T \mathbf{K}_a \Phi_a$$

The assemblage of the substructure matrices will yield the total matrices \mathbf{M}^* , \mathbf{C}^* , and \mathbf{K}^* . Due to the particular nature of the soil-structure interaction problem, the load vector has to be computed once the mass, stiffness and damping of the total system have been formed. After assembling, the Equations of the system are similar to Equation (5.14)

$$\mathbf{M}^* \ddot{\mathbf{y}} + \mathbf{C}^* \dot{\mathbf{y}} + \mathbf{K}^* \mathbf{y} = \left[-\mathbf{M}^* \mathbf{r}_c + \Phi^T \begin{Bmatrix} 0 \\ m_{gg} \\ 0 \end{Bmatrix} \right] \ddot{\mathbf{y}}_g \quad (5.19)$$

where

$$\mathbf{r}_c = -(\mathbf{K}^*)^{-1} \Phi_s^T \begin{Bmatrix} k_g \\ k_{gg} \\ 0 \end{Bmatrix} \quad (5.20)$$

and Φ_s^* is given by Equation (5.18).

Substituting (5.18) in (5.20) and (5.19), the R.H.S. of (5.19) becomes:

$$-(M^*)(K^*)^{-1} \begin{Bmatrix} \phi_s^T k_g \\ -\phi_g^T k_{sg} k_{ss}^{-1} k_{sg} + \phi_g^T k_{gg} \end{Bmatrix} + \begin{Bmatrix} 0 \\ \phi_g^T m_g \end{Bmatrix}$$

Note that the vectors (1) and (2) in (5.21) may be formed in the structure at the substructure level. The last step is to compute $M^*(K^*)^{-1}$. The complete reduced system is now ready for numerical integration. Equation (5.21) defines the procedure S3 for subsequent computations.

5.2.3.-Numerical example.

To check the methods considered in section 5.3.2 a small numerical example is carried out. A fictitious soil-structure system is modeled with a 8 degrees of freedom shear beam model that is illustrated in Figure 5.2. The fundamental period of the structure on a fixed base is 0.4 sec, and that of the soil alone is 0.5 sec. The fundamental period of the ensemble is 0.625 sec, which shows that there is significant interaction between both systems.

The soil-structure model is subjected to a free field motion equal to the W-E component of the Taft earthquake. The Equations of motion are integrated numerically by the Newmark step-by-step integration procedure. The time step is chosen sufficiently small to avoid numerical perturbation. The system is solved using the following different approaches:

- 1.- A complete run is made (8 dofs) to obtain the master solution.
- 2.- The system is reduced with sets of 1,2,3, and 4 eigenvectors and solved according to the procedure S1 explained above.
- 3.- The system is reduced with sets of 1,2,3, and 4 Wilson-Yuan Ritz vectors and solved according to the procedure S1.
- 4.- The system and load vector are reduced with sets of 1,2,3 and 4 Wilson-Yuan Ritz vectors and solved according to procedure S2.
- 5.- The system is solved with sets of Wilson-Yuan vectors in the soil and structure

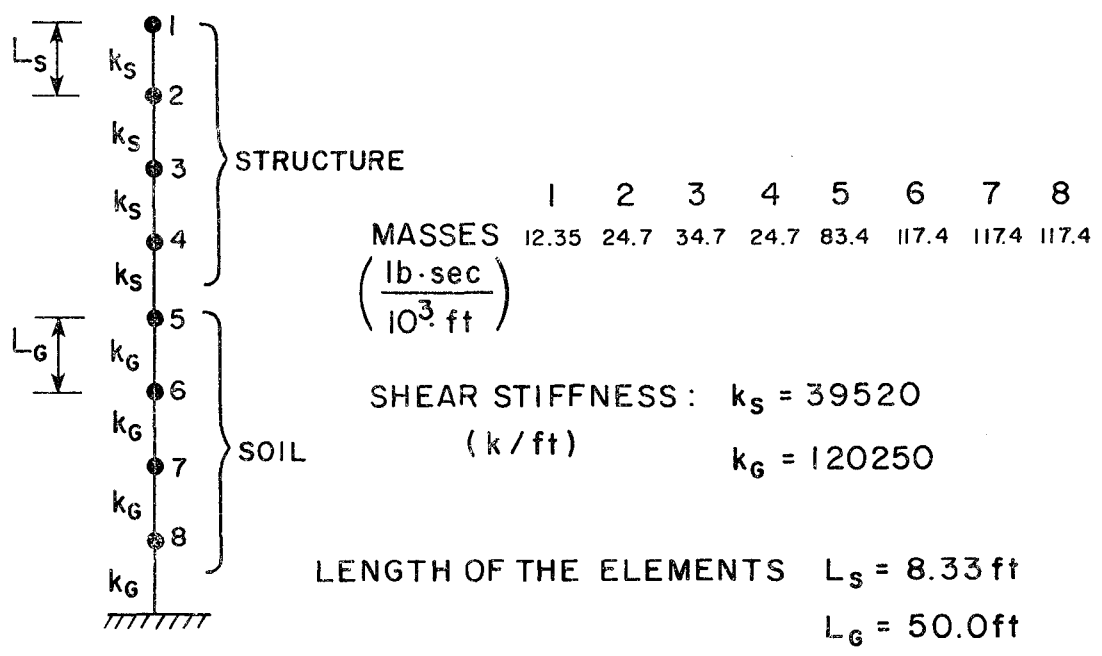


Fig 5.7.- Characteristics of a fictitious soil-structure system.

using the substructuring procedure S3.

The maximum displacements and story forces obtained by the different methods are given in Table 4. Comparisons are made with respect to the complete model. In view of the results the following comments may be made:

* All the methods give good results that converge to the complete solution as the number of Ritz vectors is increased.

* Differences between the third and fourth approaches are very small. This demonstrates that the assumption of approximating the R.H.S. of the Equation of motion with Ritz vectors is feasible.

* Errors resulting from reducing the system with eigenvectors in one side and Ritz functions in the other are of the same order of magnitude. The eigen solution provides an approximation to the the exact solution from below, whereas that provided by the Wilson-Yuan Ritz vectors oscillates with respect to it. For instance, the three vector solution with Wilson-Yuan Ritz vectors gives a better response than the eigenvectors, while the four vector solution is better using the eigenvectors, although the differences between them are very small.

* The substructuring approach also gives very good results. The solution obtained with two Ritz functions in the structure and 2 in the soil gives an approximation of the same order as that obtained with four global vectors.

Conclusion:

a) The Wilson-Yuan Ritz vectors and the eigenvectors give solutions with the same degree of approximation. Since the Ritz vectors are obtained with much less computational effort than the eigenvectors, they become a better candidate for the solution of soil-structure interaction problems where the sizes of the models are quite large.

b) The substructuring procedure defined in Section 5.3.2 renders very good results. Again due to the effectiveness and the simple way by which the Ritz vectors are obtained, this substructuring method becomes not only ideal for soil-structure interaction problems, but also for general dynamic substructuring.

1 VECTOR 2 VECTORS 3 VECTORS 4 VECTORS

	Disp	Shear	Disp	Shear	Disp	Shear	Disp	Shear
EIGENVECTORS	.355	40.59	.443	86.0	.443	86.5	.445	93.6
	.344	78.8	.422	159.6	.423	160.3	.423	160.2
	.314	71.8	.366	124.7	.366	124.6	.364	132.5
	.266	60.8	.283	73.96	.283	75.4	.277	104.3
	.202	-252.2	-.210	-444.0	-0.211	-444.3	-.211	-445.1
RITZ VECTORS 1	.559	83.3	.440	67.2	.445	87.7	.444	87.8
	.538	166.7	.423	135.8	.424	159.4	.423	161.6
	.474	166.7	.374	140.6	.364	127.7	.364	127.4
	.369	166.7	.291	-151.2	.274	139.2	.278	122.4
	.222	-583.4	-.209	-492.0	-.211	-442.2	-.211	-438.1
RITZ VECTORS 2	.754	112.3	.443	69.9	.446	90.3	.444	96.8
	.725	224.6	.426	142.3	.424	161.2	.423	161.8
	.640	224.6	.375	150.0	.363	127.3	.365	127.0
	.498	224.6	.289	-171.7	.274	154.5	.277	127.2
	.299	-783.2	-.208	-525.1	-.211	-443.1	-.211	-437.5
SUBSTRUCTURING	1 Soil/1 Str	1 Soil/2 Str	1 Soil/3 Str	2 Soil/2 Str	2 Soil/3 Str	2 Soil/3 Str	2 Soil/3 Str	2 Soil/3 Str
	.489	79.4	0.486	95.37	.488	102.7	.445	87.9
	.471	158.85	.462	174.8	.462	171.1	.424	163.1
	.417	158.7	.396	134.8	.392	163.8	.364	124.6
	.327	158.8	.300	157.9	.302	129.9	.278	128.7
	-.250	-555.7	-.239	-471.9	-.239	-467.8	-.211	-436.4

COMPLETE MODEL

Disp	Shear
.446	91.6
.426	161.0
.363	132.2
.277	112.6
-.211	-443.6

TABLE 5.4 - Maximum displacements and shears at the structure for different substructuring methods.

CHAPTER 6

SOLUTION TO THE SCATTERING AND NON-LINEAR PROBLEMS

6.1.- SCATTERING PROBLEM:

As we have seen throughout the time domain formulation, in order to solve the soil-structure interaction problem of an embedded structure by the boundary method, a scattering problem needs to be solved first. This is the only way in which the motions at the interface between soil and structure may be computed. So far, in the literature that deals with this problem, the only method that is given to solve the scattering problem is to model the scattering field with finite elements and to introduce the input motion at the rock basement, as shown in the figure below.

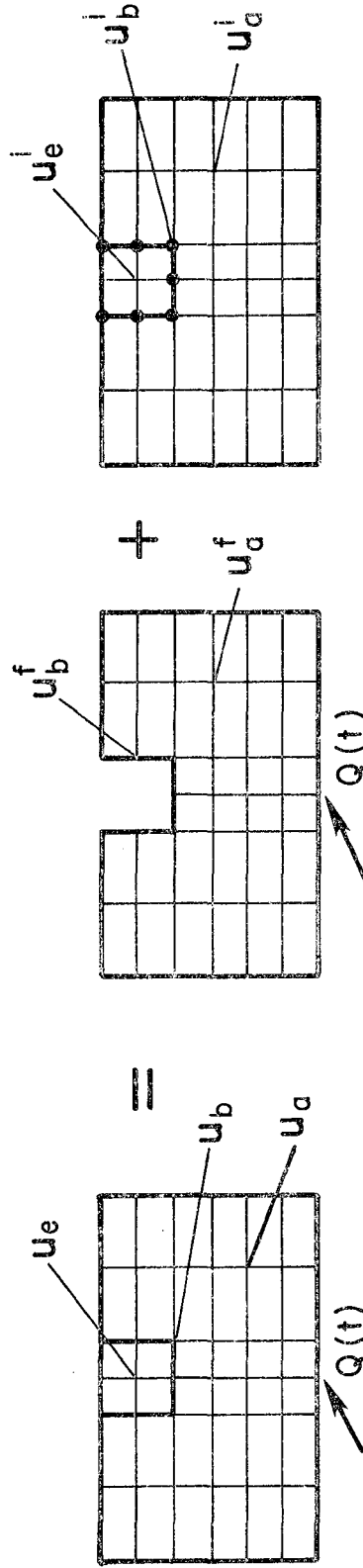
In what follows, a new method is presented that makes use of the superposition principle to define the equations of motion in terms of the free field accelerations at the excavated part of the soil. Since the motion is defined at the soil-structure interface (inside the model) the input does not interfere with the transmitting boundaries placed at the edges of the model. A reduction on the size of the model can be achieved by using the Wilson-Yuan Ritz functions as explained in Chapter 5.

Using the principle of superposition the free field problem can be divided into two parts as illustrated in Figure 6.1. The first one corresponds to the scattering problem and the second to the interaction problem. The general equations for the total system are! (Damping terms are not included for simplification.)

$$M\ddot{u} + Ku = Q(t) \quad (6.1)$$

and for the scattering:

$$M_f \ddot{u}_f + K_f u_f = Q(t) \quad (6.2)$$



(a) FREE FIELD

(b) SCATTERING PROBLEM

(c) ADDED MOTIONS

$$u = \begin{Bmatrix} u_e \\ u_b \\ u_a \end{Bmatrix}$$

$$u^f = \begin{Bmatrix} 0 \\ u_b^f \\ u_a^f \end{Bmatrix}$$

$$u^i = \begin{Bmatrix} u_e^i \\ u_b^i \\ u_a^i \end{Bmatrix}$$

• INPUT MOTION

Fig 6.1.1.- Decomposition of the free field problem for the solution of the scattering problem.

applying the superposition principle:

$$U = U_i + U_f \quad (6.3)$$

or

$$U_f = U - U_i$$

The substitution of (6.6) and (6.1) in (6.2) yields:

$$M_f \ddot{U} - M_f \ddot{U}_i + K_f U - K_f U_i = M \ddot{U} + K U$$

arranging terms:

$$M_f \ddot{U}_i + K_f U_i = (M_f - M) \ddot{U} + (K_f - K) U \quad (6.4)$$

Equation (6.4) can be solved for the added motions and U_f may be obtained from (6.3).

The physical property matrices are:

$$M = \begin{bmatrix} m_e & 0 & 0 \\ 0 & m_b & 0 \\ 0 & 0 & m_a \end{bmatrix}$$

$$K = \begin{bmatrix} k_{ee} & k_{eb} & 0 \\ k_{be} & k_{bb} & k_{ba} \\ 0 & k_{ab} & k_{aa} \end{bmatrix}$$

and

$$M_f = \begin{bmatrix} 0 & 0 & 0 \\ 0 & m_b^* & 0 \\ 0 & 0 & m_a \end{bmatrix}$$

$$K_f = \begin{bmatrix} 0 & 0 & 0 \\ 0 & k_{bb}^* & k_{ba} \\ 0 & k_{ab} & k_{aa} \end{bmatrix}$$

Equation (6.4) becomes:

$$\begin{bmatrix} 0 & 0 & 0 \\ 0 & m_b^* & 0 \\ 0 & 0 & m_a \end{bmatrix} \begin{Bmatrix} \ddot{U}_e^i \\ \ddot{U}_b^i \\ \ddot{U}_a^i \end{Bmatrix} + \begin{bmatrix} 0 & 0 & 0 \\ 0 & k_{bb}^* & k_{ba} \\ 0 & k_{ab} & k_{aa} \end{bmatrix} \begin{Bmatrix} U_b^i \\ U_a^i \end{Bmatrix} = \begin{bmatrix} -m_e & 0 & 0 \\ 0 & m_b^* - m_b & 0 \\ 0 & 0 & 0 \end{bmatrix} \begin{Bmatrix} \ddot{U}_e \\ \ddot{U}_b \\ \ddot{U}_a \end{Bmatrix} + \begin{bmatrix} -k_e & -k_{eb} & 0 \\ -k_{be} & k_{bb}^* - k_{bb} & 0 \\ 0 & 0 & 0 \end{bmatrix} \begin{Bmatrix} U_e \\ U_b \\ U_a \end{Bmatrix}$$

The first equation vanishes. The second and third become:

$$\begin{bmatrix} m_b & 0 \\ 0 & m_a \end{bmatrix} \begin{Bmatrix} \ddot{U}_b^i \\ \ddot{U}_a^i \end{Bmatrix} + \begin{bmatrix} k_b & k_{ba} \\ k_{ab} & k_{aa} \end{bmatrix} \begin{Bmatrix} U_b^i \\ U_a^i \end{Bmatrix} = \begin{Bmatrix} m_b^* - m_b \\ 0 \end{Bmatrix} \ddot{U}_b + \begin{Bmatrix} -k_{be} U_e - k_b^* U_b \\ 0 \end{Bmatrix} \quad (6.5)$$

Equation (6.5) is in terms of the added displacements. Note that the load vector is defined at the interface degrees of freedom.

Once the added motions u_b^i are known, the motions of the scattering problem are obtained from:

$$u_{fb} = u_b - u_b^i$$

Equation (6.5) can be expressed in terms of the accelerations by simply considering the total displacements as the sum of quasi-static plus dynamic displacements:

$$u^i = U^r + r \begin{Bmatrix} u_b \\ u_e \end{Bmatrix} \quad (6.6)$$

thus

$$r = \begin{bmatrix} k_b & k_{ba} \\ k_{ab} & k_{aa} \end{bmatrix}^{-1} \begin{bmatrix} k_i & k_e \\ 0 & 0 \end{bmatrix}$$

Substituting (6.6) into (6.5) we get:

$$M\ddot{U}^r + KU^r = \begin{Bmatrix} m_b^* - m_b \\ 0 \end{Bmatrix} \ddot{u}_b + Mr \begin{Bmatrix} \ddot{u}_b \\ \ddot{u}_e \end{Bmatrix} \quad (6.7)$$

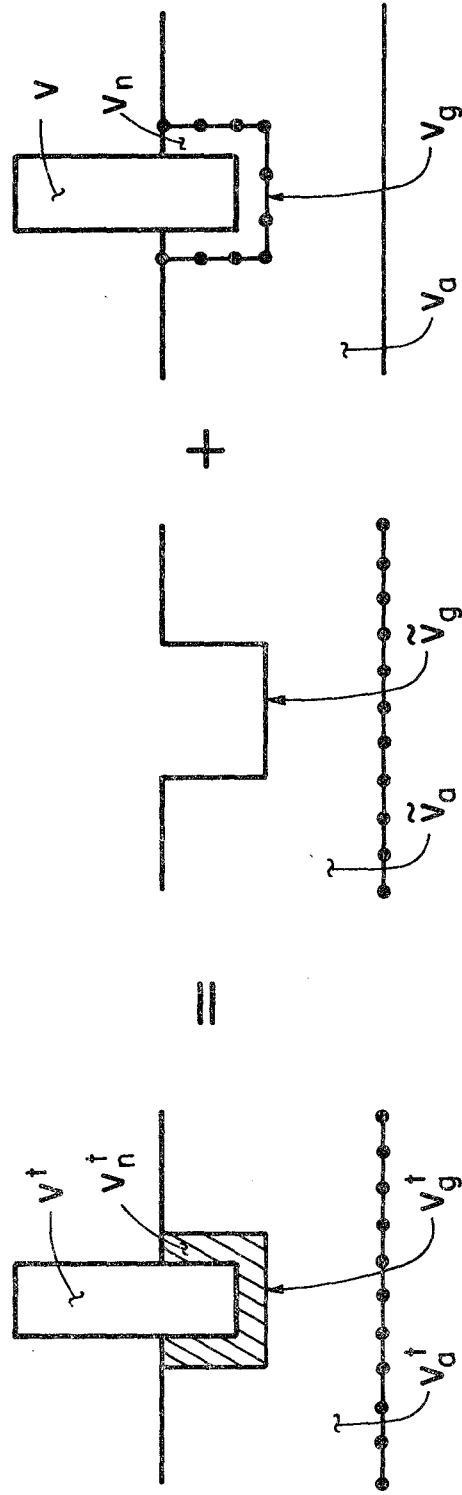
Equation (6.7) is expressed in terms of the accelerations only. This equation may be further simplified by reducing the number of degrees of freedom by the techniques explained in Chapter 5.

6.2.- NONLINEAR ANALYSIS:

The concepts used so far can be easily extended to include nonlinearities in the soil near the foundation of the structure. Consider the case of a soil-structure system in which the portion of soil close to the foundation (see Figure (6.2)) may behave nonlinearly due to the uplifting of the structure or plastic behavior of the material.

As shown in the Figure, v^t , v_n^t , v_g^t and v_a^t represent the total motions at the structure, the nonlinear part of the soil, the boundary interface, and the linear part of the soil respectively. The total displacements may be divided, as done in the boundary methods, into the added v_c^t plus the free field \tilde{v}_c^t .

$$\tilde{v}_c^t = \begin{Bmatrix} 0 \\ 0 \\ \tilde{v}_g^t \\ \tilde{v}_a^t \end{Bmatrix} \quad \text{and} \quad v_c^t = \begin{Bmatrix} v \\ v_n \\ v_g \\ v_a \end{Bmatrix}$$



(a) COMPLETE NONLINEAR PROBLEM (b) SCATTERING PROBLEM (c) ADDED PROBLEM

● POINTS AT WHICH THE INPUT MOTIONS ARE SPECIFIED.

Fig 6.2.- Two step solution for the nonlinear problem.

As can be seen the added motions contain the total displacements of the structure and the nonlinear part of the soil. Therefore Equation (3.7) that is rewritten below is perfectly suitable for nonlinear analysis in those regions.

$$[\bar{m}_c + m] \ddot{v}_c^t + [\bar{c}_s + c] \dot{v}_c^t + [\bar{k}_c + k] v_c^t = - \begin{Bmatrix} 0 \\ m_g \\ m_{gg} \\ 0 \end{Bmatrix} \ddot{v}_g - \begin{Bmatrix} 0 \\ c_g \\ c_{gg} \\ 0 \end{Bmatrix} \dot{v}_g - \begin{Bmatrix} 0 \\ k_g \\ k_{gg} \\ 0 \end{Bmatrix} v_g$$

The solution to this problem may be achieved in two steps:

1) Solve the scattering problem according to Section 6.1, in order to obtain the motions at the boundary, \ddot{v}_g , that constitute the input of the interaction problem, (Equation (3.7)).

2) Solve Equation (3.7) for the added displacements. The total displacements in the nonlinear part of the soil and the structure will be given directly. Since the nonlinearities are localized at the foundation level, the elastic part of soil and structure can be reduced by using Wilson-Yuan Ritz functions and the substructuring techniques explained in Chapter 5. The reduced elastic components can then be coupled to the nonlinear part, and only the latter needs to be modified during the response analysis, Clough and Wilson (1979).

CHAPTER 7

MODELING AND SOLUTION OF SOIL-STRUCTURE INTERACTION PROBLEMS IN THE TIME DOMAIN

7.1.- MODELING THE SOIL-STRUCTURE SYSTEM:

So far all the techniques presented are aimed at modeling the soil-structure problem in the time domain. The main concern in saving computer time and storage is to reduce the size of the finite element model and maintain at the same time a high level of accuracy. Thus, the frequency independent boundary and the reduction of the number of degrees of freedom by substructuring techniques are of most importance. In this section a general technique for geometrically modeling the soil-structure system is explained. This technique is based on the combined use of solid and axisymmetric elements to model the soil in the near and far field respectively.

Figure (7.1) shows the way of modeling a general soil-structure system. A certain structure will be represented with standard finite elements. The foundation of the structure will be attached to 8 to 27 node solid elements (see Appendix B) that will extend throughout the near field region of the soil. At a certain distance from the structure the behavior tends to be similar to that of an axisymmetric system with non axisymmetric loads. The far field then, can be modeled by several harmonic expansions of axisymmetric finite elements (See Appendix A).

In order to couple both the near and the far fields, the displacements corresponding to the solid elements at the boundary between both regions are expanded in terms of Fourier series. The corresponding displacement transformation matrices are used to transform the solid mass, stiffness, and damping matrices of the solid elements in contact with the axisymmetric mesh. All the operations are carried out at the element level. (See Appendix B).

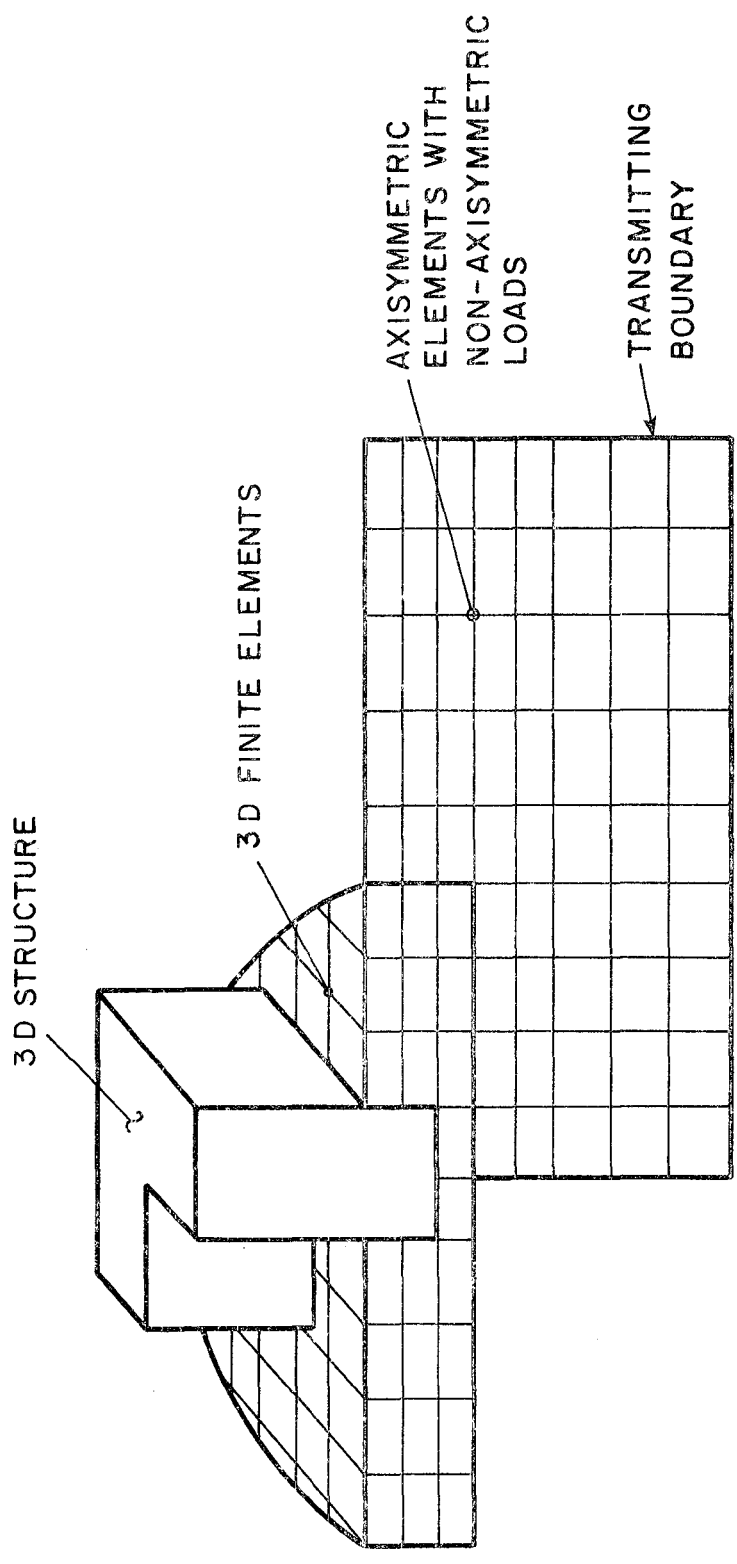


Fig 7.1.- Modeling of the soil-structure interaction problems.

The frequency independent boundary can now be attached to the edges of the model, and the substructuring techniques can be used to reduce the systems of equations. The maximum size of the element is controlled by the size of the wave length corresponding to the maximum frequency to be correctly transmitted through the finite element mesh. For linear elements the size recommended is $h = \lambda / 8$ for lumped mass matrices, where h is the length of the element and λ is the minimum wave length to be transmitted accurately, Lysmer and Kulhemeyer (1973). For quadratic elements the size of the element can be extended to $\lambda / 4$.

7.2.- DAMPING.

Generation of damping matrices presents special difficulties. The internal energy dissipation mechanisms in soils and structures depend on many factors that are difficult or almost impossible to account for analytically in a deterministic way. Usually all the damping effects are considered by defining damping ratios in the natural modes of vibration. Some of the bases for assigning those values are harmonic vibration tests, ambient vibration measurements and recorded response during earthquakes.

Damping ratios are different for different materials, and for a given material they vary with the level of strain at which that material is behaving. Thus for a soil-structure system different damping ratios will be defined; those corresponding to the different structural materials (steel-concrete), and to the different types of soil composing the site. The use of distinct damping ratios leads irremediably to nonproportional damping matrices that can not be diagonalized by the undamped mode shapes and frequencies. Due to the variation of damping ratios for different parts of the structure, the damping matrices will have to be defined at the element level.

Viscous damping has been the common assumption in time domain calculations. For a viscous mechanism the viscous forces are proportional to the velocity:

$$f_v = C \dot{v}(t)$$

Where C is the viscous damping matrix.

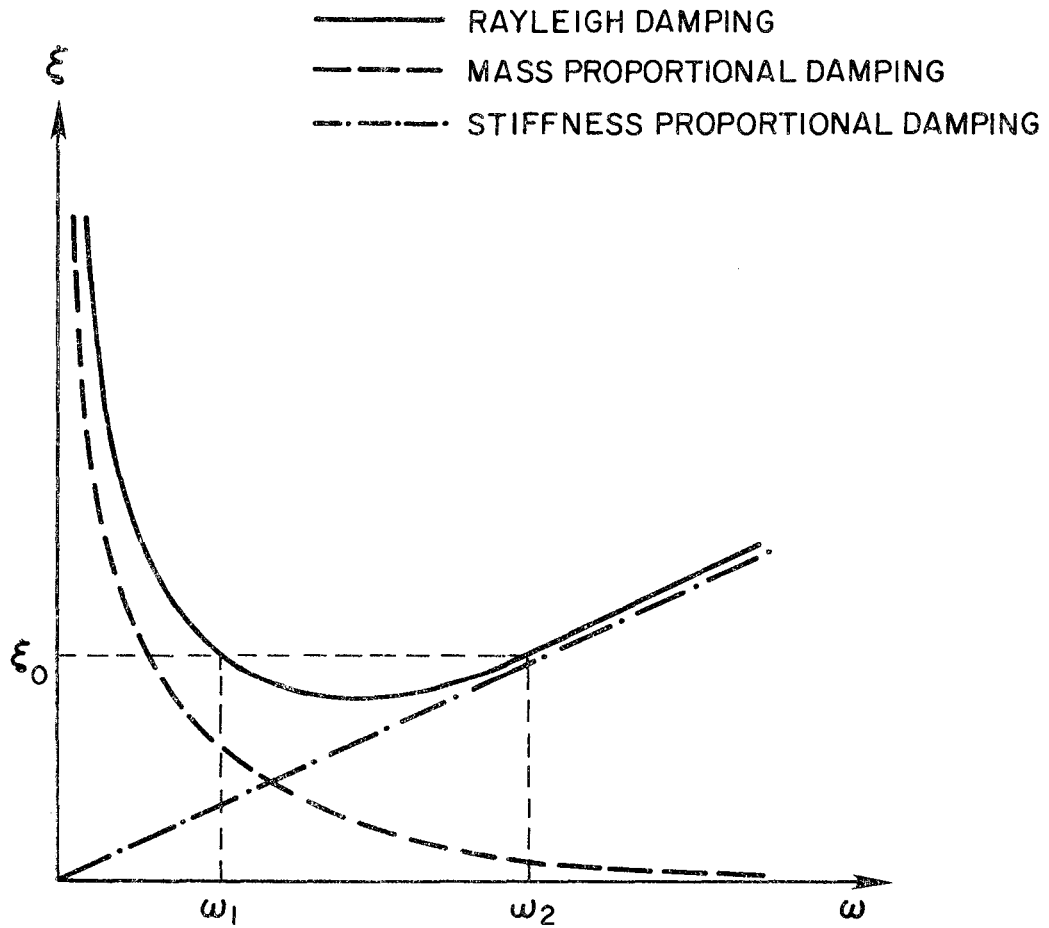


Fig 7.2.- Variation of the Rayleigh damping ratio with respect to frequency.

The matrix C can be defined in terms of Caughey series (1960) :

$$C = \sum_{n=0}^N a_n M (M^{-1}K)^n$$

This provides a proportional damping matrix. The Rayleigh damping model, proposed by Rayleigh much before the Caughey series were developed, happens to coincide with the first two terms of these series:

$$C = a M + b K$$

The coefficients a and b are obtained by matching the damping ratio at two different frequencies. Their general expression is: (Clough and Penzien 1975)

$$\begin{bmatrix} a \\ b \end{bmatrix} = \frac{2\xi}{\omega_n + \omega_m} \begin{bmatrix} \omega_n \omega_m \\ 1 \end{bmatrix} \quad (7.1)$$

where ω_1 and ω_2 are the frequencies at which a certain damping ratio ξ is specified. The damping ratio at other frequencies is defined by the following relation:

$$\xi = \frac{a}{2\omega} + \frac{b\omega}{2}$$

The variation of ξ with respect to frequency is shown in Figure (7.2). A viscous damping mechanism yields an energy loss per cycle that is dependent on frequency:

$$E = \pi C A^2 \omega$$

where ω is the frequency and A the amplitude of a harmonic excitation. Consequently, this formulation leads to large damping ratios and increasing energy loss at high frequencies, which means that the high frequency content of the response will be numerically much more damped than the low frequency content. This behavior although in agreement with the comportment of fluids and gases, is in contrast with the observation that for structural and soil materials, damping ratios differ very slightly with respect to frequency.

As a consequence, the Expression (7.1) has to be used very judiciously when applied to soil-structure systems, by selecting those values of ω_1 and ω_2 that will keep the variation of the damping ratio as constant as possible within the desired frequency interval. Kalvhati (1981), developed an optimized Rayleigh damping based on the application of least squares techniques to minimize the distance between a horizontal line of constant damping and the Rayleigh damping curve.

The hysteretic type of damping leads to a damping ratio and an energy dissipation mechanism that are independent of frequency, and consequently becomes a better candidate for the representation of soil and structural damping. A hysteretic damping mechanism is defined as that for which the damping forces are proportional to the amplitude of the displacements but have the direction of the velocity:

$$f_v = \beta k |v| \frac{\dot{v}}{|v|} \quad (7.2)$$

It can be demonstrated that the damping ratio is now constant throughout the frequency range. The energy loss per cycle is frequency independent and equal to:

$$E = 2\beta k A^2$$

where β is a hysteretic damping coefficient and k the generalized stiffness. Again A is the amplitude of the response.

The direct use of Expression (7.2) leads to a nonlinear set of dynamic equations. The nonlinearity can be eliminated in a step-by-step integration by defining the damping terms at the beginning of each time step from the values of displacements and velocities of the previous step, and by transferring them to the R.H.S. of the equation. Since the damping forces are generally small, the errors introduced are negligible provided that the numerical integration is carried out with a small time step. Kalvhati (1978). This will insure that sudden jumps in the absolute values of the displacements or the direction of the velocity do not take place.

The relation between the hysteretic damping coefficient and the damping ratio can be stated by equating the energy loss per cycle. This yields the following relation:

$$2\beta k A^2 = \pi c A^2 \omega$$

Thus

$$\beta = \pi \zeta$$

In the frequency domain the hysteretic damping can be accounted for by the use of complex stiffness matrices. The damping force is defined as

$$f_D = i n k y$$

where k is the stiffness matrix and n the hysteretic damping factor.

The energy loss per cycle is again independent of frequency and equal to

$$E = \pi n k A^2$$

Again by equating the energy loss per cycle for a viscous and hysteretic mechanism, we can get the following relation between the damping ratio and the hysteretic damping coefficient:

$$n = 2\xi$$

The general transfer function in the frequency domain becomes:

$$H(\bar{\omega}) = [k - m\bar{\omega}^2 + i n k]$$

It can be seen how easy it is to implement this type of damping in the frequency domain, but for obvious reasons is not possible to use it in the time domain.

After this discussion, the question still remains as to what is the best solution for the time domain approach. Two alternate solutions are proposed:

*- The first one is to introduce hysteretic damping at the element level with a hysteretic coefficient equal to $\beta = \pi\xi$. The time step integration of the equations of motion can be carried out explicitly by transferring the damping terms to the R.H.S. of the equation of motion and by defining them at the beginning of each time step according to the velocity and displacement of the previous step. The time step will have to be kept small for accuracy reasons.

*.- The second method consists of using several terms of the Caughey series, as explained below, so that as constant a damping ratio as possible can be maintained throughout the frequency range of interest.

In order to construct a damping matrix of those characteristics, a method is provided, Clough and Penzien (1975), to obtain the coefficients a_0, a_1, \dots, a_1 of the Caughey series. These coefficients are determined by expanding the generalized damping for each mode in terms of the Caughey series.

The final expression for the coefficients is:

$$\xi \begin{Bmatrix} 1 \\ 1 \\ \vdots \\ 1 \end{Bmatrix} = \frac{1}{2} \begin{bmatrix} \frac{1}{\omega_1} & \omega_1 & \dots & \omega_1^{2i-3} \\ \frac{1}{\omega_2} & \omega_2 & \dots & \omega_2^{2i-3} \\ \vdots & \vdots & \ddots & \vdots \\ \frac{1}{\omega_i} & \omega_i & \dots & \omega_i^{2i-3} \end{bmatrix}$$

Where ξ is the constant damping ratio, ω_i are the selected frequencies and a_i are the coefficients to be determined.

A good selection of the frequencies $\omega_1, \omega_2, \dots, \omega_i$ should provide a fairly constant damping ratio over the desired range of frequencies. ω_1 should be the fundamental frequency of the system. In order to select the rest of the frequencies a certain knowledge of the frequency characteristics of the soil-structure system is needed. Once the coefficients a_i are known the calculation of the damping matrices will be carried out at the element level.

Wilson and Penzien (1972), proposed a method to compute directly the damping matrix of the system in terms of the generalized modal damping. The expression for the total damping is in this case:

$$C = m \left[\sum_1^N \frac{2\xi_n \omega_n}{M_n} \phi_n \phi_n^T \right] m$$

where m is the mass matrix, ξ_n are the specified damping ratios, ω_n the modal frequencies, M_n the generalized modal masses and ϕ_n the mode shapes. This method has the inconvenience of having to obtain the mode shapes and frequencies for which damping ratios are specified.

Figures (7.3) and (7.4) show the variation of damping with respect to frequency for a system with damping defined with an even number of terms of the Caughey series, and by the Wilson-Penzien approach respectively. As can be seen, the latter provides a zero damping ratio for frequencies higher than ω_i . Consequently, this approach is not recommended unless provisions are made to damp the high frequency content of the system.

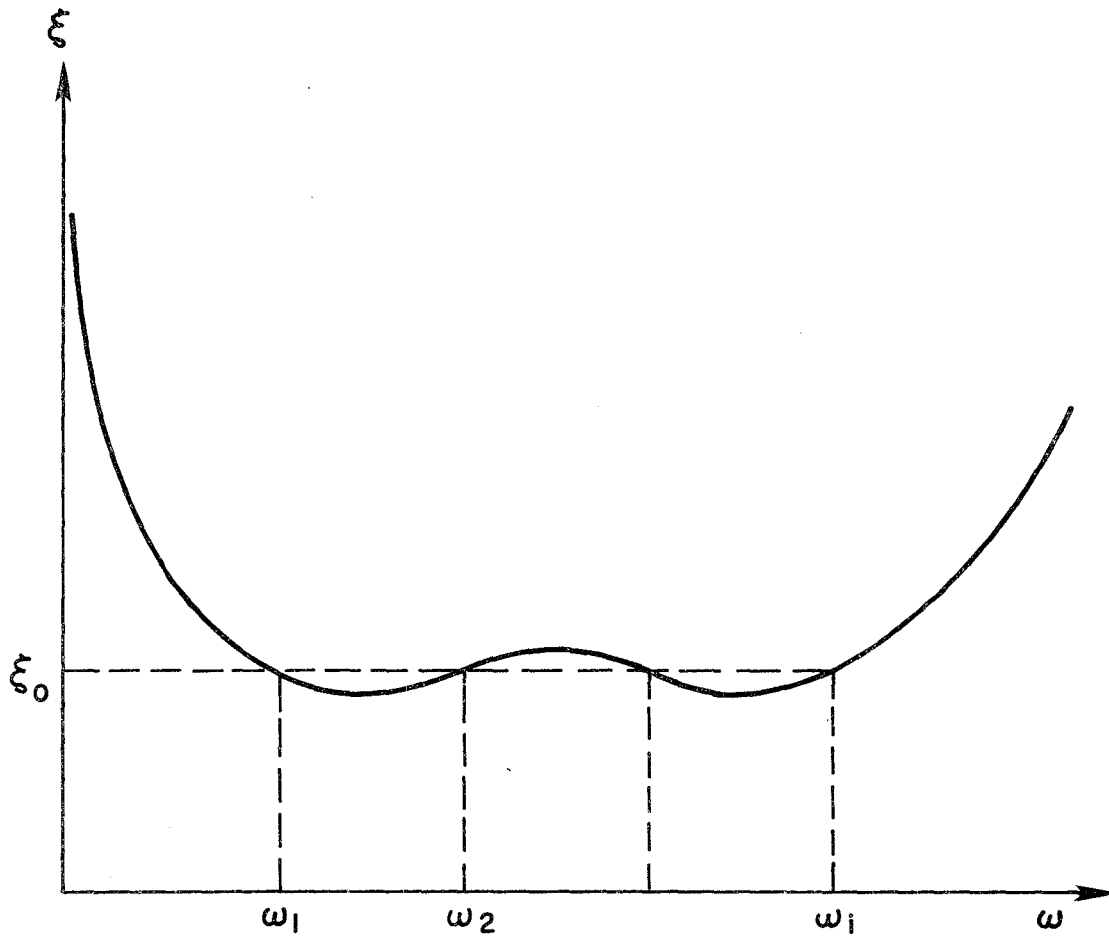


Fig 7.3.- Damping ratio versus frequency for "i" terms of the Caughey series.

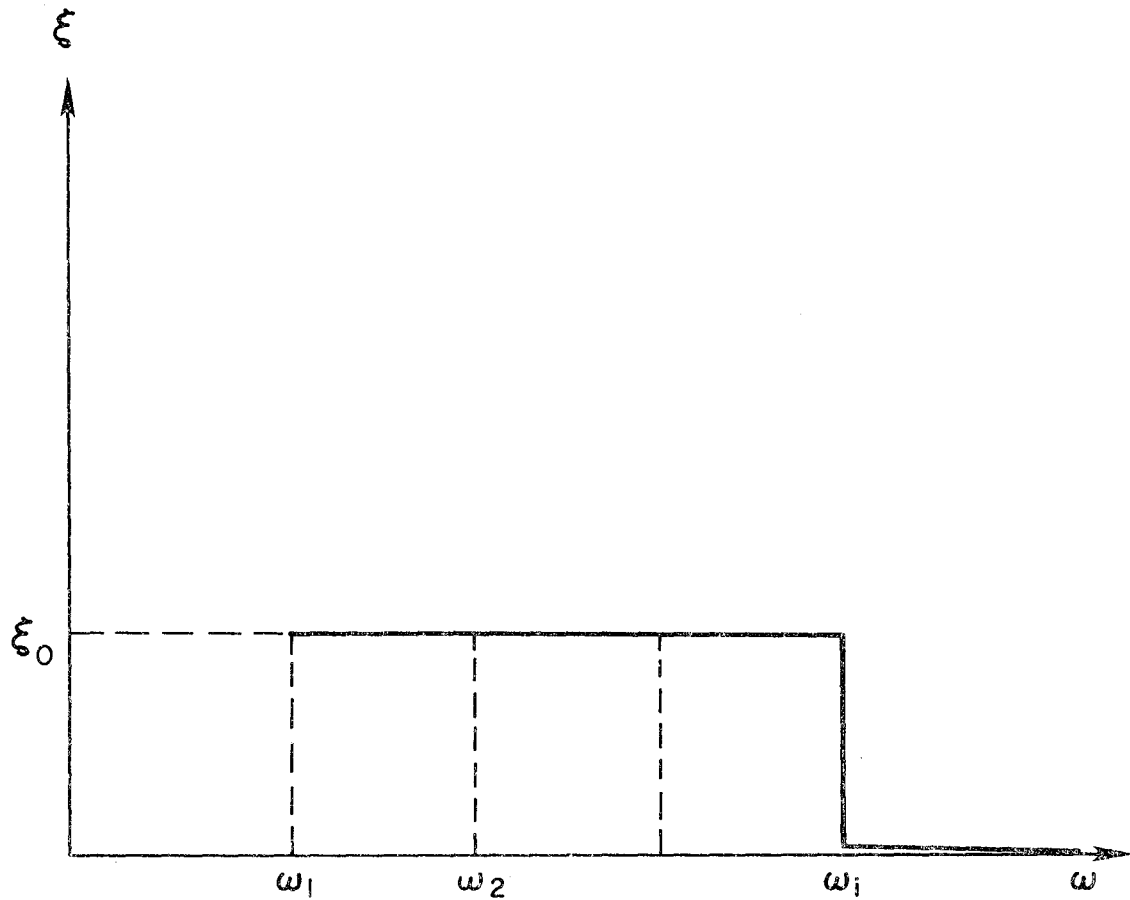


Fig 7.4.- Variation of the damping ratio obtained with Wilson's and Penzien's approach.

7.3.- NUMERICAL INTEGRATION.

Once the system of equations is formed and reduced by Ritz vectors or substructuring techniques, its numerical integration can be carried out by one of three possible ways in the time domain.

The first method is modal analysis. This well known technique makes use of the undamped eigenvalues and eigenvectors to decouple the system of equations. Each uncoupled modal equation can be solved exactly for earthquake type of loading by the linear force method. Since the major part of the response is contained in only a limited number of modes, this procedure would be perfect if it were not for the fact that, as shown above, the damping matrix is not proportional and therefore can not be decoupled by the undamped mode shapes and frequencies. Some approximate methods have been devised to overcome this limitation. They are based on energy considerations and use different damping ratios for each mode, Roesset (1973) and Tsai (1974). However, they are more suited for structural systems rather than soil-structure ones, where due to the big discontinuities in damping characteristics, specially at the radiation boundary, the mentioned methods may not be accurate.

The second way is direct integration. The term "direct integration" encompasses a large and increasing number of time marching schemes that solve the equations of motions in small increment of time. Typical examples are Newmark's method (1959), the Wilson- θ method (1973), the α method etc, (Bathe and Wilson (1973)). New methods continue to be developed to suit the specific characteristics of particular problems. Common troubles of all the direct integration methods are the spurious period elongation and amplitude modifications, which depend directly on the chosen time step, Hilbert (1976). These problems can only be overcome by shortening the time step at the expense of more time and storage. Regardless of these difficulties, the time step methods are very good candidates for the solution of linear dynamic systems and the only ones for nonlinear systems.

The third method which is valid for linear systems is to decouple the equations of motion using the complex eigenvectors. This method is prohibitive for large systems because of its numerical inefficiency, but becomes competitive with the time steps methods when the number of equations of the reduced system does not exceed 200. The main advantages of this approach being that for piece-wise linear excitation, once the set of equations is uncoupled, the time integration can be carried out inexpensively and without introducing the numerical errors inherent in the step-by-step procedures. A detailed description of this method is given in Appendix C.

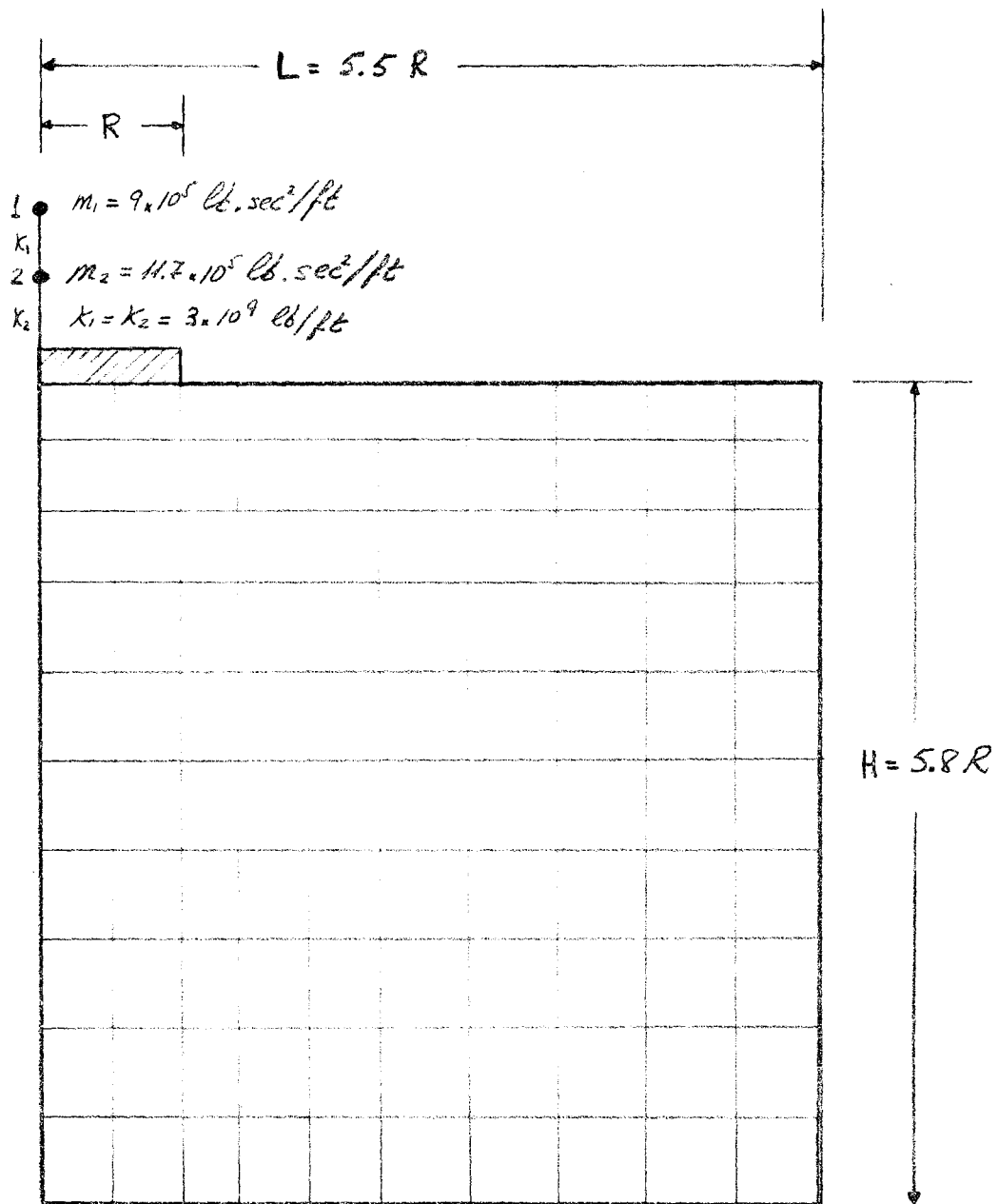
CHAPTER 8

NUMERICAL EXAMPLE

The procedures explained above have been implemented in the computer program SAP80, Wilson 1980, for the solution of soil-structure interaction problems in the time domain. To evaluate their effectiveness, a three dimensional soil structure system, whose characteristics are shown in Figure 8.1, is analyzed. The superstructure consists of a 2 degree of freedom system attached to a rigid massless circular foundation with a radius equal to 42 ft. The lumped masses are connected by frame elements. The foundation is attached to a semi-infinite halfspace with the characteristics depicted in Figure 8.1. The half-space is discretized with axisymmetric finite elements. The length and depth of the model are 5.5 and 5.8 times the radius respectively, with a total number of degrees of freedom equal to 714.

The material damping is assigned a constant value for all the frequency range and equal to 7 %. In order to represent this behaviour in the time domain 2 terms of the Caughey series are used (Rayleigh damping). The frequencies taken to match the given damping ratio are 23 and 70 rd/sec. This will insure a variation of the damping ratio of less than 0.9% (ie. 6.1 to 7.9 %) over the frequency range of $21 < \omega < 87$ rd/sec. Attached to the edges of the model is the Lysmer-Khulemeyer viscous damping boundary defined at the fundamental frequency of the system, which has been previously computed to be 25.8 rd/sec.

The frequencies of the 2 degree of freedom model on a fixed base are 34.24 and 85.38 rd/sec. The significance of the soil-interaction effects in the dynamic response of the system is apparent from the fact that the first resonant frequency for the structural response has been reduced from 34.24 to 25.80 rd/sec. The second resonant frequency varies to a lesser degree from 85.38 to 80.42 rd/sec, which means that the interaction effects will be concentrated in the first resonant mode.



$$V_p = 4000 \text{ ft/sec}$$

$$\nu = 1/3$$

$$V_s = 2000 \text{ "}$$

$$G = 1.244 \times 10^7 \text{ lb/ft}^2$$

$$\rho = 3.11 \text{ lb sec}^2/\text{ft}^4$$

$$E = 3.317 \times 10^7 \text{ "}$$

Fig 8.1.- Characteristics of the example.

The total system of equations is reduced globally with 2 different sets of Ritz vectors, the first one has 15 Ritz functions and the second 40 (2.1 and 5.6 % of the total number of degrees of freedom respectively). By running these two cases the convergence of the Ritz vector approach can be checked. The system is to be subjected to the vertical component of an earthquake excitation represented by the first 8 seconds of a given accelerogram, discretized at time intervals of 0.01 seconds and with maximum acceleration equal to 0.26 g.

The results obtained with SAP80 are to be compared with those obtained by the computer program SASSI (Lysmer et al 1981). SASSI solves the problem in the frequency domain following the volume methods explained in Chapter 2. It uses frequency dependent radiation boundaries, and complex stiffness coefficients (as explained in Chapter 7) to account for the constant damping ratio.

Figures 8.2 and 8.3 show the accelerograms at the top and bottom masses of the structural model obtained first by SAP80, with 15 Ritz functions and with numerical integration by the complex eigenvectors, and second by SASSI. As can be seen both accelerograms show minor differences only in the peak responses. The total maximum accelerations in "g" obtained by both programs are:

	DOF1	DOF2
SASSI	-0.440	-0.393
SAP80	-0.456	-0.402

The maximum discrepancy is 3.6%. Figures 8.4 and 8.5 show the response spectra at both degrees of freedom for 5% damping. As can be seen both solutions are very close. The discrepancy between the two solutions at the peak of the spectrum is 9%.

Figures 8.6 and 8.7 show the accelerograms obtained by SAP80 with 40 Ritz functions, and SASSI. Both solutions are extremely close, except for minor differences in the peak responses. This case is also solved with a Newmark constant average acceleration step-by-step method. The results are practically identical with those obtained with the complex eigenvalues, and it is not consider necessary to plot them here.

DEGREE OF FREEDOM 1

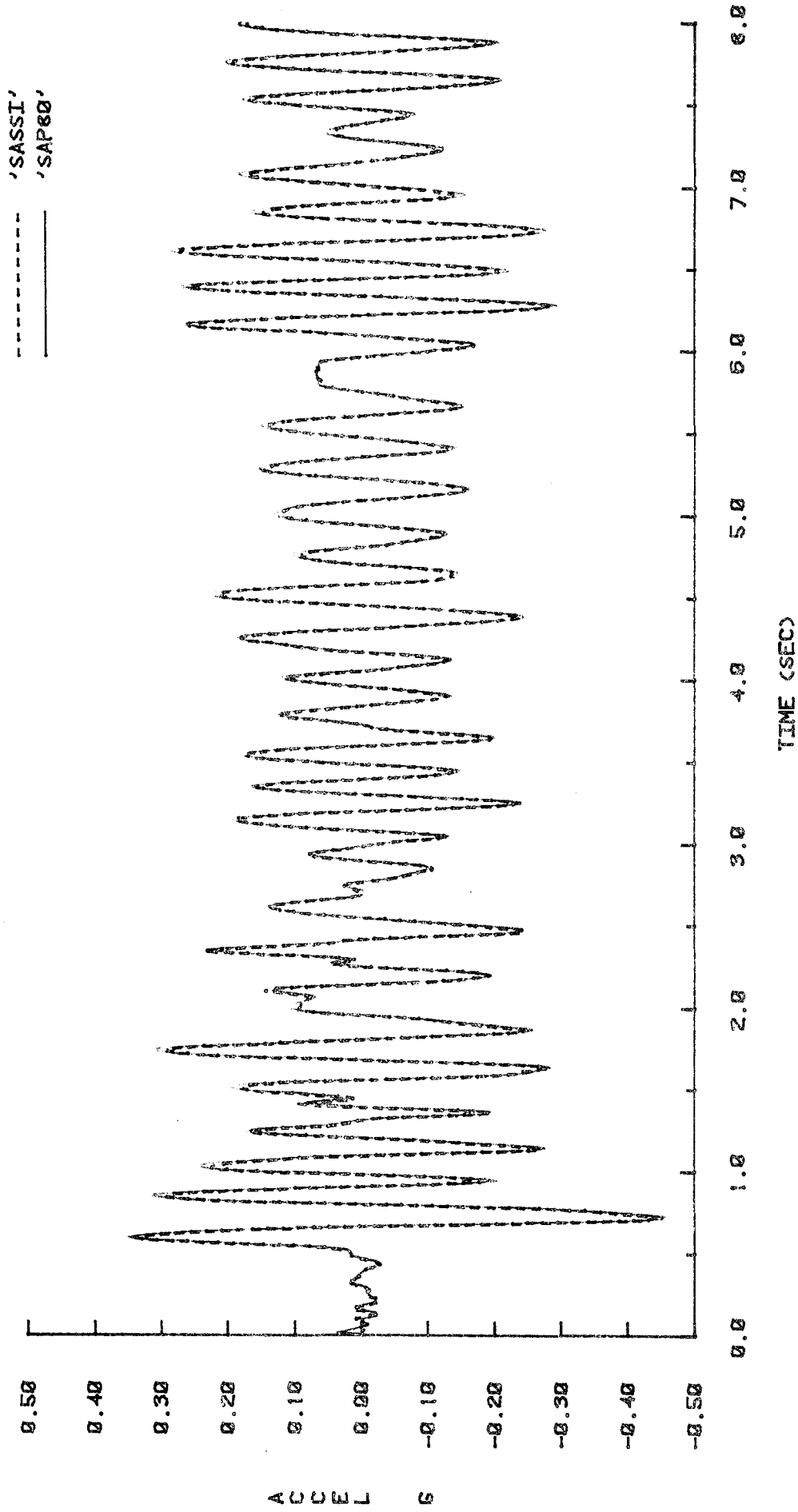


Fig 8.2.- Accelerogram at DOF1 obtained with SAP80 using 15 Ritz functions, and SASSI.

DEGREE OF FREEDOM 2

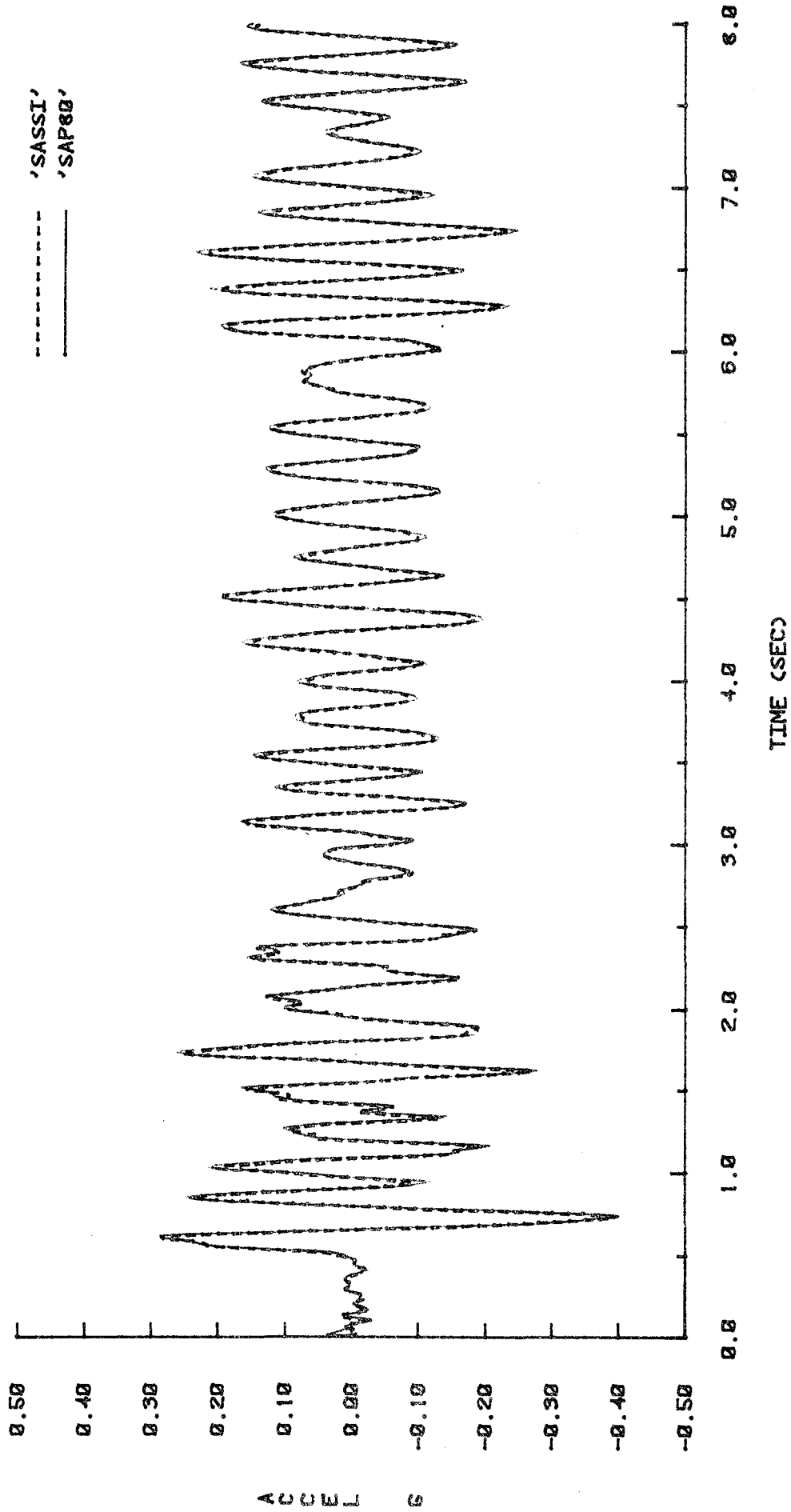


Fig 8.3.- Accelerogram at DOF2 obtained with SAP80 using 15 Ritz vectors, and SASSI.

DEGREE OF FREEDOM 1 RESPONSE SPECTRUM 5% DAMPING

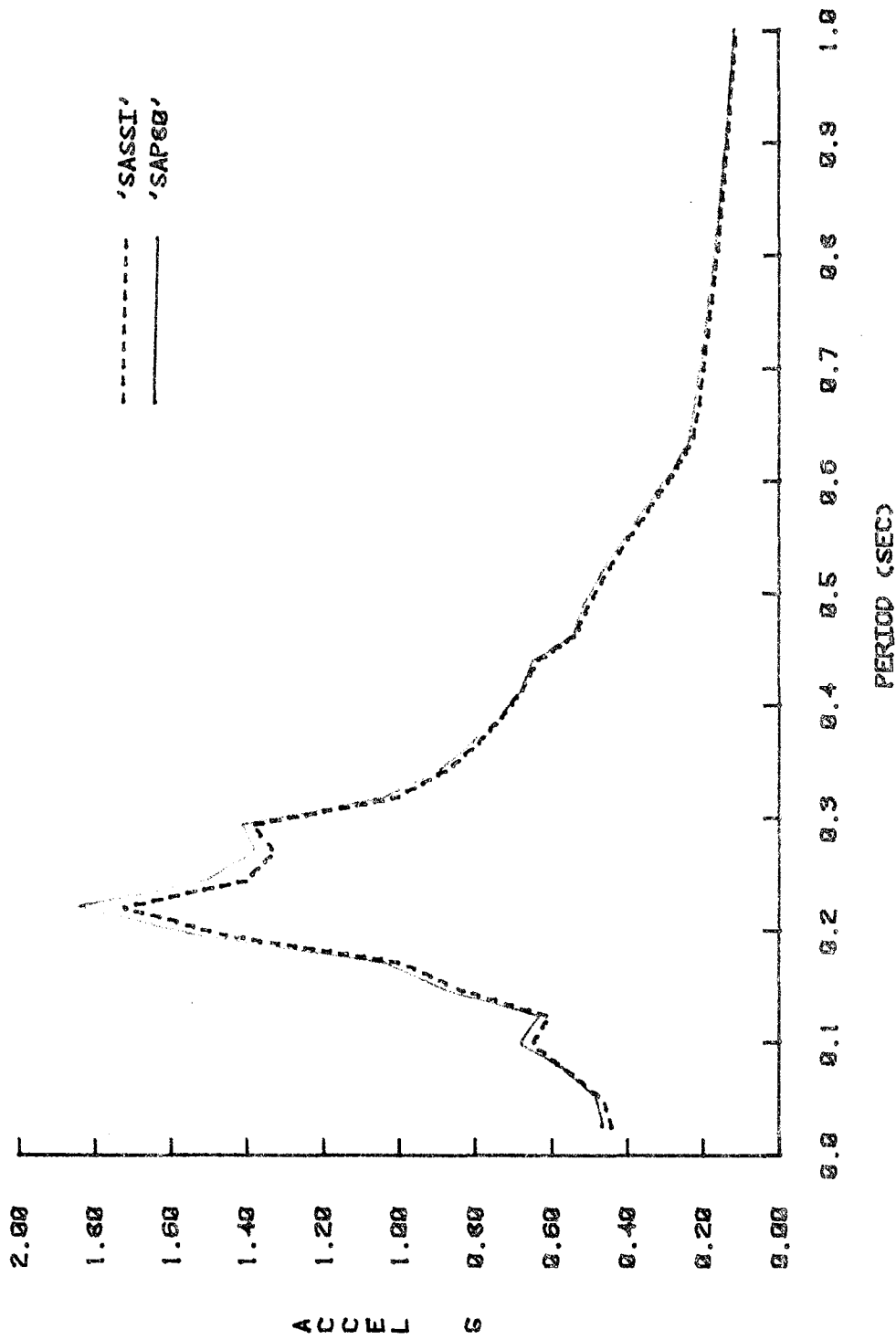


Fig 8.4.- Response spectrum at DOF1 obtained with SAP80 using 15 Ritz functions, and SASSI,

DEGREE OF FREEDOM 2 RESPONSE SPECTRUM 5% DAMPING

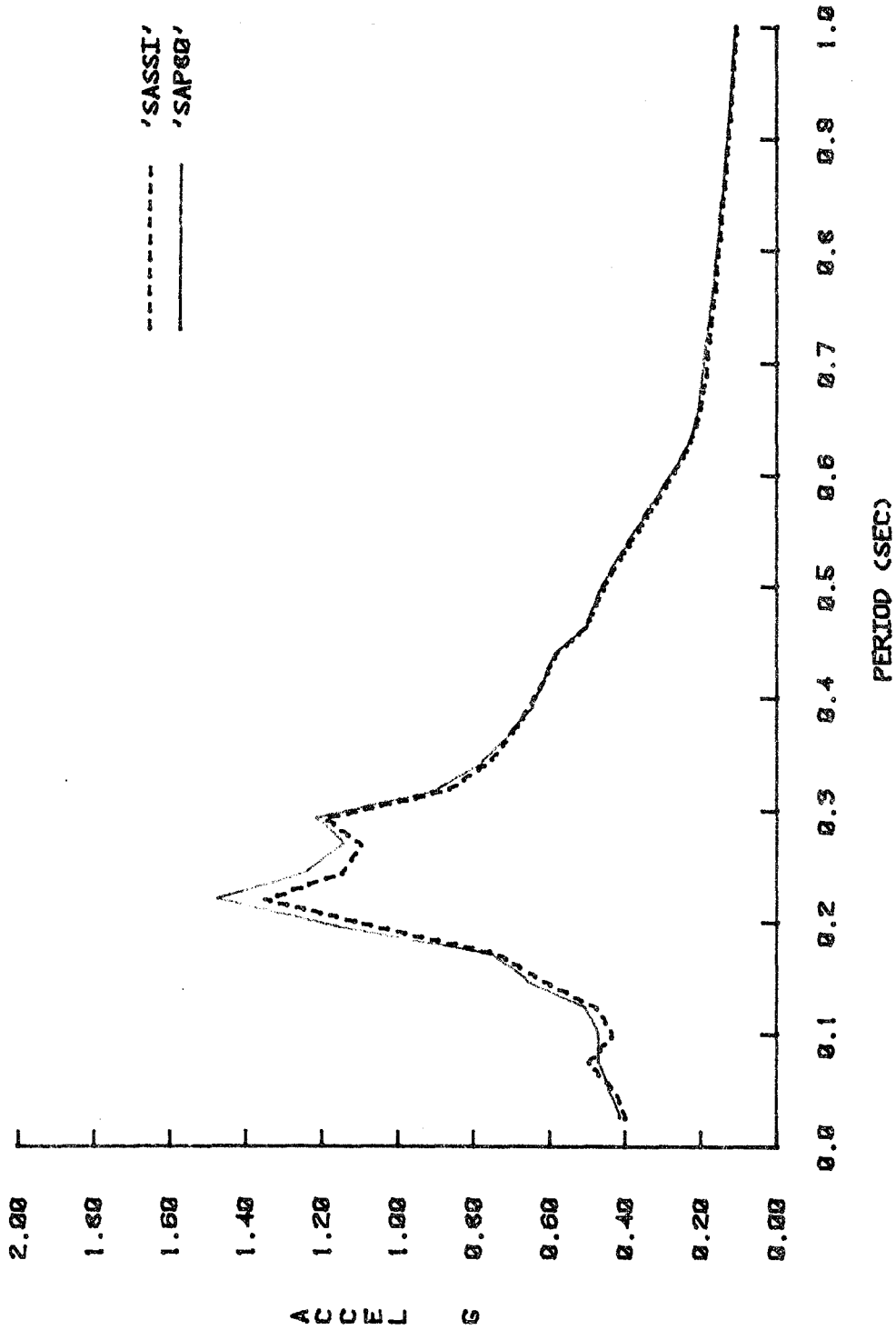


Fig 8.5.- Response spectrum at DOF2 obtained with SAP80 using 15 Ritz functions, and SASSI.

DEGREE OF FREEDOM 1

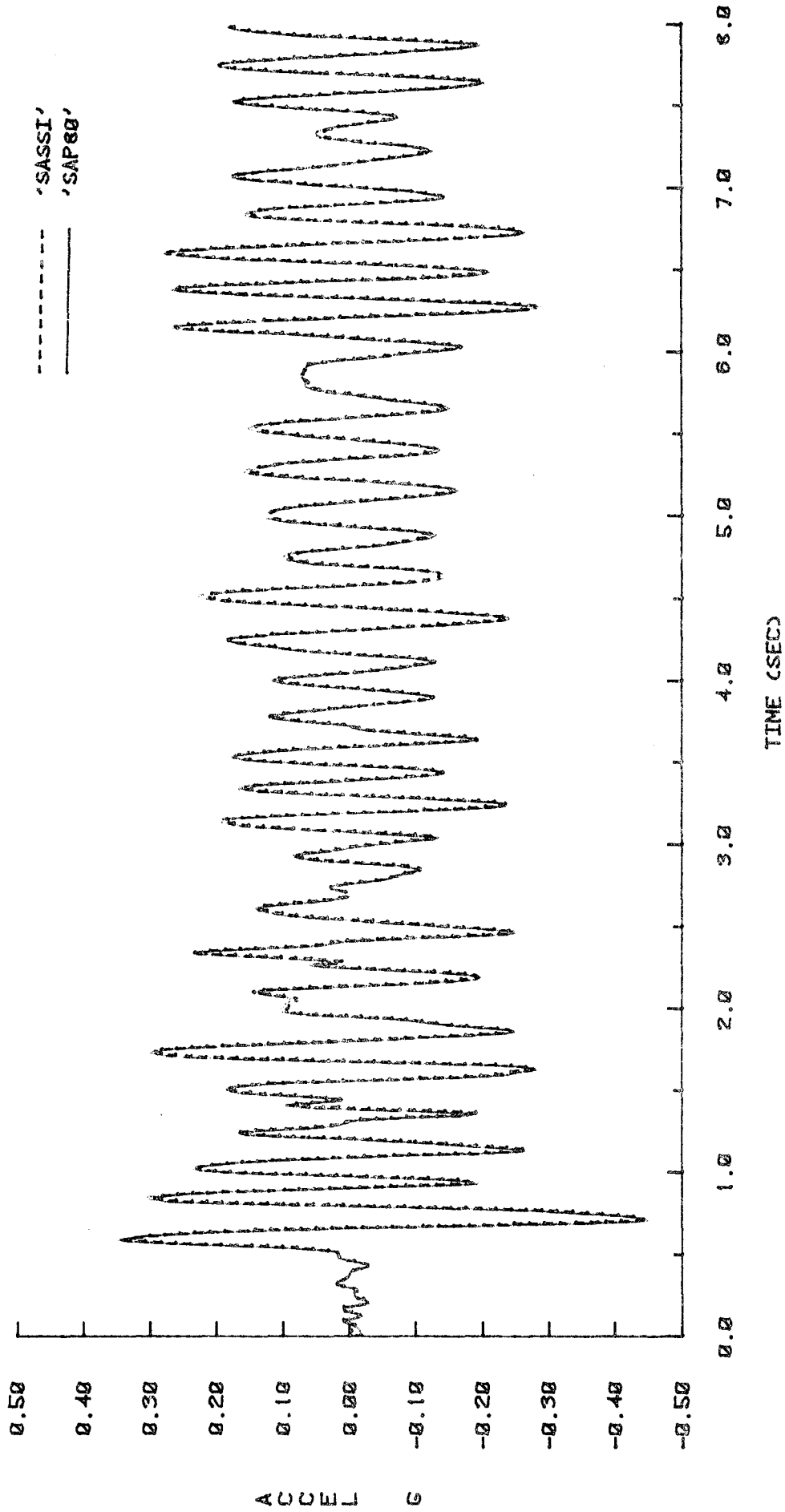


Fig 8.6.- Accelerogram at DOF1 obtained with SAP80 using 40 Ritz functions, and SASSI.

DEGREE OF FREEDOM 2

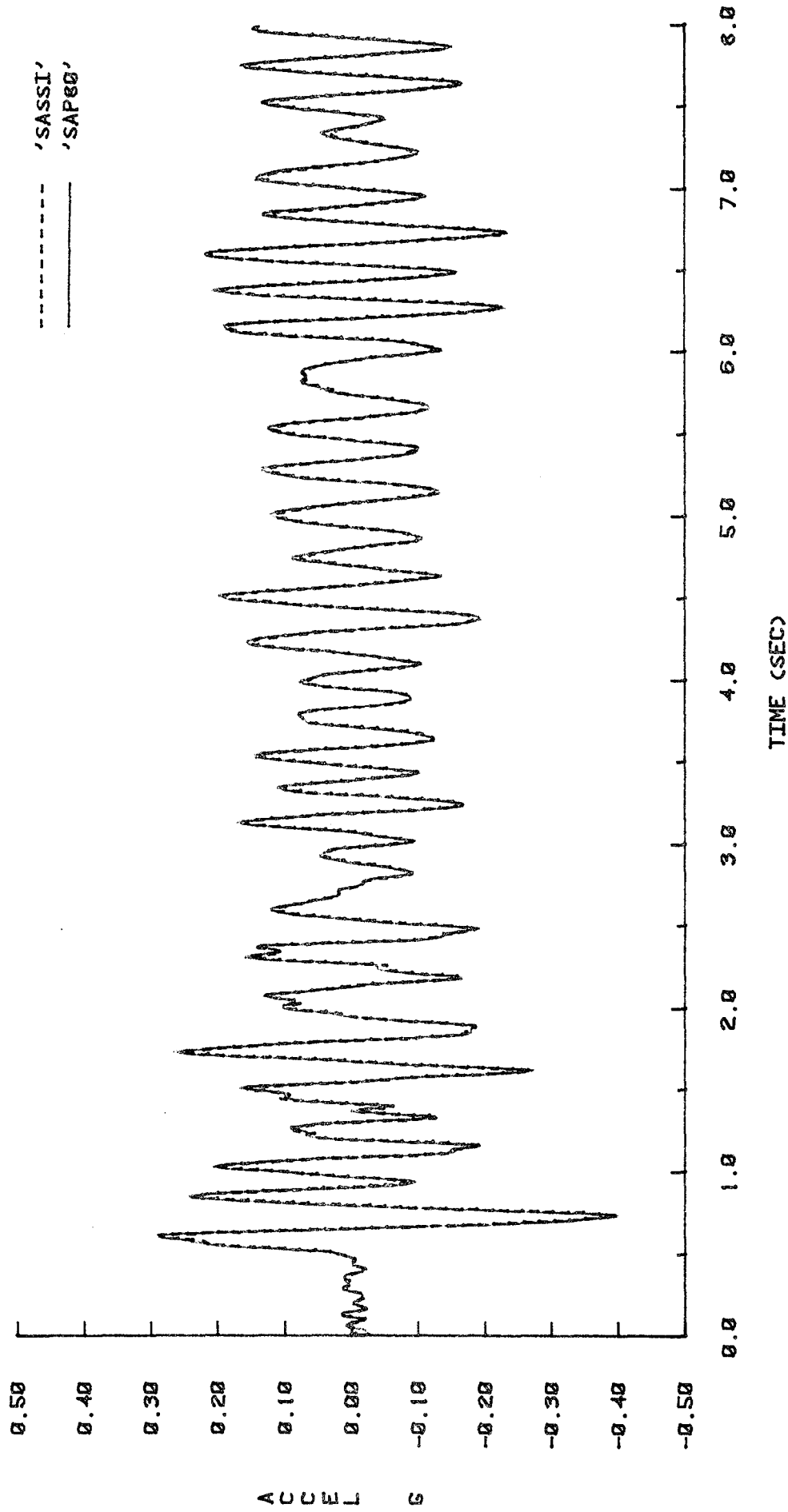


Fig 8.7.- Accelerogram at DOF2 obtained with SAP80 using 40 Ritz functions, and SASSI.

The total maximum accelerations at both degrees of freedom are now:

	DOF1	DOF2
SASSI	-0.440	-0.393
SAP80 (step-by-step)	-0.460	-0.396
SAP80 (complx eigvec)	-0.452	-0.400

The maximum discrepancy is now 2.5%. The response spectra for 5% damping shown in figures 8.8 and 8.9 show how close both solutions are. The differences in the interval of periods between 0.2 and 0.3 seconds are due to the different ways by which both methods represent the material damping. The maximum discrepancy at the peak is now 2.5%.

In order to see how important the interaction effects are in this case, the two degree of freedom model is analyzed for the given input considering its base fixed. The maximum accelerations obtained in this way are 0.647 g and 0.424g, which indicates that the reduction achieved by considering the interaction effects is of the order of 30%. This difference increases substantially when comparing the response spectra of the model with and without interaction effects, as illustrated in Figures 8.10 and 8.11. They show the drastic reduction of the response and the shifting of the resonant periods due to the interaction. A third resonant period appears at 0.293 seconds due to the participation of the soil.

The program SAP80 was run using a VAX 780 and SASSI using a CDC 7600 computer. The cpu time used by both methods are depicted in the table below:

<u>PROGRAM</u>	<u>METHOD OF INTEGRATION</u>	<u>COMPUTER</u>	<u>CPU TIME (SEC)</u>
SAP80 (15 func)	(Complex Eigvec)	VAX 780	220
SAP80 (40 func)	(Complex Eigvec)	VAX 780	515
SAP80 (40 func)	(Step-by-step)	VAX 780	506
SASSI	(Freq domain)	CDC 7600	176

DEGREE OF FREEDOM 1 RESPONSE SPECTRUM 5% DAMPING

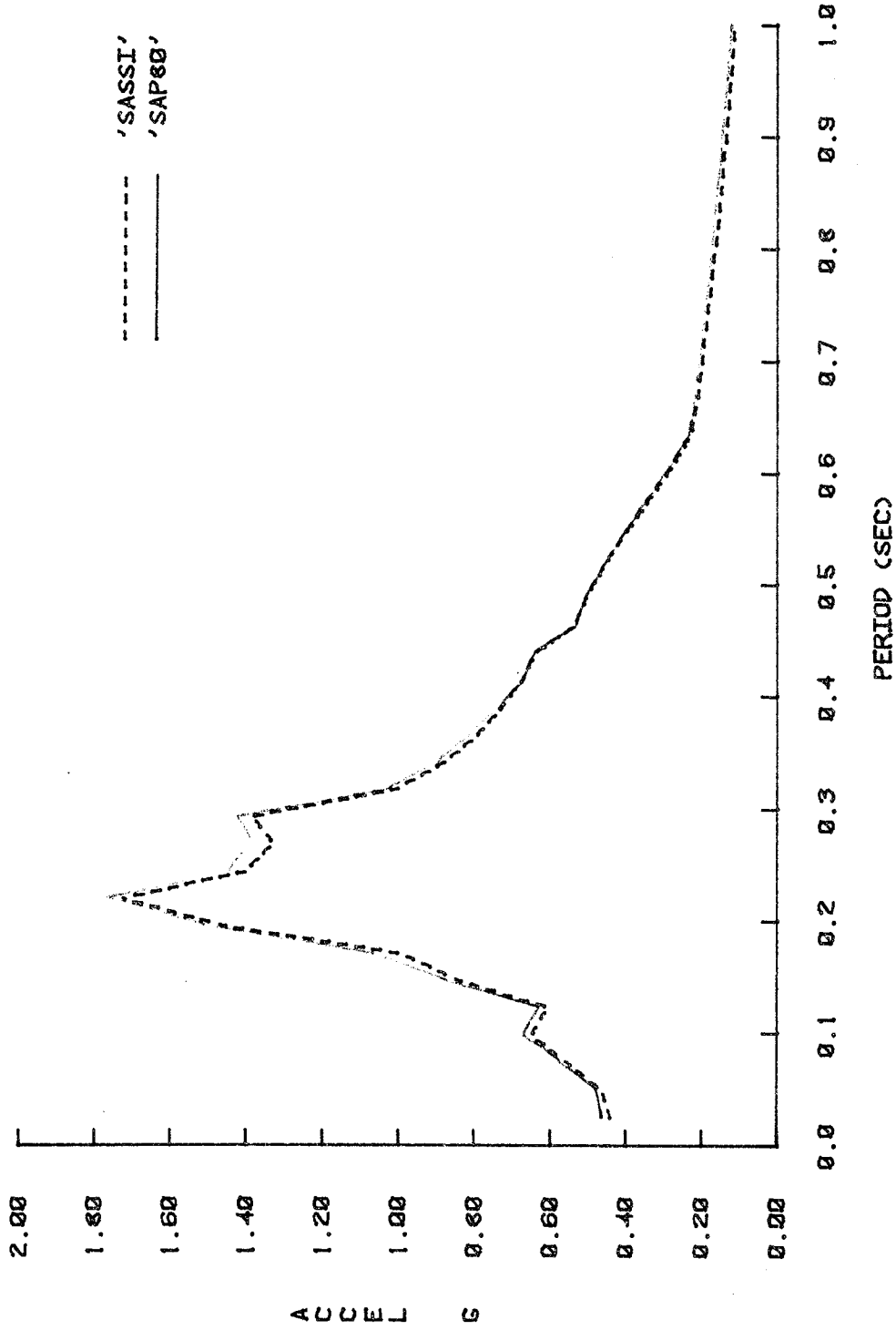


Fig 8.8.- Response spectrum at DOF1 obtained with SAP80 using 40 Ritz vectors, and SASSI.

DEGREE OF FREEDOM 2 RESPONSE SPECTRUM 5% DAMPING

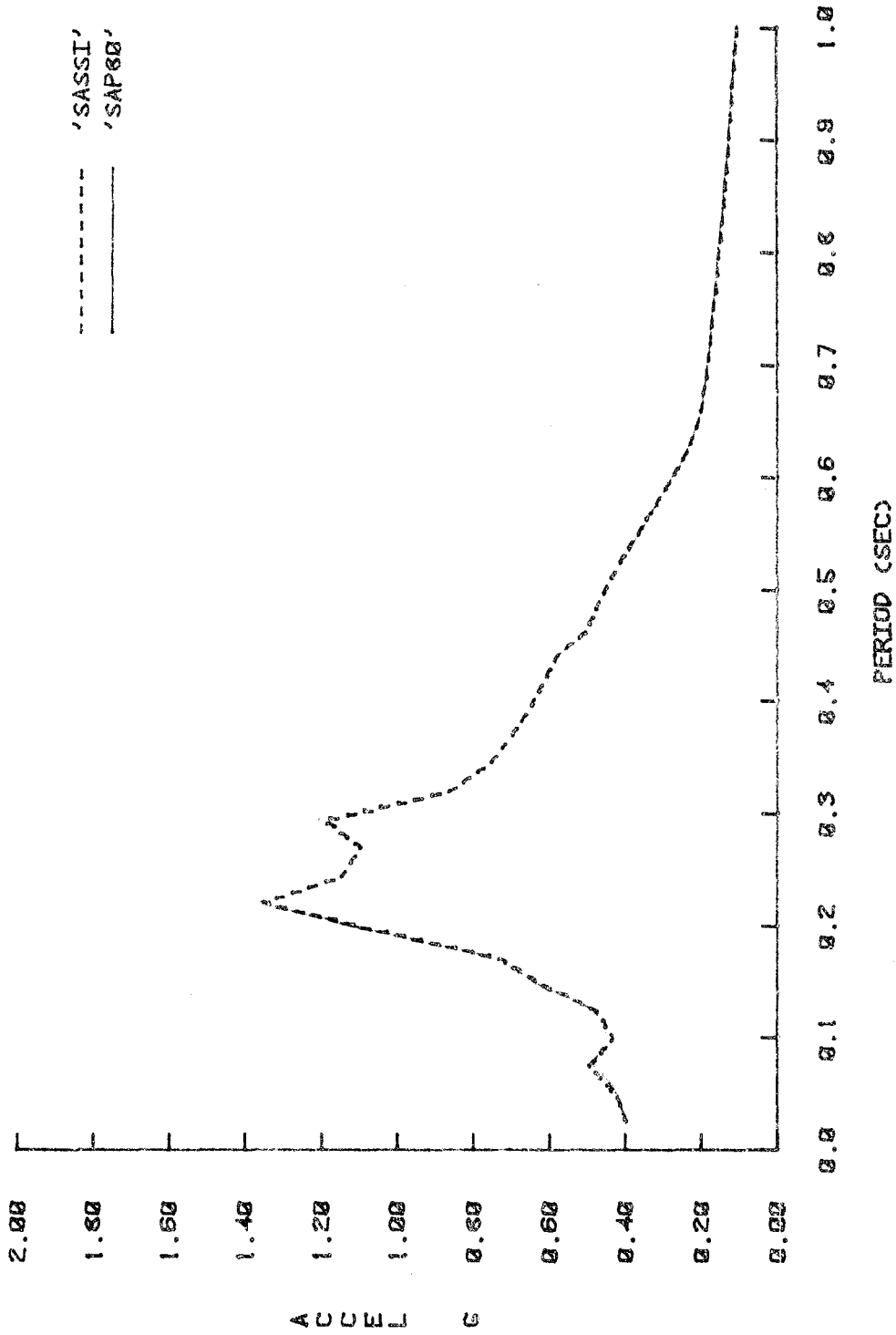


Fig 8.7.- Response spectrum at DOF2 obtained with SAP80 using 40 Ritz vectors, and SASSI.

DEGREE OF FREEDOM 1 RESPONSE SPECTRUM 5% DAMPING

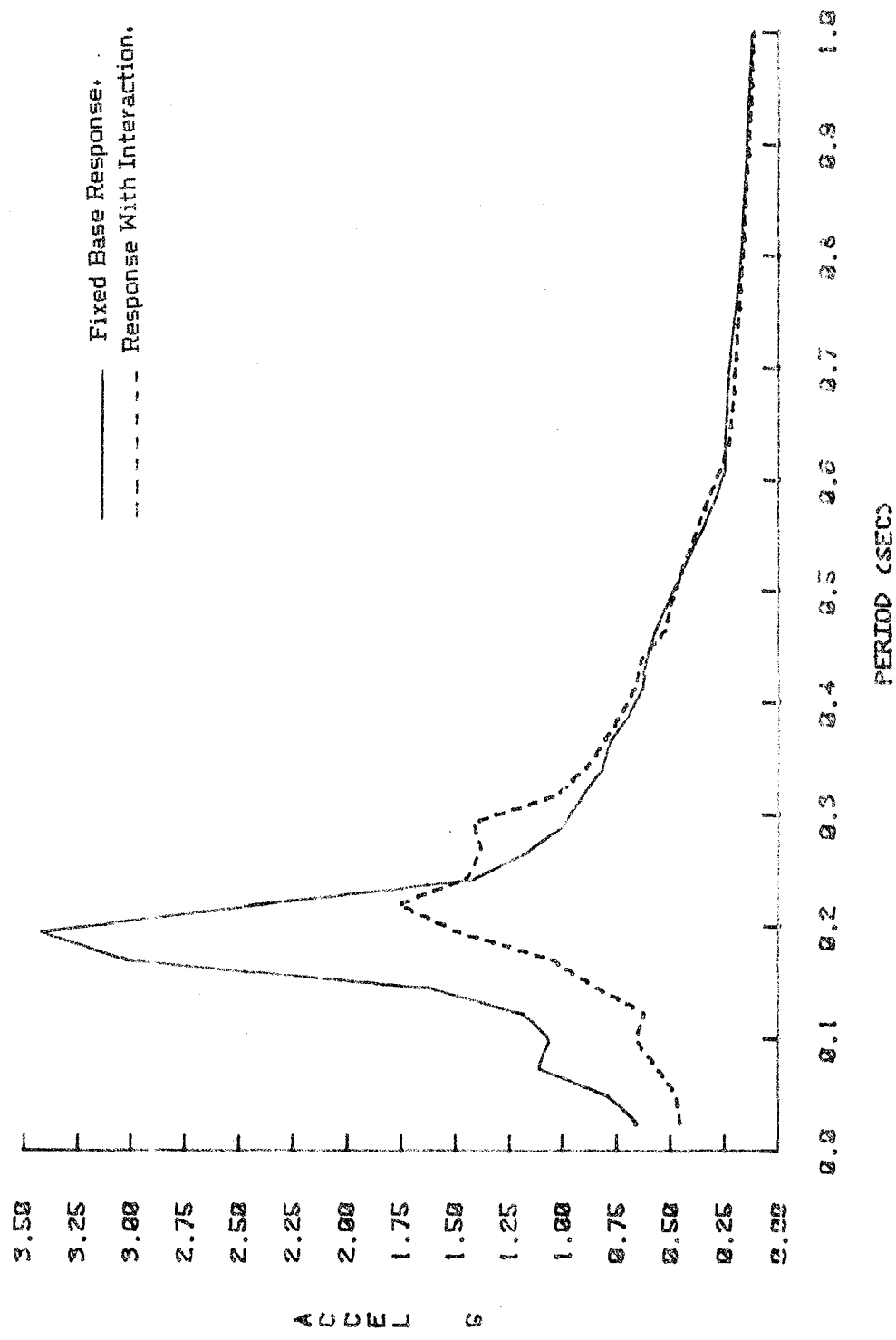


Fig 8.10.- Response spectrum at DOF1 obtained with and without interaction effects.

DEGREE OF FREEDOM 2 RESPONSE SPECTRUM 5% DAMPING

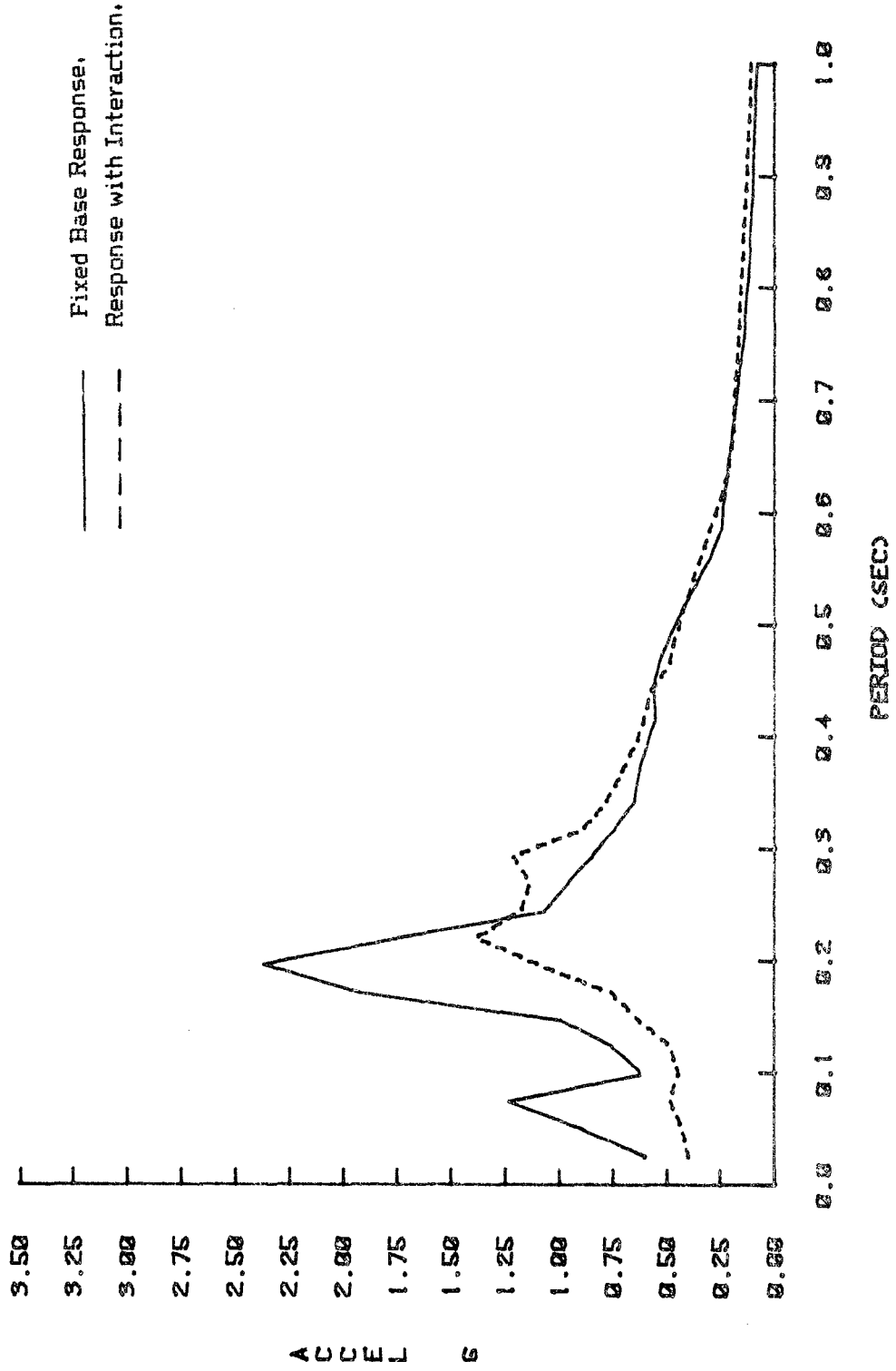


Fig 8.11.- Response spectrum at DOF2 obtained with and without interaction effects.

Assuming a factor of 16 in speed between the CDC 7600 and the VAX 780 (UNIX system), a time domain analysis may be accomplished 5 to 13 times faster than the frequency domain analysis depending on the number of Ritz vectors that are used.

It is worth noticing the little difference in computer time resulting from integrating the system of equations by step-by-step methods or by using the complex eigenvectors. The conclusions that may be drawn from this example are left for the next Chapter.

CHAPTER 9

CONCLUSIONS

The main conclusions of this study may be summarized as follows:

A time domain finite element method has been developed that solves the three dimensional soil-structure interaction problem. This new method can consider the following factors: structural embedment, arbitrary soil profile, flexibility of the foundation, spatial variations of the free-field motions, interaction between two or more structures and nonlinear effects in the structure and foundation (separation of the base mat and the soil, or nonlinear behavior of the materials).

Two different formulations may be constituted, namely the boundary and the volume methods. In the boundary methods the total soil-structure displacements are divided into the scattered and the interaction displacements. The latter are subdivided into the quasi-static and the dynamic relative displacements. This subdivision allows the load vector to be expressed only in terms of the free field accelerations at the boundary interface between the soil and the structure. Computation of the total displacements is not needed, since the total forces at the superstructure depend only on the dynamic relative displacements. The boundary methods require the solution of the scattering problem.

In the volume methods, the total motions are divided into the free field and the interaction motions. This division is possible if the properties of the buried portion of the structure are reduced by those of the soil at the same level. The subdivision of the interaction displacements into the quasi-static and the dynamic displacements leads again to a load vector that is an exclusive function of the free field accelerations. The total forces in the superstructure will depend now upon the dynamic plus the quasi-static displacements. The volume methods eliminate the need of solving the scattering problem.

Prior to any soil-structure interaction analysis a site response problem needs to be solved in order to obtain the free field motions. Even though some methods are now available that include the effect of different wave patterns, no method has yet solved the problem of considering the variation of the free field due to the fault rupture mechanism, or the location of the site with respect to the fault source or hypocenter of a given earthquake. These effects are important for sites that are located in the vicinity of active faults, and their study constitutes one of the most important problems in strong motion seismology. Until these problems are solved the input motion will remain an uncertainty.

A frequency independent radiation boundary is developed that accounts for the energy radiation through the boundaries of the finite element model. This transmitting boundary is obtained from a frequency dependent boundary defined at the fundamental frequency of the soil-structure system. This approach leads to very good approximations in soil-structure interaction problems where the total response of the structure is concentrated in a few modes close to the fundamental mode. An extensive parametric study is carried out for two and three dimensional cases with different soil conditions. Results show that placing the frequency independent transmitting boundary at distances equal to or greater than six times the radius of the foundation leads to very small errors in the compliance functions over a wide range of frequencies. The errors become negligible when material damping is included in the soil. The results obtained from the numerical example presented in Chapter 8 corroborate these findings.

Several methods have been presented for the reduction of the total number of equations of the soil-structure system that are based on the use of Ritz vectors techniques. The Ritz functions are either used globally to reduce the entire system or locally to reduce the soil and structure components separately. Following this last approach, a new method of dynamic substructuring based on component mode synthesis techniques has been developed, in which compatibility of forces and displacements between soil and structure (one or more) are achieved by imposing certain restraint conditions to the Ritz vectors.

A small numerical example is carried out that shows the excellent approximations obtained with all these methods. Results are also shown that demonstrate that the Ritz vectors give the same or greater accuracy than the classical eigenvectors of the system. The reason for this comes from the fact that the selected Ritz functions take into account the spatial distribution of the load whereas the eigenvectors are obtained independently from them. Also, since these Ritz vectors are obtained in a much simpler and computationally much faster way than the eigenvectors they become better candidates for dynamic problems.

A constant damping ratio over a desired frequency range can be achieved by taking several terms of the Caughey series, and computing its coefficients according to the method outlined in Chapter 7. The results of the numerical example shown in Chapter 8 reveal the complete adequacy of this method. In order to account for the spatial variation of the material damping, the damping matrices can be calculated at the element level.

The soil is modeled with three dimensional 8 to 27 solid elements in the near field and axisymmetric elements in the far field. Efficient computer codes have been developed for the construction of the respective stiffness and mass matrices, and for the coupling between the solid and the axisymmetric parts of the finite element mesh. Several numerical rules are tested for the integration of the 27 node solid element. The 3x3x3 Gauss quadrature provides the best results for all the examples chosen.

Nonlinear effects at the foundation level due to the uplifting of the structure and the plastification of the soil have not been given enough attention as yet, and their influence on the response of the structure are not completely known. The existing frequency domain methods cannot for obvious limitations solve these problems in a direct manner. A new formulation in the time domain has been presented to account for these nonlinearities. The dynamic substructuring techniques proposed in Chapter 5 can still be applied at the elastic parts of the system, thus, making this formulation an efficient technique of analysis. Further research is needed to put this formulation into practice to explore the consequences that the nonlinear behaviour of foundations, including soil-structure interaction effects, have on the response of structures.

The numerical integration of the reduced set of equations can be carried out by step-by-step procedures or by decoupling the system with complex eigenvectors and solving each of the uncoupled equations by the linear force method. The second approach becomes exact for piece-wise linear type of excitation, while the first always introduces errors in the amplitude and periods of the response. For reduced systems of equations (up to 100 mode shapes) the complex eigenvector approach is equivalent to the step-by-step procedures in computational efficiency and therefore becomes a better candidate for the numerical integration.

From the results obtained with the numerical example illustrated in Chapter 8, the following conclusions may be drawn:

- 1.- The total response of a soil-structure interaction problem is concentrated in only a few modes of vibration.
- 2.- A limited number of Ritz functions (10-40) in the soil suffice to represent the major effects of the wave propagation problem.
- 3.- The use of frequency independent transmitting boundaries defined at the fundamental frequency of the system gives satisfactory results.
- 4.- A constant damping ratio over a desired frequency range can be achieved by using only a few terms of the Caughey series. (2 in the example shown in Chapter 8)
- 5.- The computational work needed to solve the reduced set of equations is equal for both the step-by-step procedures and the method of complex eigenvectors. In addition, the latter approach eliminates period and amplitude errors associated with the former technique.
- 6.- The savings in computer time and storage obtained by carrying out the soil-structure analysis in the time domain when compared to the frequency domain are outstanding.

The purpose of this research has been to develop efficient numerical techniques to solve soil-structure interaction problems in the time domain. The computer program SAP80 has been used as a tool for all the numerical computations carried out throughout these studies. However, the implementation of these numerical techniques has not yet been completed for industrial use.

REFERENCES

- Arnold, R.N., Bycroft, G.N. and Warbuton G.B. (1955). "Forced Vibrations of a Body in an Infinite Elastic Solid". *Journal of Applied Mechanics*. ASME. Vol.22 #3. pp. 391-400. (1955).
- Bathe, K. J., and Wilson, E. L. (1976). "Numerical Methods in Finite Element Analysis". Prentice-Hall Inc. (1976).
- Bycroft, G.W. (1956). "Forced Vibrations of a Rigid Circular Plate on a Semi-Infinite Elastic Space or on a Elastic Stratum". *Philosophical Transactions, Royal Society of London*. pp. 327-368. 1956.
- Caughey, T. K. (1960). "Classical Normal Modes in Damped Linear Systems". *Journal of Applied Mechanics*. Vol 27. 1960. pp 269-271.
- Chen, J.C., Lysmer, J., Seed, H.B. (1981) "Analysis of Local Variations in Free Field Seismic Ground Motion." University of California Berkeley. EERC report 81/03. January 1981.
- Chopra, A.K. and Gutierrez, J.A. (1973). "Earthquake Analysis of Multistory Buildings Including Foundation Interaction". University of California. Berkeley. EERC report 73-13. June 1973.
- Chopra, A.K., Chakrabarti, P., Dasgupta, G. (1975) "Frequency Dependent Stiffness Matrices for Viscoelastic Halfspace Foundations." University of California. Berkeley. EERC report 75/22. (1975).
- Clough, R.W., and Penzien, J. (1975). "Dynamic of Structures." Magraw-Hill. (1975).
- Clough, R. W. and Wilson, E. L. (1979). "Dynamic Analysis of Large Structural Systems with Local Nonlinearities". *Computer Methods in Applied Mechanics and Engineering*. 17-18. pp 107-129 (1979).

Cundall, P. A., Kunar, R. R., Carpenter, P. C., Marti J. (1978). "Solution of infinite Dynamic Problems by Finite Modelling in the Time Domain". Proc. 2 Int. Confer. Appl. Numer. Model. Madrid, Spain. (1978).

Day, S. M. (1977). "Finite Element Analysis of Seismic Scattering Problems". PhD Dissertation. University of California. San Diego. (1977).

Dickens, J. M. (1980). "Numerical Methods for Dynamic Substructure Analysis". University of California. Berkeley. EERC report 80-20. (1980).

Gomez Masso, A., Lysmer J., Chen J.C., Seed B. (1979). "Soil Structure Interaction in Different Seismic Environments." University of California. Berkeley. EERC, report 79/18. August 1979.

Gupta, S., T.W. Lin, J. Penzien, C.S. Yen (1980) "Hybrid Modelling of Soil Structure Interaction". University of California. Berkeley. EERC report 80/9. May 1980.

Gutierrez J.A. (1976). "A Substructure Method for Earthquake Analysis of Structure-Soil Interaction." University of California. Berkeley. EERC, report 76-9. April 1976

Guyan, R. J. (1965) "Reduction of Stiffness and Mass Matrices". AIAA Journal, Vol 3. p-380. Feb (1965).

Hilber, H. M. (1976). "Analysis and Design of Numerical Integration Methods in Structural Dynamics". University of California. Berkeley. EERC report # 76-29. (1976)

Hintz, R. M. Jr and Chang, C-J. (1976). "Free interface Methods of Substructure Coupling for Dynamic Analysis". AIAA Journal, Vol 14 #11. pp 1633-1635. (Nov 1976)

Hurty, W. C., Collings, J. D. and Hart, G. C. (1971). "Dynamic Analysis of Large Structures by Modal Synthesis Techniques". Computers and Structures, Vol 1. pp 553-563. (1971)

Idriss, J.M., Kennedy, R.P. (1980). Report by the Ad Hoc Group on Soil Structure Interaction of the Committee on Nuclear Structures and Materials of the Structural Division of ASCE. "Analysis for Soil-Structure Interaction Effects for Nuclear Power Plants," January 1980.

Iguchi, M., and Luco, J.E. (1981) "Dynamic Response of Flexible Rectangular Foundations on an Elastic Half-space." Earthquake Engineering and Structural Dynamics, Vol. 9, # 3, May-June 1981.

Kausel, E., Roesset, J., and Waas, G. (1975). "Dynamic Analysis of Footings on Layered Media". J. Eng. Mech. Div. ASCE, Vol 101, # EM5, pp 679-693, Oct 1975.

Kausel, E. Whitman, A, Murray J, Elsabee, F. (1978). "The Spring Method for Embedded Foundations." Nuclear Engineering and Design , Vol. #48. (1978), pp.(377-392).

Kausel, E. and Roesset, J.M. (1975). "Dynamic Stiffness of Circular Foundations." Journal Engin. Mech. Div. ASCE, Vol.101, #EM6, pp.(771-785), December 1975.

Kaskio, J. (1970) "Steady State Response of a Circular Disk Resting on a Layered Medium". PhD Thesis, Rice University, Houston, Texas. (1970).

Khalvati, Medhi. (1978). "Numerical Methods in Soil Wave Propagation Problems". Report submitted for the Doctoral Qualifying Examination. University of California, Berkeley. Nov 1978.

Khalvati, M. (1981) "Finite Element Analysis of Interacting Soil-Structure Fluid systems with Local Nonlinearities". PhD Dissertation. University of California, Berkeley. May 1981.

Kulhemeyer, R. L., Lysmer, J. (1973). "Finite Element Method Accuracy for Wave Propagation Problems". J. Soil Mech. Found. Div. ASCE, Vol 99 # SM5, May 1973.

Kunar, R. R., Rodriguez-Ovejero L. (1980). "A Model with Non-Reflecting Boundaries for Use in Explicit Soil-Structure Interaction Analysis". Earth. Eng. Struc. Dynam. Vol 8. pp 361-374. (1980).

Luco, J.E., Westmann, R.A., (1971). "Dynamic Response of Circular Footings". Journal of the Soil Mech. and Foundation Division. ASCE Vol. 97, # EM5, pp. 1381-1395, October 1971.

Luco, J.E. and Westmann, R.A. (1972) "Dynamic Response of a Rigid Footing Bonded to an Elastic Halfspace," Journal of Applied Mechanics. ASME. Vol. 39, #E2. June (1972).

Luco, J.E. (1974). "Impedence Functions for a Rigid Foundation on a Layered Medium". Nuclear Engineering and Design. Vol. 31, 204-217. (1974).

Luco, J.E. "Vibrations of Rigid Displacement on a Layered Viscoelastic Medium." Nuclear Engineering. Vol. 36. pp.325-340. (1976).

Luco, J.E. and Wong, H.L. (1977). "Dynamic Response of Rectangular Foundation For Rayleigh Wave Excitation." Proceedings at 6th World Conference on Earthquake Engineering. Vol. 4, pp. 85-90. New Delhi, India. January 1977.

Lysmer, J., Richart, F.E.Jr. (1966) "Dynamic Response of Footings to Vertical Loadings". Journal of the Soil Mech. and Foundation Division. ASCE Vol. 92. # SM1, 65-91, January 1966.

Lysmer, J. and Kuhlemeyer, R.L. (1969). "Finite Dynamic Model for Infinite Media." Journal Engin. Mech. Div. ASCE, Vol. 95, #EM4, pp (859-877), August 1969.

Lysmer, J., Udaka, T., Seed, H.B., and Hwong, R. (1974). "LUSH- A computer Program for Complex Response Analysis of Soil-Structure Systems". University of California. Berkeley. EERC report 74-4. April 1974.

Lysmer, J., Udaka, T., Tsai, C. and Seed, H.B. (1975). " FLUSH. A Computer Program for Approximate 3-D Analysis of Soil Structure Interaction Problems." University of California Berkeley. EERC report 75-30. November 1975.

Lysmer, J. (1978). "Analytical Procedures in Soil Dynamics." University of California Berkeley. EERC, report 78-29. December 1978.

Lysmer, J., Seed, H.B. (1980) "The Seismic Soil-Structure Interaction Problems for Nuclear Facilities." Seismic Safety Margins Research Program (Phase # 1), April (1980).

Lysmer J., Raissi, M., Tajinian, F., Valdan, S., Ostandan, F. (1981). "SASSI- A System For Analysis of Soil-Structure Interaction". University of California Berkeley. Geotechnical report # 81-02. April (1981).

McNeal, R. (1971) "A Hybrid Method of Component Mode Synthesis". Computers and Structures". Vol 1, pp 581-601. (1971).

Miller, G. F. and Pursey H. (1955). "On the Partition of Energy Between Elastic Waves in a Semi-infinite Solid". Proceedings Royal Society of London, Series A, Vol 233, pp 55-59. (1955).

Newmark, N. M. (1959). "A method of Computation of Structural Dynamics", J. Eng. Mech. Div. Vol 85, 1959, pp 67-94.

Oien, M.A. "Steady State Motion of a Rigid Strip Bonded to an Elastic Halfspace," Journal of Applied Mechanics, ASME, Vol. 8, June 1971.

Roesset, J. M. and Whitman, R. V. (1973). "Modal Analysis for Structures with Foundation Interaction" J. Struct. Div. ASCE, Vol 99, #ST3, March 1973.

Roesset, J.M. and Ettouney, N.M. (1977). "Transmitting Boundaries: A Comparison ". Inter. Journal Numerical and Analytical Methods in Geomechanics, Vol. 1, pp 151-176. (1977).

Rosenblueth, E. Ed. (1980) "Design of Earthquake Resistant Structures". John Willey and Sons. (1980).

Rucker, W. (1982). "Dynamic Behavior of Rigid Foundations of Arbitrary Shape on a Half-space". Earth. Eng. Struct. Dynam. Vol 10 #4.

Savidis, S.A. and Richter, J. (1977). "Dynamic Interaction of Rigid Foundation." Proceedings at 9th Inter. Conference on Soil Mechanics and Foundations in Engineering. Vol. 2, pp. 369-374. Tokyo, Japan. (1977).

Seed, H.B., Lysmer, J. (1977). "Soil Structure Interaction Analysis by Finite Element Methods. State of The Art." Proceedings at 4th Internatl. Conference on Structural Mechanics in Reactor Technology, SMIRT 4, Vol.K Paper H 211, pp.1-11, San Francisco, August 1977.

Seed, H., Lysmer, J. (1978) "Soil-Structure Interaction Analysis by Finite Elements- State of The Art". Nuclear Engineering and Design, Vol. 46, #1 (1978), pp. 349-365.

Schnabel, P. B., Lysmer, J. and Seed, H. B. (1972). "SHAKE- A Computer Program for Earthquake Response Analysis of Horizontally Layered Sites". University of California, Berkeley. EERC report 72-12. (1972).

Smith, W. D. (1974). "A nonreflecting plane boundary for wave propagation problems". J. Comp. Phys. Vol 15, pp 492-503.

Synge, J. L. (1956). "Elastic Waves in Anisotropic Media". J. Mathem. and Physic. Vol. 35, pp 332-334. (1956)

Tsai, N. C. (1974). "Modal Damping for Soil-Structure Interaction". J. Eng Mech. Div, ASCE, Vol 100, EM2, April 1974.

Tsai, N., Niehoff, M., Swatta, M. and Madjian, A. (1974) "The Use of Frequency-Independent Soil Structure Interaction Parameters." Nuclear Engineering and Design, Vol. 31 (1974) pp 168-183.

Tzong, J.J., Gupta, S., Penzein, J. (1981). "Two Dimensional Hybrid Modelling of Soil-Structure Interaction". University of California, Berkeley. EERC report 81/11, August 1981.

Vaish and Chopra, A. (1973) "Earthquake Analysis in Structure Foundation Systems". University of California Berkeley. EERC report 73-9. April 1973.

Veletsos, A.S., and Wei, Y.T. (1971). "Lateral and Rocking Vibrations of Footings". Journal of the Soil Mech. and Foundation Division. ASCE Vol. 97. # SM9, pp.1227-1248, September 1971.

- Veletsos, A.S. and Verbic, B. (1973) "Vibrations of Viscoelastic Foundations". *Earthquake Engineering and Structural Dynamics*. Vol. 2, pp. 87-102. (1973).
- Veletsos, A.S. and Nair, V.V.D. (1974) "Torsional Vibrations of Viscoelastic Foundations". *Journal of Geotechnical Engineering Division, ASCE*, Vol. 100, pp.225-246. (1974).
- Waas, G. (1972). "Analysis Method for Footing Vibrations Through Layered Media". PhD Dissertation. University of California, Berkeley, December 1972.
- Warbuton, G.B. (1957) "Forced Vibrations of a Body on an Elastic Stratum". *Journal of Applied Mechanics, ASME*, Vol. 24, pp. 55-59. (1957).
- Wei, Y. (1971). "Steady State Response of Certain Foundation Systems", PhD Thesis. Rice University, Houston, Texas. (1971).
- White, W., Valliapan, S., Lee, I. K. (1977). "Unified Boundary for Finite Dynamic Models". *J. Eng. Mech. Div. ASCE*, Vol 103, pp 949-964. (1977).
- Wilson, E. L. and Penzien, J. "Evaluation of Orthogonal Damping Matrices" *Int. J. Num. Meth. Eng.* Vol 4. 5-10 (1972)
- Wilson, E. L., Farharmand I. and Bathe, K. J. (1973). "Nonlinear Dynamic Analysis of Complex Structures". *Inter. J. of Earthq. an Struc. Dynam.* Vol 1. 1973, pp 241-252.
- Wilson, E. L. "SAP80 Structural Analysis Programs for Small or Large Computer Systems". CEPA 1980 Fall Conference and Annual Meeting. Newport Beach, California.
- Wilson, E.L., Yuan, M-W, Dickens J.M. (1982). "Dynamic Analysis by Direct Superposition of Ritz Vectors". *Earth. Eng, Struc. Dynam.* Vol 10, pp 813-823 (1982).
- Wolf, J. P. and Obernhuber, P. (1982). "Free-field Response from Inclined SH-waves and Love waves". *Earth. Eng, Struc. Dynam.* Vol 10, pp 823-847. (1982).

Wolf, J. P. and Oberhuber, P. (1982). "Free-field Response from Inclined SV-waves P-waves and Rayleigh waves". *Earth. Eng. Struct. Dynam.* Vol 10, pp 847-871. (1982).

Wong, H. L. and Luco, J. E. (1976) "Dynamic Response of Rigid Foundations of Arbitrary Shape". *Earth. Eng. Struct. Dynam.* Vol 4, (579-587). (1976).

APPENDIX A

FINITE ELEMENT FORMULATION OF AXISYMMETRIC SOLIDS WITH NON-AXISYMMETRIC LOADS

In this Appendix a general formulation of an axisymmetric element is given that can include any number of terms in the Fourier expansion. The coordinate system is taken as the cylindrical basis r, θ, z . Since the solid is a solid of revolution, its shape is completely defined by any plane where $\theta = \text{constant}$. The body shape is defined using a finite element model for the r - z plane. Each element generates a solid torus and each node a nodal circle. The shape functions for the r, θ direction are trigonometric functions, sine and cosine, that are appropriate due to their periodic characteristics for $0 < \theta < 2\pi$.

The displacement expansion is:

$$\begin{aligned} u_r(r, \theta, z) &= \sum_{n=0}^{\infty} (V_{rn}(r, z) \cos n\theta + W_{rn} \sin n\theta) \\ u_\theta(r, \theta, z) &= \sum_{n=1}^{\infty} (V_{\theta n}(r, z) \cos n\theta + W_{\theta n} \sin n\theta) \\ u_z(r, \theta, z) &= \sum_{n=0}^{\infty} (V_{zn}(r, z) \cos n\theta + W_{zn} \sin n\theta) \end{aligned} \quad (A.1)$$

Where u_r , u_θ and u_z are the radial, circumferential, and vertical displacements respectively, and $v(r, z)$ and $w(r, z)$ are the interpolation functions. Note that for $n=0$ Equation (A.1) gives the displacement expansion for the axisymmetric components r, z , and for the pure torsion problem θ . The functions $v_n(r, z)$ and $w_n(r, z)$ can be expressed in terms of the nodal shape functions (4 to 9 node elements)

$$\tilde{v}_n(r, z) = \begin{Bmatrix} v_{rn}(r, z) \\ v_{\theta n}(r, z) \\ v_{zn}(r, z) \end{Bmatrix} = \sum_{a=1}^9 N^a(r, z) \tilde{v}_n^a \quad (A.2)$$

$$\underline{w}_n(r, z) = \begin{Bmatrix} w_{rn}(r, z) \\ w_{\theta n}(r, z) \\ w_{zn}(r, z) \end{Bmatrix} = \sum_{a=1}^q N^a(r, z) \underline{w}_n^a; \quad (A.3)$$

where N^a are the element shape functions and v^a and w^a are the nodal unknowns. Substituting (A.2) and (A.3) into (A.1) yields

$$\underline{u} = \sum_{n=0}^N \left[\sum_{a=1}^q N^a(r, z) \cos n\theta \underline{v}_n^a + \sum_1^q N^a(r, z) \sin n\theta \underline{w}_n^a \right];$$

where

$$\underline{u} = \begin{Bmatrix} u_r \\ u_\theta \\ u_z \end{Bmatrix} \quad \underline{v}_n = \begin{Bmatrix} v_r \\ v_\theta \\ v_z \end{Bmatrix}_a \quad \text{and} \quad \underline{w}_n = \begin{Bmatrix} w_r \\ w_\theta \\ w_z \end{Bmatrix}_a$$

rearranging terms gives the following expression:

$$\underline{u} = \sum_{n=0}^N \left[\sum_{a=1}^q \begin{bmatrix} N_a \cos n\theta & N_a \sin n\theta \\ N_a \sin n\theta & N_a \cos n\theta \\ N_a \cos n\theta & N_a \sin n\theta \end{bmatrix} \begin{Bmatrix} v_r \\ v_\theta \\ v_z \\ w_r \\ w_\theta \\ w_z \end{Bmatrix} \right] = \sum_0^N \left(\sum_{n=1}^q \underline{H}_n^{(a)} \underline{v}_n^{(a)} \right); \quad (A.4)$$

the reason for this rearrangement is, as will be seen later, that the stiffness matrix becomes uncoupled for each of the parts. Splitting \underline{H}_n^a , (A.4) becomes

$$\underline{u} = \sum_{n=0}^N \left(\sum_{a=1}^q \underline{c}_n \underline{H}_n^a \underline{v}_n^{(a)} \right)$$

The strain displacement relationship according to the notation and sign criteria given in Figure (A.1) is:

$$\begin{aligned} \epsilon_{rr} &= u_{r,r} \\ \epsilon_{\theta\theta} &= \frac{1}{r} u_{\theta,\theta} + u_r/r \\ \epsilon_{zz} &= u_{z,z} \\ \gamma_{r\theta} &= 2\epsilon_{r\theta} = \left(\frac{1}{r} u_{r,\theta} + u_{\theta,r} - u_\theta/r \right) \\ \gamma_{rz} &= 2\epsilon_{rz} = (u_{z,r} + u_{r,z}) \\ \gamma_{\theta z} &= 2\epsilon_{\theta z} = (u_{\theta,z} + \frac{1}{r} u_{z,\theta}) \end{aligned}$$

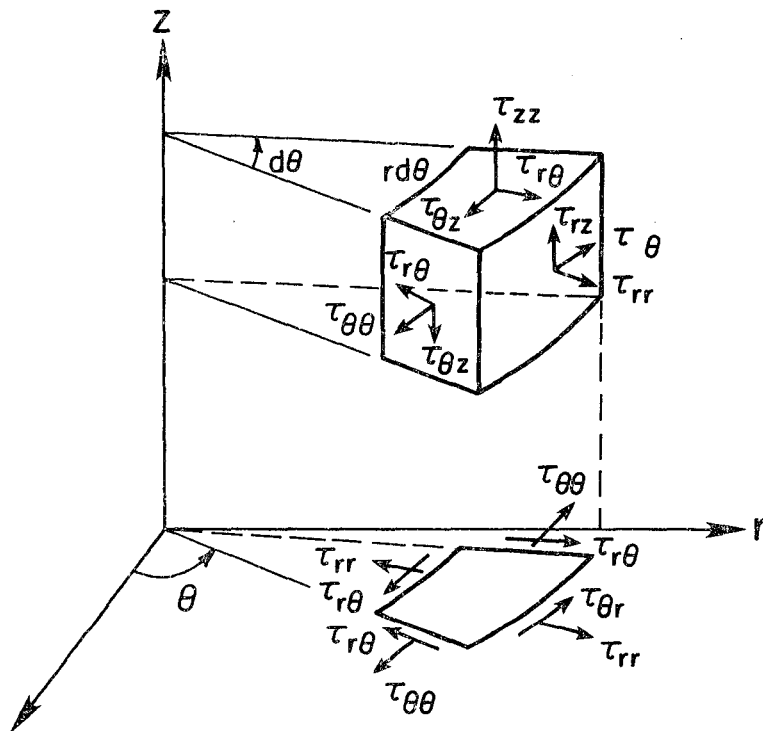


Fig A.1.- Stresses and sign criteria for axisymmetric problems.

Sustituting (A.4) in (A.5), the following relation for each harmonic can be obtained:

$$\begin{Bmatrix} \epsilon_{rr} \\ \epsilon_{\theta\theta} \\ \epsilon_{zz} \\ \gamma_{rz} \\ \gamma_{r\theta} \\ \gamma_{\theta z} \end{Bmatrix} = \sum_{a=1}^q \begin{bmatrix} N_{1r}^a \cos & 0 & 0 \\ N_{1r}^a \cos & n N_{1r}^a \cos & 0 \\ 0 & 0 & N_{1z}^a \cos \\ N_{1z}^a \cos & 0 & N_{1r}^a \cos \\ -\frac{nN_{1z}^a}{r} \sin & (N_{1r}^a - \frac{N_{1z}^a}{r}) \sin & 0 \\ 0 & N_{1z}^a \sin & -\frac{nN_{1z}^a}{r} \sin \end{bmatrix} \begin{Bmatrix} U_r \\ W_\theta \\ U_z \end{Bmatrix}^{(a)} + \begin{bmatrix} N_{1r}^a \sin & 0 & 0 \\ N_{1r}^a \sin & -\frac{n}{r} N_{1z}^a \sin & 0 \\ 0 & 0 & N_{1z}^a \sin \\ N_{1z}^a \sin & 0 & N_{1r}^a \sin \\ \frac{nN_{1z}^a}{r} \cos & (N_{1r}^a - \frac{N_{1z}^a}{r}) \cos & 0 \\ 0 & N_{1z}^a \cos & \frac{nN_{1z}^a}{r} \cos \end{bmatrix} \begin{Bmatrix} W_r \\ U_\theta \\ W_z \end{Bmatrix}^{(a)} \quad (A.7)$$

or in simplified notation

$$\underline{\underline{\epsilon}} = \sum_{n=1}^N \sum_{a=1}^q \left[B_1^{na} \quad \dots \quad B_2^{na} \right] \begin{Bmatrix} U_n^a \\ W_n^a \end{Bmatrix} \quad (A.8)$$

It is worth noting that without considering the sin and cos the following relation is satisfied

$$B_1^a(n) = B_2^a(-n)$$

Equation (A.8) can also be expressed in the following manner:

$$\underline{\underline{\epsilon}} = \sum_{n=1}^N \left[B_1^{n1} B_2^{n1} \quad \dots \quad B_1^{nq} B_2^{nq} \right] \begin{Bmatrix} U_n^1 \\ W_n^1 \\ \vdots \\ U_n^q \\ W_n^q \end{Bmatrix} = \sum_{n=1}^N \underline{\underline{B}} \underline{\underline{U}} \quad (A.9)$$

where $\underline{\underline{B}}$ represents the strain-displacement transformation matrix of the whole element.

The constitutive equations for cylindrically orthotropic or isotropic materials are:

$$\begin{Bmatrix} \sigma_{rr} \\ \sigma_{\theta\theta} \\ \sigma_{zz} \\ \tau_{rz} \\ \tau_{r\theta} \\ \tau_{\theta z} \end{Bmatrix} = \begin{bmatrix} C_{rr} & C_{r\theta} & C_{rz} & & & \\ C_{\theta r} & C_{\theta\theta} & C_{\theta z} & & & \\ C_{zr} & C_{z\theta} & C_{zz} & & & \\ & & & G_{rz} & & \\ & & & & G_{r\theta} & \\ & & & & & G_{\theta z} \end{bmatrix} \begin{Bmatrix} \epsilon_{rr} \\ \epsilon_{\theta\theta} \\ \epsilon_{zz} \\ 2\epsilon_{rz} \\ 2\epsilon_{r\theta} \\ 2\epsilon_{\theta z} \end{Bmatrix} = \underline{\underline{D}} \underline{\underline{\epsilon}} \quad (A.10)$$

STIFFNESS MATRIX.

The strain energy functional for an element is:

$$E_e = \frac{1}{2} \int_0^{2\pi} \int_A \sum_n^N \sum_{m=0}^N \underline{v}^T \underline{B}^T \underline{D} \underline{B} \underline{v} r d\theta dA \quad (A.11)$$

Due to the orthogonality conditions of the trigonometric functions, the double summation in (A.11) can be converted in a single one.

$$E_e = \frac{1}{2} \int_0^{2\pi} \int_A \underline{v}^T \underline{B}^T \underline{D} \underline{B} \underline{v} r dA \quad \begin{array}{l} \xi=1 \text{ for } n \neq 0 \\ \xi=2 \text{ for } n = 0 \end{array} \quad (A.12)$$

It is worth noting that :

a) Each harmonic n will produce an uncoupled stiffness matrix.

b) the vector \underline{v} contains 6 degrees of freedom per node and per harmonic. A planar 9 node element will therefore give $9 \times 6 = 54$ degrees of freedom.

c) The matrix \underline{B} is 6×54 therefore the product $\underline{B}^T \underline{D} \underline{B}$ will provide a stiffness matrix of order 54×54 . Due to the rearrangement shown above the stiffness matrix can be divided into two of order 27×27 . For simplicity we can carry out the product shown above by the subdivision of \underline{B} as given in Equation (A.8) and depicted in Figure (A.2)

$$\underline{k}_{ab} = \int_{ne} \underline{B}_a^T \underline{D} \underline{B}_b r dV = \int_{ne} \underline{T}_{ab} r dA d\theta$$

where

$$\underline{T}_{ab} = \underline{B}_a^T \underline{D} \underline{B}_b$$

After integrating with respect to θ , \underline{k}_{ab} becomes:

$$\underline{k}_{ab} = \int_A \begin{bmatrix} T_{11} & T_{12} & T_{13} & & & \\ T_{21} & T_{22} & T_{23} & & & \\ T_{31} & T_{32} & T_{33} & & & \\ & & & T_{11} & -T_{12} & T_{13} \\ & & & -T_{21} & T_{22} & -T_{23} \\ & & & T_{31} & -T_{32} & T_{33} \end{bmatrix} r dA = \int_A [\underline{k}] r dA$$

The numerical integration will be carried out in the following manner:

$$\underline{k}_{ab} = \sum_{i=1}^M w_i |J|_i [\underline{k}_i] r_i$$

where M represents the total number of Gauss points used in the integration.

NODE	1	2	3	4	5	6	7	8	9
K_{11}	K_{12}	K_{13}							
					K_{ab}				

Fig A.2.- Element matrix per harmonic. The order of each cell is 6x6.

MASS MATRIX.

The element kinetic energy is

$$T_e = \frac{1}{2} \int_0^{2\pi} \int_A \rho \sum_{\tilde{n}} \sum_{\tilde{m}} \dot{v}_{\tilde{n}}^T H_{\tilde{n}}^T H_{\tilde{m}} \dot{v}_{\tilde{m}} r d\theta dA$$

where $H_{\tilde{n}}$ is defined in Equation (A.4). Again taking into account the orthogonality of the trigonometric functions, the functional can be expressed as

$$T = \frac{1}{2} \rho \pi \int_A \sum_{\tilde{n}} \dot{v}_{\tilde{n}}^T \left[\int_{\tilde{n}} H_{\tilde{n}}^T H_{\tilde{n}} r dA \right] \dot{v}_{\tilde{n}}$$

Each harmonic will produce an uncoupled mass matrix. The consistent mass will be

$$M_{as} = \rho \pi \int_A H_{\tilde{n}}^T H_{\tilde{n}} r dA$$

This can be lumped to the diagonal terms by scaling:

$$M_{aa} = \left(\rho \pi \int_A H_{\tilde{n}}^T H_{\tilde{n}} r dA \right) \frac{M_t}{\sum M_{ii}} \quad (A.13)$$

where M_t represents the total mass of the element. Numerical integration will give :

$$M_{aa} = \sum_{i=1}^N w_i |J_i| \rho \pi \int (H_{\tilde{n}}^T)_i (H_{\tilde{n}})_i r_i \frac{M_t}{\sum M_{aa}}$$

BODY FORCES.

The energy term corresponding to one element is:

$$E = \int_{vol} \tilde{u}^T \tilde{b} dV = \sum_{n=0}^N \int_{vol} \tilde{v}^T H \tilde{c}_n \tilde{b} dVol \quad (A.14)$$

The body forces can be expanded in terms of the Fourier Series

$$\tilde{b} = \begin{Bmatrix} b_r \\ b_\theta \\ b_z \end{Bmatrix} = \sum_n \begin{Bmatrix} b_{nr}^1 \cos n\theta + b_{nr}^2 \sin n\theta \\ b_{n\theta}^1 \cos n\theta + b_{n\theta}^2 \sin n\theta \\ b_{nz}^1 \cos n\theta + b_{nz}^2 \sin n\theta \end{Bmatrix} = \sum_{n=0}^N \tilde{c}_n \tilde{b}$$

and (A.14) becomes

$$E = \sum_n \sum_m \int_{vol} \left(\sum_{a=1}^2 \tilde{v}^{aT} H^a \tilde{c}_n \right) \tilde{c}_m \tilde{b}_m dVol$$

Again due to orthogonality conditions:

$$E = \rho \pi \sum_n \sum_{\tilde{n}} \tilde{v}^{aT} \int_A H^a \tilde{b}_n r dA$$

After imposing the stationarity condition to the energy functional one can obtain the nodal forces for a given harmonic n .

$$F_n^{(a)} = \oint_{Area} N_n^a \underline{d}_n r dA \quad (A.15)$$

TEMPERATURE LOADS.

Again the energy term is:

$$E_T = \int_{Vol} \underline{\epsilon}^T(\underline{\epsilon}) dVol = \sum_{n=0}^N \int_{Vol} \underline{v}_n^T \underline{B}_n^T \underline{D} \underline{\alpha} (T-T_r) dVol$$

where

$$\underline{\alpha} (T-T_r) = \begin{bmatrix} \alpha_r \\ \alpha_\theta \\ \alpha_z \\ 0 \\ 0 \\ 0 \end{bmatrix} (T-T_r) = \begin{bmatrix} \alpha_r \Delta t^1 C_n + \alpha_r \Delta t^2 S_n \\ \alpha_\theta \Delta t^1 C_n + \alpha_\theta \Delta t^2 S_n \\ \alpha_z \Delta t^1 C_n + \alpha_z \Delta t^2 S_n \\ 0 \\ 0 \\ 0 \end{bmatrix}$$

Since

$$(T-T_r) = \Delta t (t) = \sum_n (\Delta t^1 \cos n\theta + \Delta t^2 \sin n\theta)$$

where the temperature distribution has been expanded as a Fourier series. α_i are the coefficients of thermal expansion. Substituting (A.17) in (A.16)

$$E_T = \sum_n^N \sum_m^M \int_{Vol} \underline{\epsilon}^T (\underline{v}_n^T \underline{B}_n^T) \underline{C} \underline{\epsilon}_m dVol = \oint_{Area} \sum_n^N \underline{\epsilon}^T (\underline{v}_n^T \underline{B}_n^T) \underline{C} \underline{\epsilon}_n r dA$$

By the stationarity of the functional the thermal loads become:

$$F_n^{(a)} = \oint_{Area} \underline{B}_n^T \underline{C} \underline{\epsilon}_n r dA$$

PRESSURE LOADS.

They can be treated as body forces. Expression (A.15) can now be used but integrating not over the volume but over the area where the pressure is applied

$$F_n^{(2)} = 9\pi \int_{\tilde{A}} N_n^a p_n dA$$

now

$$p_n = \begin{Bmatrix} p_n \\ p_0 \\ p_2 \end{Bmatrix}_n = \sum_i H_n^a p^a$$

and the pressure loads can be expanded in Fourier series leading to:

$$F_n^{(2)} = 9\pi \int_{\tilde{A}} N_n^a H_n^a p_n^{(a)} r dA$$

APPENDIX B

8 TO 27 NODE SOLID FINITE ELEMENT

A solid isoparametric finite element is defined in this Appendix that has a variable number of nodes (8-27). Also, some aspects concerning numerical integration are considered. Finally, an expansion of the displacements in the solid element in terms of Fourier series is developed so that a solid finite element can be coupled with an axisymmetric mesh.

B.1.- FORMULATION.

The system of local coordinates for each element is defined in Figure (B.1). In an isoparametric element the coordinates can be defined in terms of the shape functions:

$$\begin{aligned}x &= \sum_1^N H_i(r, s, t) x_i \\y &= \sum_1^N H_i(r, s, t) y_i \\z &= \sum_1^N H_i(r, s, t) z_i\end{aligned}\tag{B.1}$$

The same functions are used to expand the displacements:

$$\begin{aligned}u_x &= \sum_1^N H_i(r, s, t) u_x^i \\u_y &= \sum_1^N H_i(r, s, t) u_y^i \\u_z &= \sum_1^N H_i(r, s, t) u_z^i\end{aligned}\tag{B.2}$$

The shape functions are defined by a serendipity type of formulation that starts with the basic nodal linear functions to which the quadratic terms are added. Table 1 shows all the basic interpolation functions. Table 2 illustrates the generation of the shape functions by the serendipity approach.

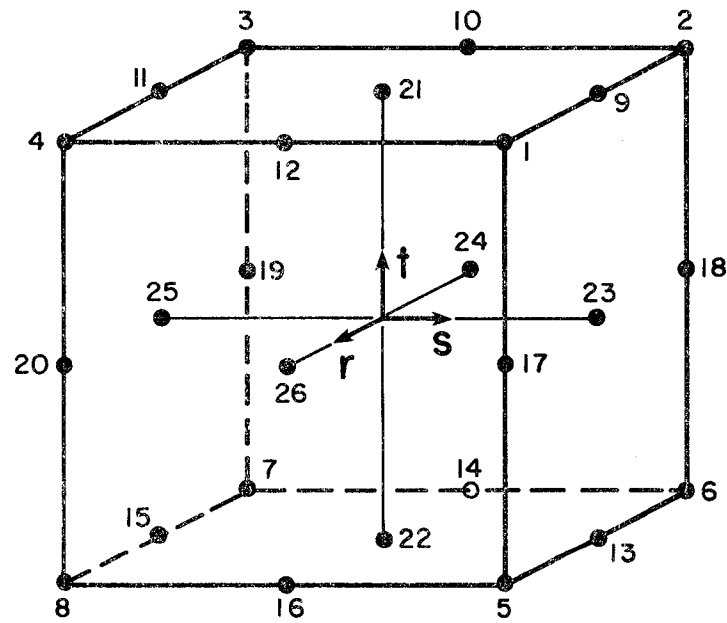


Fig B.1.- Local numbering and coordinate system.

$$\begin{array}{lll}
 R = (1+r) & \bar{R} = (1-r) & R^* = (1-r^2) \\
 S = (1+s) & \bar{S} = (1-s) & S^* = (1-s^2) \\
 T = (1+t) & \bar{T} = (1-t) & T^* = (1-t^2)
 \end{array}$$

$$\begin{array}{lll}
 l_1 = 1/8 R S T & l_9 = 1/4 R^* S T & l_{21} = 1/2 R^* S^* T \\
 l_2 = 1/8 \bar{R} S T & l_{10} = 1/4 \bar{R} S^* T & l_{22} = 1/2 R^* S^* \bar{T} \\
 l_3 = 1/8 \bar{R} \bar{S} T & l_{11} = 1/4 R^* \bar{S} T & l_{23} = 1/2 R^* S T^* \\
 l_4 = 1/8 R \bar{S} T & l_{12} = 1/4 R S^* T & l_{24} = 1/2 \bar{R} S^* T^* \\
 l_5 = 1/8 R S \bar{T} & l_{13} = 1/4 R^* S \bar{T} & l_{25} = 1/2 R^* \bar{S} T^* \\
 l_6 = 1/8 \bar{R} S \bar{T} & l_{14} = 1/4 \bar{R} S^* \bar{T} & l_{26} = 1/2 R S^* T^* \\
 l_7 = 1/8 \bar{R} \bar{S} \bar{T} & l_{15} = 1/4 R^* \bar{S} \bar{T} & l_{27} = 1/2 R^* S^* T^* \\
 l_8 = 1/8 R \bar{S} \bar{T} & l_{16} = 1/4 R S^* \bar{T} & \\
 & l_{17} = 1/4 R S T^* & \\
 & l_{18} = 1/4 \bar{R} S T^* & \\
 & l_{19} = 1/4 \bar{R} \bar{S} T^* & \\
 & l_{20} = 1/4 R \bar{S} T^* &
 \end{array}$$

Table B.1.- Basic interpolation functions.

The displacement functions given in (B.2) can also be written in the following form

$$\begin{Bmatrix} u_x \\ u_y \\ u_z \end{Bmatrix} = \sum_{a=1}^{27} \begin{bmatrix} N_{a,x} & 0 & 0 \\ 0 & N_{a,y} & 0 \\ 0 & 0 & N_{a,z} \end{bmatrix} \begin{Bmatrix} u_x^a \\ u_y^a \\ u_z^a \end{Bmatrix} = \sum \tilde{H}_a \underline{u}^a \quad (B.3)$$

The strain-displacement relationship is:

$$\begin{aligned} \epsilon_x &= u_{x,x} \\ \epsilon_y &= u_{y,y} \\ \epsilon_z &= u_{z,z} \\ \gamma_{xy} &= u_{x,y} + u_{y,x} \\ \gamma_{yz} &= u_{y,z} + u_{z,y} \\ \gamma_{zx} &= u_{z,x} + u_{x,z} \end{aligned} \quad (B.4)$$

Combining (B.5) and (B.3), gives

$$\begin{Bmatrix} \epsilon_x \\ \epsilon_y \\ \epsilon_z \\ \gamma_{xy} \\ \gamma_{yz} \\ \gamma_{zx} \end{Bmatrix} = \sum_1^{27} \begin{bmatrix} N_{a,x} & 0 & 0 \\ 0 & N_{a,y} & 0 \\ 0 & 0 & N_{a,z} \\ N_{a,y} & N_{a,x} & 0 \\ 0 & N_{a,z} & N_{a,y} \\ N_{a,z} & 0 & N_{a,x} \end{bmatrix} \begin{Bmatrix} u_x^a \\ u_y^a \\ u_z^a \end{Bmatrix} = \sum_1^{27} \tilde{D}_a \underline{u}^a \quad (B.5)$$

Considering the case of orthotropic or isotropic materials the constitutive equations take the following form:

$$\underline{\sigma} = \begin{bmatrix} C_{xx} & C_{xy} & C_{xz} & 0 & 0 & 0 \\ C_{yx} & C_{yy} & C_{yz} & 0 & 0 & 0 \\ C_{zx} & C_{zy} & C_{zz} & 0 & 0 & 0 \\ 0 & 0 & 0 & G_{xy} & 0 & 0 \\ 0 & 0 & 0 & 0 & G_{yz} & 0 \\ 0 & 0 & 0 & 0 & 0 & G_{zx} \end{bmatrix} \quad (B.6)$$

STIFFNESS MATRIX.

The stiffness matrix is obtained from the strain energy expression as was done for the axisymmetric case:

$$\underline{\underline{K}}_{ab}^e = \int_{vol} \underline{\underline{B}}_a^T \underline{\underline{C}} \underline{\underline{B}}_b \, dvol \quad (B.7)$$

where $\underline{\underline{K}}_{ab}$ represents the 3x3 matrix shown in the figure (A.2). The computation of $\underline{\underline{S}}_{ab} = \underline{\underline{B}}_a^T \underline{\underline{C}} \underline{\underline{B}}_b$ is straightforward. By using numerical quadrature:

$$\underline{\underline{K}}_{ab}^e = \sum_{i=1}^M w_i (\underline{\underline{B}}_a^T \underline{\underline{C}} \underline{\underline{B}}_b) |J|_i$$

MASS MATRIX.

As for the axisymmetric element, the expression for the consistent mass matrix is

$$\underline{\underline{M}}_{ab} = \int_{vol} \rho \underline{\underline{H}}_a^T \underline{\underline{H}}_b \, dvol \quad (B.8)$$

where $\underline{\underline{M}}_{ab}$ constitutes a 3x3 cell of the total element mass matrix. By scaling the diagonal terms of the consistent mass matrix we can obtain the lumped mass matrix:

$$\underline{\underline{M}}_{aa} = \frac{M_t}{\sum \underline{\underline{M}}_{aa}} \int_{vol} \underline{\underline{H}}_a^T \underline{\underline{H}}_a \, dvol \quad (B.9)$$

BODY FORCES.

From the energy term:

$$\int_{vol} \underline{\underline{u}}^T \underline{\underline{b}} \, dvol = \int_{vol} (\sum \underline{\underline{H}}_a^T \underline{\underline{u}}_a^T) \underline{\underline{b}} \, dvol$$

and the nodal forces are

$$\underline{\underline{F}}^{(a)} = \int_{vol} \underline{\underline{H}}_a^T \underline{\underline{b}} \, dvol \quad (B.11)$$

SURFACE LOADS

These loads are defined identically to (B.11)

$$\underline{\underline{F}}^{(a)} = \int_{Sur} \underline{\underline{H}}_a^T \underline{\underline{p}} \, dArea$$

where p is now the surface pressure. The integration is carried out over the surface integral instead of over the volume as was done for the body forces.

B.2- NUMERICAL INTEGRATION

Numerical integration for the calculation of the stiffness, mass and loads matrices at the element level is carried out by quadrature rules. Some authors have obtained savings in computer time and storage by adopting quadrature rules with a smaller number of points than the Gaussian rules. Irons (1971) and Hellen (1972) demonstrated that quadrature rules that use 13 and 14 points for solid elements with 20 nodes are of the same accuracy as the 3x3x3 Gauss quadrature. The aim of this study is to find a reduced quadrature that similar to the 20 node element, will give to the 27 node element the same degree of accuracy as the 3*3*3 Gauss integration rule.

The general expression for an integration rules is:

$$\int_{-1}^1 \int_{-1}^1 \int_{-1}^1 f(x,y,z) dx dy dz = A_1 f(0,0,0) + B_6 \{ f(-b,0,0) + f(b,0,0) + \dots \} + C_{12} \{ f(-c,-c,-c) + f(-c,-c,c) + \dots \} + D_{12} \{ f(-d,-d,0) + f(-d,d,0) + \dots \}$$

Where the capital letters represent the weights and the lower case letters the coordinates of the quadrature points. The rules and their respective points and weights are shown in Table 3. The errors introduced in the different polynomials that are included in the stiffness matrix are given in Table 4.

The solutions to three different problems: a beam, plate bending and solid deformation, are illustrated in Tables 5, 6 and 7. As it can be seen the 14 point rules give very oscillatory results and in some cases are totally unreliable, as in the plate bending and solid problems. The 15 point rule gives much better results. The use of the central point considerably increases the accuracy of the integration process. However, for the plate problem it gives some oscillatory results that become much more pronounced for the solid problem. The use of the 21 point rule does not lead to noticeable improvements. The oscillations disappear for the plate problem but remain in the solid problem. It is worth noticing, that the average of all the oscillatory results coincides with the master solution given by 3x3x3 Gauss integration rule.

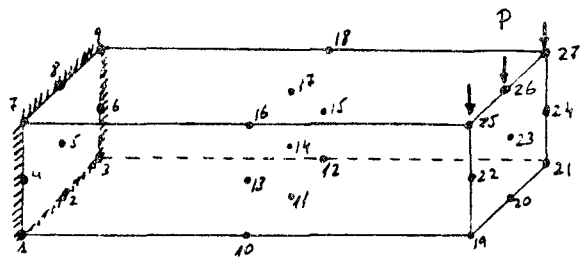
RULE	WEIGHTS				COORDINATES		
	A	B ₆	C ₈	D ₁₂	b	c	d
14a		0.0001	.999925		.7071134	.57736109	
14b		.88642659	.33518005		.79582243	.758786911	
15b	.71213744	.68622723	.39635239		.84841801	.72766244	
15	-.39506173	.98765432	.30864198		.77459667	.77459667	
21a	1.024		0.008	0.57600		1.2909945	.7453559
21b	1.5802469		.06172839	.49382716		.77459667	.77459667
21c	.3731778		.07871720	.58309038		.881917104	.683130051

Table B.3.- Points and weights of the interpolation rules.

RULE	SIX DEGREE TERMS			EIGHTH DEGREE TERMS		
	r^6	r^4s^2	$r^2s^2t^2$	r^6s^2	r^4s^4	$r^4s^2t^2$
14a	1.14	0.53	0.30	0.38	0.32	0.18
14b	-0.18	-0.02	0.22	-0.09	-0.03	0.12
15	-0.16	0.00	0.24	-0.06	0.00	0.14
15b	-0.16	-0.06	0.17	-0.13	-0.07	0.07
21a	0.06	0.16	0.00	0.33	0.39	0.31
21b	-0.18	0.00	-0.19	-0.06	0.00	-0.11
21c	0.37	0.00	0.00	0.04	-0.02	-0.05
3x3x3G	-0.18	0.00	0.00	-0.06	0.00	0.00

Table B.4.- Errors of rules.

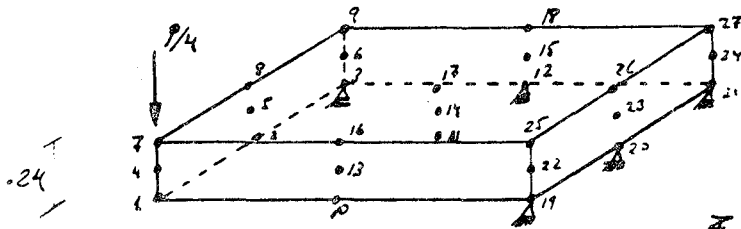
$E = 100$
 $G = 40$
 $A = 4.0$



EXACT DEFLECTIONS
 $\delta = 17.63$

JOINT	14a	14b	15	15b	21a	21b	21c	21.3.36
19	-14.01	-14.21	-14.27	-14.14	-14.18	-14.16	-14.28	-14.06
20	-19.31	-14.68	-14.76	-14.60	"	"	"	"
21	-14.01	-14.21	-14.27	-14.14	"	"	"	"
22	-19.38	-14.67	-14.75	-14.59	"	"	"	"
23	-16.68	-14.09	-14.08	-14.12	"	"	"	"
24	-19.38	-14.67	-14.75	-14.59	"	"	"	"
25	-14.01	-14.21	-14.27	-14.14	"	"	"	"
26	-19.31	-14.68	-14.76	-14.60	"	"	"	"
27	-14.01	-14.21	-14.27	-14.14	"	"	"	"

Table B.5.- Tip deflections of a cantilever beam.



$E = 26000$

$\nu = 0.3$

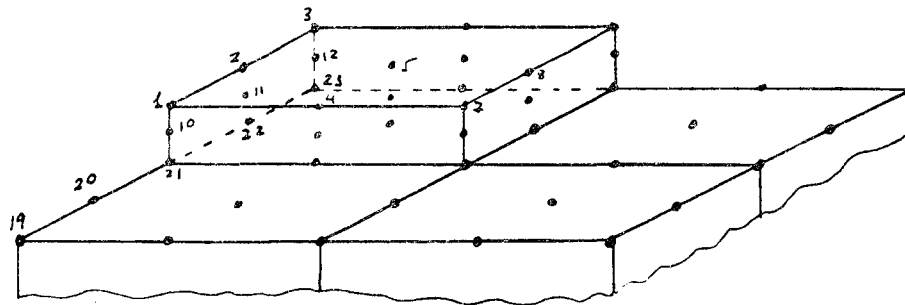
$P = 1.0$

Exact deflection at Node 7

$\delta = -0.203$

Joint	14a	14b	15	15b	21c	21b	21a	32.36
1	-0.562	-0.163	-0.137	-0.139	-0.141	-0.140	-0.143	-0.140
4	0.233	-0.202	-0.136	"	"	"	"	"
7	-0.585	-0.163	-0.137	"	"	"	"	"
2	0.171	-0.155	-0.101	-0.105	-0.105	-0.105	-0.107	-0.105
5	-0.027	-0.128	-0.102	"	"	"	"	"
8	0.177	-0.155	-0.101	"	"	"	"	"
10	0.171	-0.155	"	"	"	"	"	"
13	-0.027	-0.128	-0.103	"	"	"	"	"
16	0.177	-0.155	-0.101	"	"	"	"	"
11	0.028	-0.097	-0.077	-0.078	-0.079	-0.078	-0.080	-0.079
14	"	"	"	"	"	"	"	"
17	"	"	"	"	"	"	"	"

Table B.6.- Plate bending problem.



Joint	14a	14b	15	15b	21c	21a	21b	3a,3b,3c
1	0.0446	-0.464	-0.468	-0.459	-0.557	-0.403	-0.589	-0.538
2	-0.805	-0.613	-0.616	-0.609	-0.479	-0.536	-0.491	"
3	0.033	-0.464	-0.468	-0.459	-0.557	-0.403	-0.589	"
10	-0.806	-0.613	-0.616	-0.609	-0.479	-0.536	-0.491	"
11	-0.598	-0.512	-0.505	-0.525	-0.635	-0.668	-0.639	"
12	-0.801	-0.613	-0.616	-0.609	-0.479	-0.536	-0.491	"
21	-0.022	-0.465	-0.469	-0.459	-0.557	-0.403	-0.589	"
22	-0.802	-0.613	-0.616	-0.609	-0.479	-0.536	-0.491	"
23	0.017	-0.464	-0.468	-0.459	-0.557	-0.403	-0.589	"
19	0.342	-0.100	-0.092	-0.114	-0.114	-0.134	-0.168	-0.128
20	-0.408	-0.199	-0.209	-0.185	-0.215	-0.199	-0.199	-0.207

Table B.7.- Solid deformation problem. Vertical uniform load on top element.

The reasons for the oscillatory nature of the response lies in the higher order terms (see Table 1) in the stiffness matrix that are not integrated exactly. These errors do not affect the overall response of the structure, because the average displacements coincide with those given by the 3x3x3 Gauss quadrature. However, they have a definite influence in the local response at the element level.

Based on the above discussion, it may be concluded that the 15 and 21 point quadrature rules have to be used carefully. All the results will have to be averaged at the nodes of each element to obtain reliable answers for solid deformation problems. However their use, especially the 15 point rule, will lead to substantial savings in computer time.

B.3.- COUPLING BETWEEN SOLID AND AXISYMMETRIC MESHES.

According to the sign criteria and the configuration illustrated in Figure (B.2) the x, y, and z components of the displacements can be transformed into the cylindrical components as follows:

$$\begin{aligned} u_x &= -u_\theta \sin \theta - u_r \cos \theta \\ u_y &= -u_\theta \cos \theta + u_r \sin \theta \\ u_z &= u_z \end{aligned} \quad (B.12)$$

or in matrix form

$$\underline{\underline{u}}_c = \begin{Bmatrix} u_x \\ u_y \\ u_z \end{Bmatrix} = \begin{bmatrix} -\cos \theta & -\sin \theta & 0 \\ -\sin \theta & \cos \theta & 0 \\ 0 & 0 & 1 \end{bmatrix} \begin{Bmatrix} u_\theta \\ u_r \\ u_z \end{Bmatrix} = \underline{\underline{T}} \underline{\underline{u}}_r \quad (B.13)$$

The displacements in cylindrical coordinates are expanded in Fourier series as was done for the axisymmetric elements.

$$\underline{\underline{u}}_r = \underline{\underline{v}}_0 + \underline{\underline{c}}^1 \underline{\underline{v}}_1 + \underline{\underline{s}}^1 \underline{\underline{w}}_1 + \underline{\underline{c}}^2 \underline{\underline{v}}_2 + \underline{\underline{s}}^2 \underline{\underline{w}}_2 \quad (B.14)$$

where

$$\underline{\underline{v}}_0 = \begin{Bmatrix} v_0 \\ v_r \\ v_z \end{Bmatrix}_0 \quad \underline{\underline{v}}_n = \begin{Bmatrix} v_\theta \\ v_r \\ v_z \end{Bmatrix}_n \quad \underline{\underline{w}}_n = \begin{Bmatrix} w_\theta \\ w_r \\ w_z \end{Bmatrix}_n$$

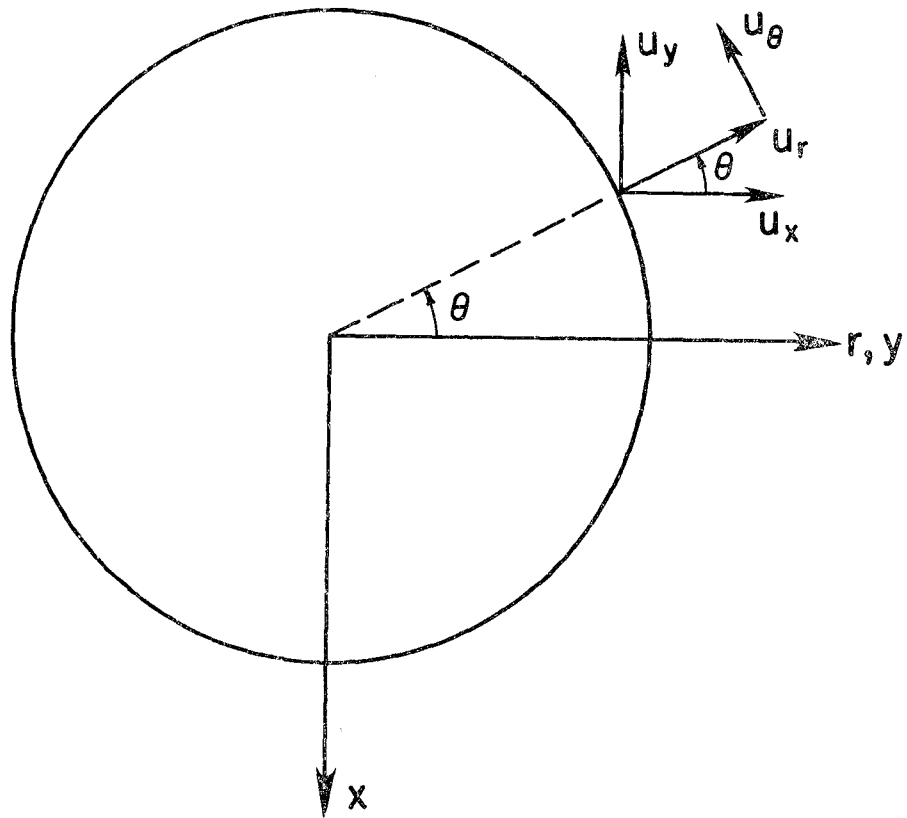


Fig B.2.- Transformation of rectangular cartesian coordinates into cylindrical ones.

and

$$\tilde{C}^n = \begin{bmatrix} \sin n\theta & 0 & 0 \\ 0 & \cos n\theta & 0 \\ 0 & 0 & \cos n\theta \end{bmatrix} \quad \text{and} \quad \tilde{S}^n = \begin{bmatrix} \cos n\theta & 0 & 0 \\ 0 & \sin n\theta & 0 \\ 0 & 0 & \sin n\theta \end{bmatrix}$$

The substitution of (B.13) into (B.14) renders:

$$\underline{u}_x = \underline{T} \underline{v}_0 + \underline{T} \underline{C}' \underline{v}_1 + \underline{T} \underline{S}' \underline{w}_1 + \underline{T} \underline{C}'' \underline{w}_2 + \dots$$

Expression (B.15) defines the general transformation of rectangular coordinates into a Fourier series expansion. If this transformation is carried out for all the nodes of the boundary interface between a solid mesh and an axisymmetric mesh, a perfect coupling may be obtained. These transformations can be accomplished in an efficient way at the element level.

For a general isolated mesh, the stiffness matrix will have the shape shown in Figure (B.3) before and after the transformation. \mathbf{K}_s represents the part of the stiffness that remains in rectangular coordinates, \mathbf{K}_i the axisymmetric stiffness for each harmonic, \mathbf{K}_{si} the coupling stiffness between both parts and \mathbf{K}_{ii} represents the coupling terms between harmonics. If a given solid mesh is a part of an ensemble that has axisymmetry, the coupling terms between harmonics, \mathbf{K}_{oi} , will vanish after adding all the element stiffness matrices along the circumference. (The harmonics are orthogonal in the interval $0 - 2\pi$). As a consequence, the stiffness matrix will have the form shown in Figure (B.4), where all the coupling terms between harmonics have vanished.

When using a profile solver a more efficient configuration of the stiffness matrix is obtained by rearranging the terms as shown in the same Figure.

REFERENCES.

Irons, B. M. "Quadrature Rules for Brick Based Finite Elements", Int. J. Numer. Meth. Engin., Vol 3, pp. 293-294, (1971)

Hellen, T. K. "Effective Quadrature Rules for Quadratic Solid Isoparametric Finite Elements", Int. J. Num. Meth. Engin. Vol 4, pp 597-600, (1972).

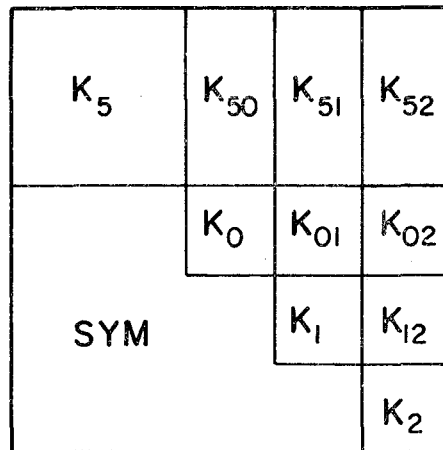


Fig B.3.- Layout of the coupled solid-axisymmetric stiffness matrix.

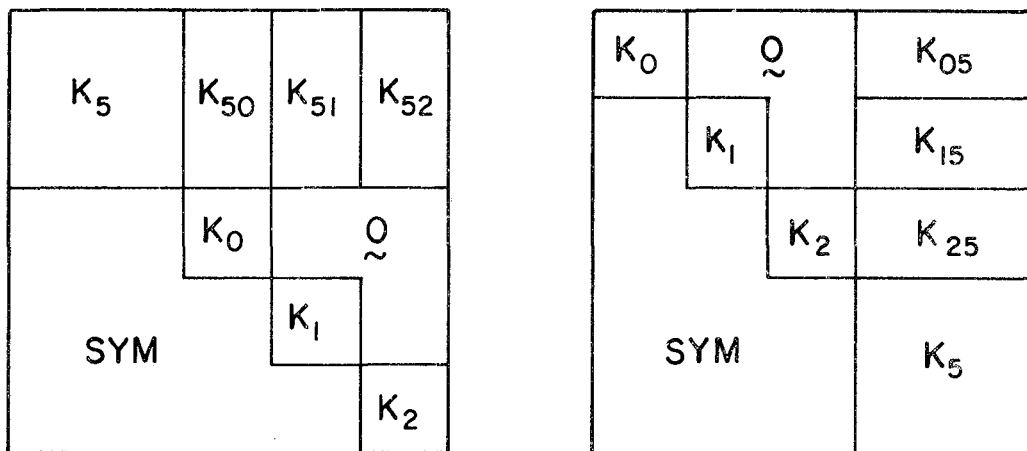


Fig B.4.- Layout of the stiffness matrix convenient for a profile solver when there is axisymmetry at the boundary.

APPENDIX C

SOLUTION OF THE EQUATIONS OF MOTION WITH THE COMPLEX MODE SHAPES

A summary of the analytical method based on the complex eigenvectors for the integration of the equations of motion is given below. The beginning of the formulation is taken from Dynamics of Structures (Hurty and Rubinstein 1964) and later it is extended by the author to include the case of earthquake type of excitation.

Consider a system of n equations of motion for a soil-structure system:

$$\underline{m} \ddot{\underline{q}} + \underline{c} \dot{\underline{q}} + \underline{k} \underline{q} = \underline{p}(t) = \underline{p} \ddot{u}_g(t) \quad (C.1)$$

where \underline{u}_g is a given ground motion and \underline{p} is a load distribution vector. The system of second order equations can be transformed into a system of $2n$ first order equations, Foss (1958), by adding the following matrix identity:

$$\underline{m} \dot{\underline{q}} - \underline{m} \dot{\underline{q}} = 0 \quad (C.2)$$

Thus (C.1) becomes:

$$\begin{bmatrix} \underline{c} & \underline{m} \\ \underline{m} & 0 \end{bmatrix} \begin{Bmatrix} \dot{\underline{q}} \\ \underline{q} \end{Bmatrix} + \begin{bmatrix} \underline{k} & 0 \\ 0 & -\underline{m} \end{bmatrix} \begin{Bmatrix} \underline{q} \\ \dot{\underline{q}} \end{Bmatrix} = \begin{Bmatrix} \underline{p}(t) \\ 0 \end{Bmatrix} \quad (C.3)$$

or in simplified notation:

$$A \{ \dot{y} \} + B \{ y \} = Y \quad (C.4)$$

It is worth noting that A and B are real and symmetric, however neither of them is positive definite. Therefore the eigen-solution will give complex eigenvalues and eigenvectors. The transformation

$$y = \{ \phi \} e^{\rho t} \quad (C.5)$$

leads to the following eigenvalue problem

$$\rho A \phi + B \phi = 0$$

After having condensed out all the massless degrees of freedom, B will have an inverse and Equation (C.5) can be written as follows:

$$B^{-1}A \phi = 1/p \phi$$

or

$$D\phi = \lambda \phi \quad (C.6)$$

where

$$D = -B^{-1}A = - \begin{bmatrix} k^{-1}c & -k^{-1}m \\ I & 0 \end{bmatrix}$$

Equation (C.6) represents a standard eigenvalue problem, but with D being non symmetric. The system (C.6) will lead to $2n$ eigenvalues and eigenvectors that are real or complex in conjugate pairs. The usual procedure in structural dynamics has been to solve (C.6) by inverse iteration. Jennings affirms that the reduction of Equation (C.6) to upper Hessenberg form and the subsequent use of the QR method for the eigen-solution leads to a very efficient algorithm for systems of up to a few hundred equations. The total number of operations is approximately $4n^3$, of which only one-fifth are required for the reduction to upper Hessenberg form. Now if

$$\lambda = u + iv$$

p will be

$$p = \alpha + i\beta$$

where

$$\alpha = u/(u^2 + v^2) \quad (C.7)$$

$$\beta = -v/(u^2 + v^2)$$

and

$$y = \phi e^{pt} = \phi e^{\alpha t} e^{i\beta t}$$

For a damped system, α is negative and the term $e^{\alpha t}$ represents the decay of the amplitude of the mode. β represents the damped frequency. If p is expressed in polar form:

$$p = (\alpha^2 + \beta^2)^{1/2} e^{i\psi}$$

, ψ represents the phase angle between velocities and displacements. The orthogonality condition of the eigenvectors is easily seen.

Hence

$$\phi_i^T A \phi_i = a_i \quad ; \quad \phi_i^T B \phi_i = B_i$$

and

$$\rho a_i + B_i = 0 \tag{C.8}$$

The next step is to uncouple Equation (C.4). Pre and postmultiplying by one obtains:

$$\phi^T A \phi \dot{z}_r + \phi^T B \phi \dot{z}_r = \phi^T Y(t)$$

or

$$a_i \dot{z}_i + B_i z_i = \phi_i^T Y(t)$$

and substituting (C.8)

$$a_i \dot{z}_i - \rho_i a_i z_i = \phi_i^T Y(t)$$

Dividing by a_i

$$\dot{z}_i - \rho_i z_i = \phi_i^T Y(t) / a_i \tag{C.9}$$

Equation (C.9) has a companion complex conjugate given by

$$\dot{z}_i^* - \bar{\rho}_i z_i^* = \bar{\phi}_i^T Y(t) / \bar{a}_i \tag{C.10}$$

Now

$$\begin{Bmatrix} \dot{q} \\ q \end{Bmatrix} = \phi e^{\rho t} = \begin{Bmatrix} \phi_u \\ \phi_e \end{Bmatrix} e^{\rho t}$$

and

$$\phi_e e^{\rho t} = (\phi_u e^{\rho t})' = \phi_u \rho e^{\rho t}$$

Thus

$$\begin{Bmatrix} \dot{q} \\ q \end{Bmatrix} = \begin{Bmatrix} \phi_u \\ \phi_u \rho \end{Bmatrix} \tilde{z}$$

For a general type of load $Q(t)$ the term $\phi_i^T Y$ becomes:

$$\phi_i^T Y = \begin{bmatrix} \phi_u^{i^T} & \rho \phi_u^i \end{bmatrix} \begin{Bmatrix} Q(t) \\ 0 \end{Bmatrix} = \phi_u^{i^T} Q(t)$$

and for earthquake type of load:

$$\phi_i^T Y = -(\phi_u^i)^T M \underline{L} \ddot{v}_g(t) = -(\phi_u^i)^T L \ddot{v}_g(t)$$

where \mathbf{p} is the load distribution vector and \ddot{v}_g is a given accelerogram. Continuing the derivation for the later case, Equation (C.9) becomes:

$$\dot{z}_i - \rho_i z_i = (\phi_i^T)^T \mathcal{L}_i \ddot{v}_g(t) / a_i \quad (C.11)$$

the discrete representation of a typical accelerogram makes $\ddot{v}_g(t)$ vary linearly in each time interval. Thus for each time step Equation (C.11) becomes:

$$\dot{z}_i - \rho_i z_i = (a + bt) \mathcal{L}_i$$

where \mathcal{L}_i is complex and equal to:

$$\mathcal{L}_i = \phi_i^T \mathbf{p} / a_i$$

and the coefficients a and b are

$$a = \ddot{v}_g(t_0)$$

$$b = (\ddot{v}_g(t_1) - \ddot{v}_g(t_0)) / \Delta t$$

The solution to Equation (C.12) is:

$$z_i(t) = A_i + B_i t + C_i e^{-\rho_i t} e^{\rho_i t}$$

where

$$A_i = -\frac{b \mathcal{L}_i}{\rho_i^2} - \frac{a \mathcal{L}_i}{\rho_i}$$

$$B_i = -\frac{b \mathcal{L}_i}{\rho_i}$$

$$C_i = z_i(t_0) - A_i$$

At the end of the integration, \mathbf{z}_1 will be a row vector and the n generalized coordinates will constitute a matrix of dimensions $n \times nt$, where nt is the total number of time steps. The solution in geometric coordinates will be:

$$q(t) = 2 \operatorname{Reals} \{ \phi_u z_n \}$$

The number 2 comes from the fact that a solution of complex pairs is being summed. The imaginary part vanishes for obvious reasons.

REFERENCES.

Hurty, W. C. and Rubinstein, M.F. "Dynamic of Structures". Prentice-Hall, Inc. (1964).

Jennings, A. "Matrix Computations for Engineers and Scientists". John Willey and Sons.

Foss, K. A. (1958) "Coordinates that uncouple the equations of motions of damped linear dynamic systems". J. Appl. Mech. ASME 25, pp. 361-364. (1958).

EARTHQUAKE ENGINEERING RESEARCH CENTER REPORTS

NOTE: Numbers in parentheses are Accession Numbers assigned by the National Technical Information Service; these are followed by a price code. Copies of the reports may be ordered from the National Technical Information Service, 5285 Port Royal Road, Springfield, Virginia, 22161. Accession Numbers should be quoted on orders for reports (PB --- ---) and remittance must accompany each order. Reports without this information were not available at time of printing. The complete list of EERC reports (from EERC 67-1) is available upon request from the Earthquake Engineering Research Center, University of California, Berkeley, 47th Street and Hoffman Boulevard, Richmond, California 94804.

- UCB/EERC-77/01 "PLUSH - A Computer Program for Probabilistic Finite Element Analysis of Seismic Soil-Structure Interaction," by M.P. Romo Organista, J. Lysmer and H.B. Seed - 1977 (PB81 177 651)A05
- UCB/EERC-77/02 "Soil-Structure Interaction Effects at the Humboldt Bay Power Plant in the Ferndale Earthquake of June 7, 1975," by J.E. Valera, H.B. Seed, C.F. Tsai and J. Lysmer - 1977 (PB 265 795)A04
- UCB/EERC-77/03 "Influence of Sample Disturbance on Sand Response to Cyclic Loading," by K. Mori, H.B. Seed and C.K. Chan - 1977 (PB 267 352)A04
- UCB/EERC-77/04 "Seismological Studies of Strong Motion Records," by J. Shoja-Taheri - 1977 (PB 269 655)A10
- UCB/EERC-77/05 Unassigned
- UCB/EERC-77/06 "Developing Methodologies for Evaluating the Earthquake Safety of Existing Buildings," by No. 1 - B. Bresler; No. 2 - B. Bresler, T. Okada and D. Zisling; No. 3 - T. Okada and B. Bresler; No. 4 - V.V. Bertero and B. Bresler - 1977 (PB 267 354)A08
- UCB/EERC-77/07 "A Literature Survey - Transverse Strength of Masonry Walls," by Y. Omote, R.L. Mayes, S.W. Chen and R.W. Clough - 1977 (PB 277 933)A07
- UCB/EERC-77/08 "DRAIN-TABS: A Computer Program for Inelastic Earthquake Response of Three Dimensional Buildings," by R. Guendelman-Israel and G.H. Powell - 1977 (PB 270 693)A07
- UCB/EERC-77/09 "SUBWALL: A Special Purpose Finite Element Computer Program for Practical Elastic Analysis and Design of Structural Walls with Substructure Option," by D.Q. Le, H. Peterson and E.P. Popov - 1977 (PB 270 567)A05
- UCB/EERC-77/10 "Experimental Evaluation of Seismic Design Methods for Broad Cylindrical Tanks," by D.P. Clough (PB 272 280)A13
- UCB/EERC-77/11 "Earthquake Engineering Research at Berkeley - 1976," - 1977 (PB 273 507)A09
- UCB/EERC-77/12 "Automated Design of Earthquake Resistant Multistory Steel Building Frames," by N.D. Walker, Jr. - 1977 (PB 276 526)A09
- UCB/EERC-77/13 "Concrete Confined by Rectangular Hoops Subjected to Axial Loads," by J. Vallenias, V.V. Bertero and E.P. Popov - 1977 (PB 275 165)A06
- UCB/EERC-77/14 "Seismic Strain Induced in the Ground During Earthquakes," by Y. Sugimura - 1977 (PB 284 201)A04
- UCB/EERC-77/15 Unassigned
- UCB/EERC-77/16 "Computer Aided Optimum Design of Ductile Reinforced Concrete Moment Resisting Frames," by S.W. Zagajeski and V.V. Bertero - 1977 (PB 280 137)A07
- UCB/EERC-77/17 "Earthquake Simulation Testing of a Stepping Frame with Energy-Absorbing Devices," by J.M. Kelly and D.F. Tsztoo - 1977 (PB 273 506)A04
- UCB/EERC-77/18 "Inelastic Behavior of Eccentrically Braced Steel Frames under Cyclic Loadings," by C.W. Roeder and E.P. Popov - 1977 (PB 275 526)A15
- UCB/EERC-77/19 "A Simplified Procedure for Estimating Earthquake-Induced Deformations in Dams and Embankments," by F.I. Makdisi and H.B. Seed - 1977 (PB 276 820)A04
- UCB/EERC-77/20 "The Performance of Earth Dams during Earthquakes," by H.B. Seed, F.I. Makdisi and P. de Alba - 1977 (PB 276 821)A04
- UCB/EERC-77/21 "Dynamic Plastic Analysis Using Stress Resultant Finite Element Formulation," by P. Lukkunapvasit and J.M. Kelly - 1977 (PB 275 453)A04
- UCB/EERC-77/22 "Preliminary Experimental Study of Seismic Uplift of a Steel Frame," by R.W. Clough and A.A. Huckelbridge 1977 (PB 278 769)A08
- UCB/EERC-77/23 "Earthquake Simulator Tests of a Nine-Story Steel Frame with Columns Allowed to Uplift," by A.A. Huckelbridge - 1977 (PB 277 944)A09
- UCB/EERC-77/24 "Nonlinear Soil-Structure Interaction of Skew Highway Bridges," by M.-C. Chen and J. Penzien - 1977 (PB 276 176)A07
- UCB/EERC-77/25 "Seismic Analysis of an Offshore Structure Supported on Pile Foundations," by D.D.-N. Liou and J. Penzien 1977 (PB 283 180)A06
- UCB/EERC-77/26 "Dynamic Stiffness Matrices for Homogeneous Viscoelastic Half-Planes," by G. Dasgupta and A.K. Chopra - 1977 (PB 279 654)A06

- UCB/EERC-77/27 "A Practical Soft Story Earthquake Isolation System," by J.M. Kelly, J.M. Eidinger and C.J. Derham - 1977 (PB 276 814)A07
- UCB/EERC-77/28 "Seismic Safety of Existing Buildings and Incentives for Hazard Mitigation in San Francisco: An Exploratory Study," by A.J. Meltsner - 1977 (PB 281 970)A05
- UCB/EERC-77/29 "Dynamic Analysis of Electrohydraulic Shaking Tables," by D. Rea, S. Abedi-Hayati and Y. Takahashi 1977 (PB 282 569)A04
- UCB/EERC-77/30 "An Approach for Improving Seismic - Resistant Behavior of Reinforced Concrete Interior Joints," by B. Galunic, V.V. Bertero and E.P. Popov - 1977 (PB 290 870)A06
- UCB/EERC-78/01 "The Development of Energy-Absorbing Devices for Aseismic Base Isolation Systems," by J.M. Kelly and D.F. Tsztoo - 1978 (PB 284 978)A04
- UCB/EERC-78/02 "Effect of Tensile Prestrain on the Cyclic Response of Structural Steel Connections, by J.G. Bouwkamp and A. Mukhopadhyay - 1978
- UCB/EERC-78/03 "Experimental Results of an Earthquake Isolation System using Natural Rubber Bearings," by J.M. Eidinger and J.M. Kelly - 1978 (PB 281 686)A04
- UCB/EERC-78/04 "Seismic Behavior of Tall Liquid Storage Tanks," by A. Niwa - 1978 (PB 284 017)A14
- UCB/EERC-78/05 "Hysteretic Behavior of Reinforced Concrete Columns Subjected to High Axial and Cyclic Shear Forces," by S.W. Zagajski, V.V. Bertero and J.G. Bouwkamp - 1978 (PB 283 858)A13
- UCB/EERC-78/06 "Three Dimensional Inelastic Frame Elements for the ANSR-I Program," by A. Riahi, D.G. Row and G.H. Powell - 1978 (PB 295 755)A04
- UCB/EERC-78/07 "Studies of Structural Response to Earthquake Ground Motion," by O.A. Lopez and A.K. Chopra - 1978 (PB 282 790)A05
- UCB/EERC-78/08 "A Laboratory Study of the Fluid-Structure Interaction of Submerged Tanks and Caissons in Earthquakes," by R.C. Byrd - 1978 (PB 284 957)A08
- UCB/EERC-78/09 Unassigned
- UCB/EERC-78/10 "Seismic Performance of Nonstructural and Secondary Structural Elements," by I. Sakamoto - 1978 (PB81 154 593)A05
- UCB/EERC-78/11 "Mathematical Modelling of Hysteresis Loops for Reinforced Concrete Columns," by S. Nakata, T. Sproul and J. Penzien - 1978 (PB 298 274)A05
- UCB/EERC-78/12 "Damageability in Existing Buildings," by T. Blejwas and B. Bresler - 1978 (PB 80 166 978)A05
- UCB/EERC-78/13 "Dynamic Behavior of a Pedestal Base Multistory Building," by R.M. Stephen, E.L. Wilson, J.G. Bouwkamp and M. Button - 1978 (PB 286 650)A08
- UCB/EERC-78/14 "Seismic Response of Bridges - Case Studies," by R.A. Imbsen, V. Nutt and J. Penzien - 1978 (PB 286 503)A10
- UCB/EERC-78/15 "A Substructure Technique for Nonlinear Static and Dynamic Analysis," by D.G. Row and G.H. Powell - 1978 (PB 288 077)A10
- UCB/EERC-78/16 "Seismic Risk Studies for San Francisco and for the Greater San Francisco Bay Area," by C.S. Oliveira - 1978 (PB 81 120 115)A07
- UCB/EERC-78/17 "Strength of Timber Roof Connections Subjected to Cyclic Loads," by P. Gülkan, R.L. Mayes and R.W. Clough - 1978 (HUD-000 1491)A07
- UCB/EERC-78/18 "Response of K-Braced Steel Frame Models to Lateral Loads," by J.G. Bouwkamp, R.M. Stephen and E.P. Popov - 1978
- UCB/EERC-78/19 "Rational Design Methods for Light Equipment in Structures Subjected to Ground Motion," by J.L. Sackman and J.M. Kelly - 1978 (PB 292 357)A04
- UCB/EERC-78/20 "Testing of a Wind Restraint for Aseismic Base Isolation," by J.M. Kelly and D.E. Chitty - 1978 (PB 292 833)A03
- UCB/EERC-78/21 "APOLLO - A Computer Program for the Analysis of Pore Pressure Generation and Dissipation in Horizontal Sand Layers During Cyclic or Earthquake Loading," by P.P. Martin and H.B. Seed - 1978 (PB 292 835)A04
- UCB/EERC-78/22 "Optimal Design of an Earthquake Isolation System," by M.A. Bhatti, K.S. Pister and E. Polak - 1978 (PB 294 735)A06
- UCB/EERC-78/23 "MASH - A Computer Program for the Non-Linear Analysis of Vertically Propagating Shear Waves in Horizontally Layered Deposits," by P.P. Martin and H.B. Seed - 1978 (PB 293 101)A05
- UCB/EERC-78/24 "Investigation of the Elastic Characteristics of a Three Story Steel Frame Using System Identification," by I. Kaya and H.D. McNiven - 1978 (PB 296 225)A06
- UCB/EERC-78/25 "Investigation of the Nonlinear Characteristics of a Three-Story Steel Frame Using System Identification," by I. Kaya and H.D. McNiven - 1978 (PB 301 363)A05

- UCB/EERC-78/26 "Studies of Strong Ground Motion in Taiwan," by Y.M. Hsiung, B.A. Bolt and J. Penzien - 1978 (PB 298 436)A06
- UCB/EERC-78/27 "Cyclic Loading Tests of Masonry Single Piers: Volume 1 - Height to Width Ratio of 2," by P.A. Hidalgo, R.L. Mayes, H.D. McNiven and R.W. Clough - 1978 (PB 296 211)A07
- UCB/EERC-78/28 "Cyclic Loading Tests of Masonry Single Piers: Volume 2 - Height to Width Ratio of 1," by S.-W.J. Chen, P.A. Hidalgo, R.L. Mayes, R.W. Clough and H.D. McNiven - 1978 (PB 296 212)A09
- UCB/EERC-78/29 "Analytical Procedures in Soil Dynamics," by J. Lysmer - 1978 (PB 298 445)A06
- UCB/EERC-79/01 "Hysteretic Behavior of Lightweight Reinforced Concrete Beam-Column Subassemblages," by B. Forzani, E.P. Popov and V.V. Bertero - April 1979 (PB 298 267)A06
- UCB/EERC-79/02 "The Development of a Mathematical Model to Predict the Flexural Response of Reinforced Concrete Beams to Cyclic Loads, Using System Identification," by J. Stanton & H. McNiven - Jan. 1979 (PB 295 875)A10
- UCB/EERC-79/03 "Linear and Nonlinear Earthquake Response of Simple Torsionally Coupled Systems," by C.L. Kan and A.K. Chopra - Feb. 1979 (PB 298 262)A06
- UCB/EERC-79/04 "A Mathematical Model of Masonry for Predicting its Linear Seismic Response Characteristics," by Y. Mengi and H.D. McNiven - Feb. 1979 (PB 298 266)A06
- UCB/EERC-79/05 "Mechanical Behavior of Lightweight Concrete Confined by Different Types of Lateral Reinforcement," by M.A. Manrique, V.V. Bertero and E.P. Popov - May 1979 (PB 301 114)A06
- UCB/EERC-79/06 "Static Tilt Tests of a Tall Cylindrical Liquid Storage Tank," by R.W. Clough and A. Niwa - Feb. 1979 (PB 301 167)A06
- UCB/EERC-79/07 "The Design of Steel Energy Absorbing Restrainers and Their Incorporation into Nuclear Power Plants for Enhanced Safety: Volume 1 - Summary Report," by P.N. Spencer, V.F. Zackay, and E.R. Parker - Feb. 1979 (UCB/EERC-79/07)A09
- UCB/EERC-79/08 "The Design of Steel Energy Absorbing Restrainers and Their Incorporation into Nuclear Power Plants for Enhanced Safety: Volume 2 - The Development of Analyses for Reactor System Piping," "Simple Systems" by M.C. Lee, J. Penzien, A.K. Chopra and K. Suzuki "Complex Systems" by G.H. Powell, E.L. Wilson, R.W. Clough and D.G. Row - Feb. 1979 (UCB/EERC-79/08)A10
- UCB/EERC-79/09 "The Design of Steel Energy Absorbing Restrainers and Their Incorporation into Nuclear Power Plants for Enhanced Safety: Volume 3 - Evaluation of Commercial Steels," by W.S. Owen, R.M.N. Pelloux, R.O. Ritchie, M. Faral, T. Ohhashi, J. Toplosky, S.J. Hartman, V.F. Zackay and E.R. Parker - Feb. 1979 (UCB/EERC-79/09)A04
- UCB/EERC-79/10 "The Design of Steel Energy Absorbing Restrainers and Their Incorporation into Nuclear Power Plants for Enhanced Safety: Volume 4 - A Review of Energy-Absorbing Devices," by J.M. Kelly and M.S. Skinner - Feb. 1979 (UCB/EERC-79/10)A04
- UCB/EERC-79/11 "Conservatism in Summation Rules for Closely Spaced Modes," by J.M. Kelly and J.L. Sackman - May 1979 (PB 301 328)A03
- UCB/EERC-79/12 "Cyclic Loading Tests of Masonry Single Piers; Volume 3 - Height to Width Ratio of 0.5," by P.A. Hidalgo, R.L. Mayes, H.D. McNiven and R.W. Clough - May 1979 (PB 301 321)A08
- UCB/EERC-79/13 "Cyclic Behavior of Dense Course-Grained Materials in Relation to the Seismic Stability of Dams," by N.G. Banerjee, H.B. Seed and C.K. Chan - June 1979 (PB 301 373)A13
- UCB/EERC-79/14 "Seismic Behavior of Reinforced Concrete Interior Beam-Column Subassemblages," by S. Viathanatepa, E.P. Popov and V.V. Bertero - June 1979 (PB 301 326)A10
- UCB/EERC-79/15 "Optimal Design of Localized Nonlinear Systems with Dual Performance Criteria Under Earthquake Excitations," by M.A. Bhatti - July 1979 (PB 80 167 109)A06
- UCB/EERC-79/16 "OPTDYN - A General Purpose Optimization Program for Problems with or without Dynamic Constraints," by M.A. Bhatti, E. Polak and K.S. Pister - July 1979 (PB 80 167 091)A05
- UCB/EERC-79/17 "ANGR-II, Analysis of Nonlinear Structural Response, Users Manual," by D.P. Mondkar and G.H. Powell July 1979 (PB 80 113 301)A05
- UCB/EERC-79/18 "Soil Structure Interaction in Different Seismic Environments," A. Gomez-Masso, J. Lysmer, J.-C. Chen and H.B. Seed - August 1979 (PB 80 101 520)A04
- UCB/EERC-79/19 "ARMA Models for Earthquake Ground Motions," by M.K. Chang, J.W. Kwiatkowski, R.F. Nau, R.M. Oliver and K.S. Pister - July 1979 (PB 301 166)A05
- UCB/EERC-79/20 "Hysteretic Behavior of Reinforced Concrete Structural Walls," by J.M. Vallenias, V.V. Bertero and E.P. Popov - August 1979 (PB 80 165 905)A12
- UCB/EERC-79/21 "Studies on High-Frequency Vibrations of Buildings - 1: The Column Effect," by J. Lubliner - August 1979 (PB 80 158 553)A03
- UCB/EERC-79/22 "Effects of Generalized Loadings on Bond Reinforcing Bars Embedded in Confined Concrete Blocks," by S. Viathanatepa, E.P. Popov and V.V. Bertero - August 1979 (PB 81 124 018)A14
- UCB/EERC-79/23 "Shaking Table Study of Single-Story Masonry Houses, Volume 1: Test Structures 1 and 2," by P. Gülkan, R.L. Mayes and R.W. Clough - Sept. 1979 (HUD-000 1763)A12
- UCB/EERC-79/24 "Shaking Table Study of Single-Story Masonry Houses, Volume 2: Test Structures 3 and 4," by P. Gülkan, R.L. Mayes and R.W. Clough - Sept. 1979 (HUD-000 1836)A12
- UCB/EERC-79/25 "Shaking Table Study of Single-Story Masonry Houses, Volume 3: Summary, Conclusions and Recommendations," by R.W. Clough, R.L. Mayes and P. Gülkan - Sept. 1979 (HUD-000 1837)A06

- UCB/EERC-79/26 "Recommendations for a U.S.-Japan Cooperative Research Program Utilizing Large-Scale Testing Facilities," by U.S.-Japan Planning Group - Sept. 1979(PB 301 407)A06
- UCB/EERC-79/27 "Earthquake-Induced Liquefaction Near Lake Amatitlan, Guatemala," by H.B. Seed, I. Arango, C.K. Chan, A. Gomez-Masso and R. Grant de Ascoli - Sept. 1979(NUREG-CRI341)A03
- UCB/EERC-79/28 "Infill Panels: Their Influence on Seismic Response of Buildings," by J.W. Axley and V.V. Bertero Sept. 1979(PB 80 163 371)A10
- UCB/EERC-79/29 "3D Truss Bar Element (Type 1) for the ANSR-II Program," by D.P. Mondkar and G.H. Powell - Nov. 1979 (PB 80 169 709)A02
- UCB/EERC-79/30 "2D Beam-Column Element (Type 5 - Parallel Element Theory) for the ANSR-II Program," by D.G. Row, G.H. Powell and D.P. Mondkar - Dec. 1979(PB 80 167 224)A03
- UCB/EERC-79/31 "3D Beam-Column Element (Type 2 - Parallel Element Theory) for the ANSR-II Program," by A. Riahi, G.H. Powell and D.P. Mondkar - Dec. 1979(PB 80 167 216)A03
- UCB/EERC-79/32 "On Response of Structures to Stationary Excitation," by A. Der Kiureghian - Dec. 1979(PB 80166 929)A03
- UCB/EERC-79/33 "Undisturbed Sampling and Cyclic Load Testing of Sands," by S. Singh, H.B. Seed and C.K. Chan Dec. 1979(ADA 087 298)A07
- UCB/EERC-79/34 "Interaction Effects of Simultaneous Torsional and Compressional Cyclic Loading of Sand," by P.M. Griffin and W.N. Houston - Dec. 1979(ADA 092 352)A15
- UCB/EERC-80/01 "Earthquake Response of Concrete Gravity Dams Including Hydrodynamic and Foundation Interaction Effects," by A.K. Chopra, P. Chakrabarti and S. Gupta - Jan. 1980(AD-A087297)A10
- UCB/EERC-80/02 "Rocking Response of Rigid Blocks to Earthquakes," by C.S. Yim, A.K. Chopra and J. Penzien - Jan. 1980 (PB80 166 002)A04
- UCB/EERC-80/03 "Optimum Inelastic Design of Seismic-Resistant Reinforced Concrete Frame Structures," by S.W. Zagajeski and V.V. Bertero - Jan. 1980(PB80 164 635)A06
- UCB/EERC-80/04 "Effects of Amount and Arrangement of Wall-Panel Reinforcement on Hysteretic Behavior of Reinforced Concrete Walls," by R. Iliya and V.V. Bertero - Feb. 1980(PB81 122 525)A09
- UCB/EERC-80/05 "Shaking Table Research on Concrete Dam Models," by A. Niwa and R.W. Clough - Sept. 1980(PB81 122 368)A06
- UCB/EERC-80/06 "The Design of Steel Energy-Absorbing Restrainers and their Incorporation into Nuclear Power Plants for Enhanced Safety (Vol 1A): Piping with Energy Absorbing Restrainers: Parameter Study on Small Systems," by G.H. Powell, C. Oughourlian and J. Simons - June 1980
- UCB/EERC-80/07 "Inelastic Torsional Response of Structures Subjected to Earthquake Ground Motions," by Y. Yamazaki April 1980(PB81 122 327)A08
- UCB/EERC-80/08 "Study of X-Braced Steel Frame Structures Under Earthquake Simulation," by Y. Ghanaat - April 1980 (PB81 122 335)A11
- UCB/EERC-80/09 "Hybrid Modelling of Soil-Structure Interaction," by S. Gupta, T.W. Lin, J. Penzien and C.S. Yeh May 1980(PB81 122 319)A07
- UCB/EERC-80/10 "General Applicability of a Nonlinear Model of a One Story Steel Frame," by B.I. Sveinsson and H.D. McNiven - May 1980(PB81 124 877)A06
- UCB/EERC-80/11 "A Green-Function Method for Wave Interaction with a Submerged Body," by W. Kioka - April 1980 (PB81 122 269)A07
- UCB/EERC-80/12 "Hydrodynamic Pressure and Added Mass for Axisymmetric Bodies," by F. Nilrat - May 1980(PB81 122 343)A08
- UCB/EERC-80/13 "Treatment of Non-Linear Drag Forces Acting on Offshore Platforms," by B.V. Dao and J. Penzien May 1980(PB81 153 413)A07
- UCB/EERC-80/14 "2D Plane/Axisymmetric Solid Element (Type 3 - Elastic or Elastic-Perfectly Plastic) for the ANSR-II Program," by D.P. Mondkar and G.H. Powell - July 1980(PB81 122 350)A03
- UCB/EERC-80/15 "A Response Spectrum Method for Random Vibrations," by A. Der Kiureghian - June 1980(PB81 122 301)A03
- UCB/EERC-80/16 "Cyclic Inelastic Buckling of Tubular Steel Braces," by V.A. Zayas, E.P. Popov and S.A. Mahin June 1980(PB81 124 885)A10
- UCB/EERC-80/17 "Dynamic Response of Simple Arch Dams Including Hydrodynamic Interaction," by C.S. Porter and A.K. Chopra - July 1980(PB81 124 000)A13
- UCB/EERC-80/18 "Experimental Testing of a Friction Damped Aseismic Base Isolation System with Fail-Safe Characteristics," by J.M. Kelly, K.E. Beucke and M.S. Skinner - July 1980(PB81 148 595)A04
- UCB/EERC-80/19 "The Design of Steel Energy-Absorbing Restrainers and their Incorporation into Nuclear Power Plants for Enhanced Safety (Vol 1B): Stochastic Seismic Analyses of Nuclear Power Plant Structures and Piping Systems Subjected to Multiple Support Excitations," by M.C. Lee and J. Penzien - June 1980
- UCB/EERC-80/20 "The Design of Steel Energy-Absorbing Restrainers and their Incorporation into Nuclear Power Plants for Enhanced Safety (Vol 1C): Numerical Method for Dynamic Substructure Analysis," by J.M. Dickens and E.L. Wilson - June 1980
- UCB/EERC-80/21 "The Design of Steel Energy-Absorbing Restrainers and their Incorporation into Nuclear Power Plants for Enhanced Safety (Vol 2): Development and Testing of Restraints for Nuclear Piping Systems," by J.M. Kelly and M.S. Skinner - June 1980
- UCB/EERC-80/22 "3D Solid Element (Type 4-Elastic or Elastic-Perfectly-Plastic) for the ANSR-II Program," by D.P. Mondkar and G.H. Powell - July 1980(PB81 123 242)A03
- UCB/EERC-80/23 "Gap-Friction Element (Type 5) for the ANSR-II Program," by D.P. Mondkar and G.H. Powell - July 1980 (PB81 122 285)A03

- UCB/EERC-80/24 "U-Bar Restraint Element (Type 11) for the ANSR-II Program," by C. Oughourlian and G.H. Powell July 1980(PB81 122 293)A03
- UCB/EERC-80/25 "Testing of a Natural Rubber Base Isolation System by an Explosively Simulated Earthquake," by J.M. Kelly - August 1980(PB81 201 360)A04
- UCB/EERC-80/26 "Input Identification from Structural Vibrational Response," by Y. Hu - August 1980(PB81 152 308)A05
- UCB/EERC-80/27 "Cyclic Inelastic Behavior of Steel Offshore Structures," by V.A. Zayas, S.A. Mahin and E.P. Popov August 1980(PB81 196 180)A15
- UCB/EERC-80/28 "Shaking Table Testing of a Reinforced Concrete Frame with Biaxial Response," by M.G. Oliva October 1980(PB81 154 304)A10
- UCB/EERC-80/29 "Dynamic Properties of a Twelve-Story Prefabricated Panel Building," by J.G. Bouwkamp, J.P. Kollegger and R.M. Stephen - October 1980(PB82 117 128)A06
- UCB/EERC-80/30 "Dynamic Properties of an Eight-Story Prefabricated Panel Building," by J.G. Bouwkamp, J.P. Kollegger and R.M. Stephen - October 1980(PB81 200 313)A05
- UCB/EERC-80/31 "Predictive Dynamic Response of Panel Type Structures Under Earthquakes," by J.P. Kollegger and J.G. Bouwkamp - October 1980(PB81 152 316)A04
- UCB/EERC-80/32 "The Design of Steel Energy-Absorbing Restrainers and their Incorporation into Nuclear Power Plants for Enhanced Safety (Vol 3): Testing of Commercial Steels in Low-Cycle Torsional Fatigue," by P. Spencer, E.R. Parker, E. Jongewaard and M. Drory
- UCB/EERC-80/33 "The Design of Steel Energy-Absorbing Restrainers and their Incorporation into Nuclear Power Plants for Enhanced Safety (Vol 4): Shaking Table Tests of Piping Systems with Energy-Absorbing Restrainers," by S.F. Stiemer and W.G. Godden - Sept. 1980
- UCB/EERC-80/34 "The Design of Steel Energy-Absorbing Restrainers and their Incorporation into Nuclear Power Plants for Enhanced Safety (Vol 5): Summary Report," by P. Spencer
- UCB/EERC-80/35 "Experimental Testing of an Energy-Absorbing Base Isolation System," by J.M. Kelly, M.S. Skinner and K.E. Beucke - October 1980(PB81 154 072)A04
- UCB/EERC-80/36 "Simulating and Analyzing Artificial Non-Stationary Earthquake Ground Motions," by R.F. Nau, R.M. Oliver and K.S. Pister - October 1980(PB81 153 397)A04
- UCB/EERC-80/37 "Earthquake Engineering at Berkeley - 1980," - Sept. 1980(PB81 205 374)A09
- UCB/EERC-80/38 "Inelastic Seismic Analysis of Large Panel Buildings," by V. Schricker and G.H. Powell - Sept. 1980 (PB81 154 338)A13
- UCB/EERC-80/39 "Dynamic Response of Embankment, Concrete-Gravity and Arch Dams Including Hydrodynamic Interaction," by J.F. Hall and A.K. Chopra - October 1980(PB81 152 324)A11
- UCB/EERC-80/40 "Inelastic Buckling of Steel Struts Under Cyclic Load Reversal," by R.G. Black, W.A. Wenger and E.P. Popov - October 1980(PB81 154 312)A08
- UCB/EERC-80/41 "Influence of Site Characteristics on Building Damage During the October 3, 1974 Lima Earthquake," by P. Repetto, I. Arango and H.B. Seed - Sept. 1980(PB81 161 739)A05
- UCB/EERC-80/42 "Evaluation of a Shaking Table Test Program on Response Behavior of a Two Story Reinforced Concrete Frame," by J.M. Blondet, R.W. Clough and S.A. Mahin
- UCB/EERC-80/43 "Modelling of Soil-Structure Interaction by Finite and Infinite Elements," by F. Medina - December 1980(PB81 229 270)A04
- UCB/EERC-81/01 "Control of Seismic Response of Piping Systems and Other Structures by Base Isolation," edited by J.M. Kelly - January 1981 (PB81 200 735)A05
- UCB/EERC-81/02 "OPTNSR - An Interactive Software System for Optimal Design of Statically and Dynamically Loaded Structures with Nonlinear Response," by M.A. Bhatti, V. Ciampi and K.S. Pister - January 1981 (PB81 213 851)A09
- UCB/EERC-81/03 "Analysis of Local Variations in Free Field Seismic Ground Motions," by J.-C. Chen, J. Lysmer and H.B. Seed - January 1981 (AD-A099508)A13
- UCB/EERC-81/04 "Inelastic Structural Modeling of Braced Offshore Platforms for Seismic Loading," by V.A. Zayas, P.-S.B. Shing, S.A. Mahin and E.P. Popov - January 1981(PB82 138 777)A07
- UCB/EERC-81/05 "Dynamic Response of Light Equipment in Structures," by A. Der Kiureghian, J.L. Sackman and B. Nour-Omid - April 1981 (PB81 218 497)A04
- UCB/EERC-81/06 "Preliminary Experimental Investigation of a Broad Base Liquid Storage Tank," by J.G. Bouwkamp, J.P. Kollegger and R.M. Stephen - May 1981(PB82 140 385)A03
- UCB/EERC-81/07 "The Seismic Resistant Design of Reinforced Concrete Coupled Structural Walls," by A.E. Aktan and V.V. Bertero - June 1981(PB82 113 353)A11
- UCB/EERC-81/08 "The Undrained Shearing Resistance of Cohesive Soils at Large Deformations," by M.R. Pyles and H.B. Seed - August 1981
- UCB/EERC-81/09 "Experimental Behavior of a Spatial Piping System with Steel Energy Absorbers Subjected to a Simulated Differential Seismic Input," by S.F. Stiemer, W.G. Godden and J.M. Kelly - July 1981

- UCB/EERC-81/10 "Evaluation of Seismic Design Provisions for Masonry in the United States," by B.I. Sveinsson, R.L. Mayes and H.D. McNiven - August 1981
- UCB/EERC-81/11 "Two-Dimensional Hybrid Modelling of Soil-Structure Interaction," by T.-J. Tzong, S. Gupta and J. Penzien - August 1981 (PB82 142 118)A04
- UCB/EERC-81/12 "Studies on Effects of Infills in Seismic Resistant R/C Construction," by S. Brokken and V.V. Bertero - September 1981
- UCB/EERC-81/13 "Linear Models to Predict the Nonlinear Seismic Behavior of a One-Story Steel Frame," by H. Valdimarsson, A.H. Shah and H.D. McNiven - September 1981 (PB82 138 793)A07
- UCB/EERC-81/14 "TLUSH: A Computer Program for the Three-Dimensional Dynamic Analysis of Earth Dams," by T. Kagawa, L.H. Mejia, H.B. Seed and J. Lysmer - September 1981 (PB82 139 940)A06
- UCB/EERC-81/15 "Three Dimensional Dynamic Response Analysis of Earth Dams," by L.H. Mejia and H.B. Seed - September 1981 (PB82 137 274)A12
- UCB/EERC-81/16 "Experimental Study of Lead and Elastomeric Dampers for Base Isolation Systems," by J.M. Kelly and S.B. Hodder - October 1981 (PB82 166 182)A05
- UCB/EERC-81/17 "The Influence of Base Isolation on the Seismic Response of Light Secondary Equipment," by J.M. Kelly - April 1981 (PB82 255 266)A04
- UCB/EERC-81/18 "Studies on Evaluation of Shaking Table Response Analysis Procedures," by J. Marcia Blondet - November 1981 (PB82 197 278)A10
- UCB/EERC-81/19 "DELIGHT.STRUCT: A Computer-Aided Design Environment for Structural Engineering," by R.J. Balling, K.S. Pister and E. Polak - December 1981 (PB82 218 496)A07
- UCB/EERC-81/20 "Optimal Design of Seismic-Resistant Planar Steel Frames," by R.J. Balling, V. Ciampi, K.S. Pister and E. Polak - December 1981 (PB82 220 179)A07
- UCB/EERC-82/01 "Dynamic Behavior of Ground for Seismic Analysis of Lifeline Systems," by T. Sato and A. Der Kiureghian - January 1982 (PB82 218 926)A05
- UCB/EERC-82/02 "Shaking Table Tests of a Tubular Steel Frame Model," by Y. Ghanaat and R. W. Clough - January 1982 (PB82 220 161)A07
- UCB/EERC-82/03 "Experimental Behavior of a Spatial Piping System with Shock Arrestors and Energy Absorbers under Seismic Excitation," by S. Schneider, H.-M. Lee and G. W. Godden - May 1982
- UCB/EERC-82/04 "New Approaches for the Dynamic Analysis of Large Structural Systems," by E. L. Wilson - June 1982 (PB83 148 080)A05
- UCB/EERC-82/05 "Model Study of Effects of Damage on the Vibration Properties of Steel Offshore Platforms," by F. Shahriyar and J. G. Bouwkamp - June 1982
- UCB/EERC-82/06 "States of the Art and Practice in the Optimum Seismic Design and Analytical Response Prediction of R/C Frame-Wall Structures," by A. E. Aktan and V. V. Bertero - July 1982 (PB83 147 736)A05
- UCB/EERC-82/07 "Further Study of the Earthquake Response of a Broad Cylindrical Liquid-Storage Tank Model," by G. C. Manos and R. W. Clough - July 1982 (PB83 147 744)A11
- UCB/EERC-82/08 "An Evaluation of the Design and Analytical Seismic Response of a Seven Story Reinforced Concrete Frame - Wall Structure," by F. A. Charney and V. V. Bertero - July 1982
- UCB/EERC-82/09 "Fluid-Structure Interactions: Added Mass Computations for Incompressible Fluid," by J. S.-H. Kuo - August 1982
- UCB/EERC-82/10 "Joint-Opening Nonlinear Mechanism: Interface Smeared Crack Model," by J. S.-H. Kuo - August 1982 (PB83 149 195)A05
- UCB/EERC-82/11 "Dynamic Response Analysis of Tchi Dam," by R. W. Clough, R. M. Stephen and J. S.-H. Kuo - August 1982 (PB83 147 496)A06
- UCB/EERC-82/12 "Prediction of the Seismic Responses of R/C Frame-Coupled Wall Structures," by A. E. Aktan, V. V. Bertero and M. Piazza - August 1982 (PB83 149 203)A09
- UCB/EERC-82/13 "Preliminary Report on the SMART 1 Strong Motion Array in Taiwan," by B. A. Bolt, C. H. Loh, J. Penzien, Y. B. Tsai and Y. T. Yeh - August 1982
- UCB/EERC-82/14 "Shaking-Table Studies of an Eccentrically X-Braced Steel Structure," by M. S. Yang - September 1982
- UCB/EERC-82/15 "The Performance of Stairways in Earthquakes," by C. Roha, J. W. Axley and V. V. Bertero - September 1982

- UCB/EERC-82/16 "The Behavior of Submerged Multiple Bodies in Earthquakes," by W.-G. Liao - September 1982
- UCB/EERC-82/17 "Effects of Concrete Types and Loading Conditions on Local Bond-Slip Relationships," by A. D. Cowell, E. P. Popov and V. V. Bertero - September 1982
- UCB/EERC-82/18 "Mechanical Behavior of Shear Wall Vertical Boundary Members: An Experimental Investigation," by M. T. Wagner and V. V. Bertero - October 1982
- UCB/EERC-82/19 "Experimental Studies of Multi-support Seismic Loading on Piping Systems," by J. M. Kelly and A. D. Cowell - November 1982
- UCB/EERC-82/20 "Generalized Plastic Hinge Concepts for 3D Beam-Column Elements," by P. F.-S. Chen and G. H. Powell - November 1982
- UCB/EERC-82/21 "ANSR-III: General Purpose Computer Program for Nonlinear Structural Analysis," by C. V. Oughourlian and G. H. Powell - November 1982
- UCB/EERC-82/22 "Solution Strategies for Statically Loaded Nonlinear Structures," by J. W. Simons and G. H. Powell - November 1982
- UCB/EERC-82/23 "Analytical Model of Deformed Bar Anchorages under Generalized Excitations," by V. Ciampi, R. Eligehausen, V. V. Bertero and E. P. Popov - November 1982
- UCB/EERC-82/24 "A Mathematical Model for the Response of Masonry Walls to Dynamic Excitations," by H. Sucuođlu, Y. Mengi and H. D. McNiven - November 1982
- UCB/EERC-82/25 "Earthquake Response Considerations of Broad Liquid Storage Tanks," by F. J. Cambra - November 1982
- UCB/EERC-82/26 "Computational Models for Cyclic Plasticity, Rate Dependence and Creep," by B. Mosaddad and G. H. Powell - November 1982
- UCB/EERC-82/27 "Inelastic Analysis of Piping and Tubular Structures," by M. Mahasuverachai and G. H. Powell - November 1982
- UCB/EERC-83/01 "The Economic Feasibility of Seismic Rehabilitation of Buildings by Base Isolation," by J. M. Kelly - January 1983
- UCB/EERC-83/02 "Seismic Moment Connections for Moment-Resisting Steel Frames," by E. P. Popov - January 1983
- UCB/EERC-83/03 "Design of Links and Beam-to-Column Connections for Eccentrically Braced Steel Frames," by E. P. Popov and J. O. Malley - January 1983
- UCB/EERC-83/04 "Numerical Techniques for the Evaluation of Soil-Structure Interaction Effects in the Time Domain," by E. Bayo and E. L. Wilson - February 1983

